12. SITE 641[1]

Shipboard Scientific Party[2]

HOLE 641A

Date occupied: 8 June 1985

Date departed: 10 June 1985

Time on hole: 1 day, 18 hr

Position: 42°09.3′N, 12°10.9′W

Water depth (sea level, corrected m, echo-sounding): 4636

Water depth (rig floor, corrected m, echo-sounding): 4646

Bottom felt (m, drill pipe): 4646

Penetration (m): 63.6

Number of cores: 7

Total length of cored section (m): 63.6

Total core recovered (m): 40.34

Core recovery (%): 63.4

Deepest sedimentary unit cored:
Depth sub-bottom (m): 63.6
Nature: green-gray calcareous clay
Age: late Albian
Measured vertical sound velocity (km/s): 1.55

HOLE 641B

Date occupied: 10 June 1985

Date departed: 11 June 1985

Time on hole: 12 hr

Position: 42°09.3′N, 12°10.9′W

Water depth (sea level, corrected m, echo-sounding): 4639

Water depth (rig floor, corrected m, echo-sounding): 4649

Bottom felt (m, drill pipe): 4649

Penetration (m): 35

Number of cores: 0

Total length of cored section (m): 0

Total core recovered (m): 0

Core recovery (%): 0

HOLE 641C

Date occupied: 11 June 1985

Date departed: 15 June 1985

Time on hole: 4 days, 2 hr

Position: 42°09.3′N, 12°10.9′W

Water depth (sea level, corrected m, echo-sounding): 4640

Water depth (rig floor, corrected m, echo-sounding): 4650

Bottom felt (m, drill pipe): 4650

Penetration (m): 305.2

Number of cores: 16

Total length of cored section (m): 154.3

Total core recovered (m): 112.52

Core recovery (%): 72.9

Deepest sedimentary unit cored:
Depth sub-bottom (m): 305.2
Nature: calcareous microturbidites, marlstone, and clayey limestone
Age: late Barremian
Measured vertical sound velocity (km/s): 1.91

Principal results: Drilling at Site 641, upslope and east of Site 638 (Fig. 1), completed the coring of the upper part of the syn-rift sediments and cored the lower part of the post-rift sequence, supplementing the cores from Site 638. The main objectives were (1) to date the break-up unconformity on the Galicia margin and to document the timing of the cessation of rifting and (2) to recover the Upper Cretaceous–Albian interval, especially the Albian–Cenomanian black shales and strata at the Cenomanian/Turonian boundary. Major results are summarized in Figure 2.

The sedimentary section comprises six lithologic units as follows:

Lithologic Unit I, 0–53.6 m: Upper Cretaceous to Pleistocene. Slumped brown clay, marl, and calcareous ooze (0–15.7 m) overlying Upper Cretaceous brown clay.

---

[1] Boillot, G., Winterer, E. L., Meyer, A. W., et al., *Proc. Init. Repts. (Pt. A), ODP*, 103.

[2] Gilbert Boillot (Co-Chief Scientist), Laboratoire de Géodynamique Sous-Marine, Université Pierre et Marie Curie, B.P. 48, 06230,Villefranche-sur-Mer, France; Edward L. Winterer (Co-Chief Scientist), Graduate Research Division A-012-W, Scripps Institution of Oceanography, La Jolla, CA 92093; Audrey W. Meyer (ODP Staff Scientist), Ocean Drilling Program, Texas A&M University, College Station, TX 77843-3469; Joseph Applegate, Department of Geology, Florida State University, Tallahassee, FL 32306; Miriam Baltuck, Department of Geology, Tulane University, New Orleans, LA 70118 (current address: NASA Headquarters, Code EEL, Washington, D.C. 20546); James A. Bergen, Department of Geology, Florida State University, Tallahassee, FL 32306; M. C. Comas, Departamento Estratigrafia y Paleontologia, Facultad de Ciencias, Universidad de Granada, 18001 Granada, Spain; Thomas A. Davies, Institute for Geophysics, University of Texas at Austin, 4920 North IH 35, Austin, TX 78751; Keith Dunham, Department of Atmospheric and Oceanic Sciences, University of Michigan, 2455 Hayward Avenue, Ann Arbor, MI 48109 (current address: P.O. Box 13, Pequat Lakes, MN 56478); Cynthia A. Evans, Department of Geology, Colgate University, Hamilton, NY 13346 (current address: Lamont-Doherty Geological Observatory, Palisades, NY 10964); Jacques Girardeau, Laboratoire de Materiaux Terrestres, I.P.G., 4 Place Jussieu, 75252 Paris Cedex 05, France; David Goldberg, Lamont-Doherty Geological Observatory, Palisades, NY 10964; Janet Haggerty, Department of Geology, University of Tulsa, 600 S. College Avenue, Tulsa, OK 74104; Lubomir F. Jansa, Atlantic Geoscience Center, Bedford Institute of Oceanography, Dartmouth, Nova Scotia B2Y 4A2, Canada; Jeffrey A. Johnson, Department of Earth and Space Sciences, University of California, Los Angeles, CA 90024 (current address: 9449 Briar Forest Drive, No. 3544, Houston, TX 77063); Junzo Kasahara, Earthquake Research Institute, University of Tokyo, 1,1,1 Yayoi, Bunkyo, Tokyo 113, Japan (current address: Nippon Schlumberger K. K., 2-1 Fuchinobe, 2-Chome, Sagamihara-shi, Kanagawa-ken, 229, Japan); Jean-Paul Loreau, Laboratoire de Géologie, Museum National D'Histoire Naturelle, 43 Rue Buffon, 75005 Paris, France; Emilio Luna, Hispanoil, Pez Volador No. 2, 28007 Madrid, Spain; Michel Moullade, Laboratoire de Géologie et Micropaleontologie Marines, Université de Nice, Parc Valrose, 06034 Nice Cedex, France; James Ogg, Geological Research Division A-012, Scripps Institution of Oceanography, La Jolla, CA 92093 (current address: Dept. Earth and Atmospheric Sciences, Purdue University, W. Lafayette, IN 47907); Massimo Sarti, Istituto di Geologia, Universitá di Ferrara, Corso Ercole d'Este, 32, 44100 Ferrara, Italy; Jürgen Thurow, Institut und Museum für Geologie und Paleontologie, Universität Tübingen, Sigwartstr. 10, D-7400 Tübingen, Federal Republic of Germany; Mark A. Williamson, Atlantic Geoscience Centre, Geological Survey of Canada, Bedford Institute of Oceanography, Box 1006, Dartmouth, Nova Scotia B2Y 4A2, Canada (current address: Shell Canada Ltd., P.O. Box 100, Stn. M, Calgary, Alberta T2P 2H5, Canada).

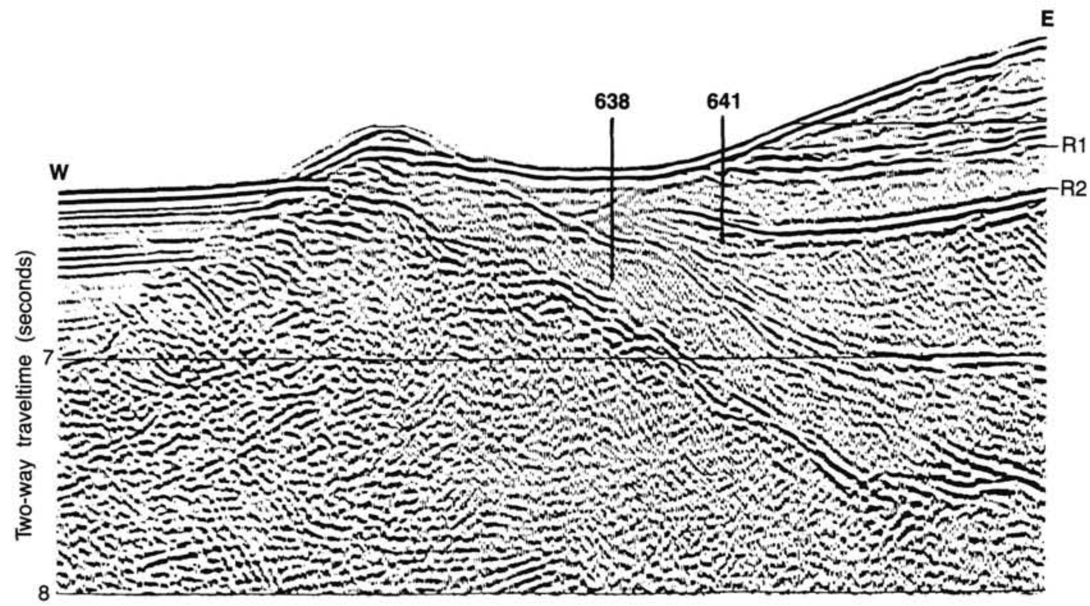

Figure 1. IFP seismic line GP-101 (courtesy of L. Montadert), showing location of Sites 638 and 641 and reflectors R1 and R2 described in text. Location of profile shown in Figure 3.

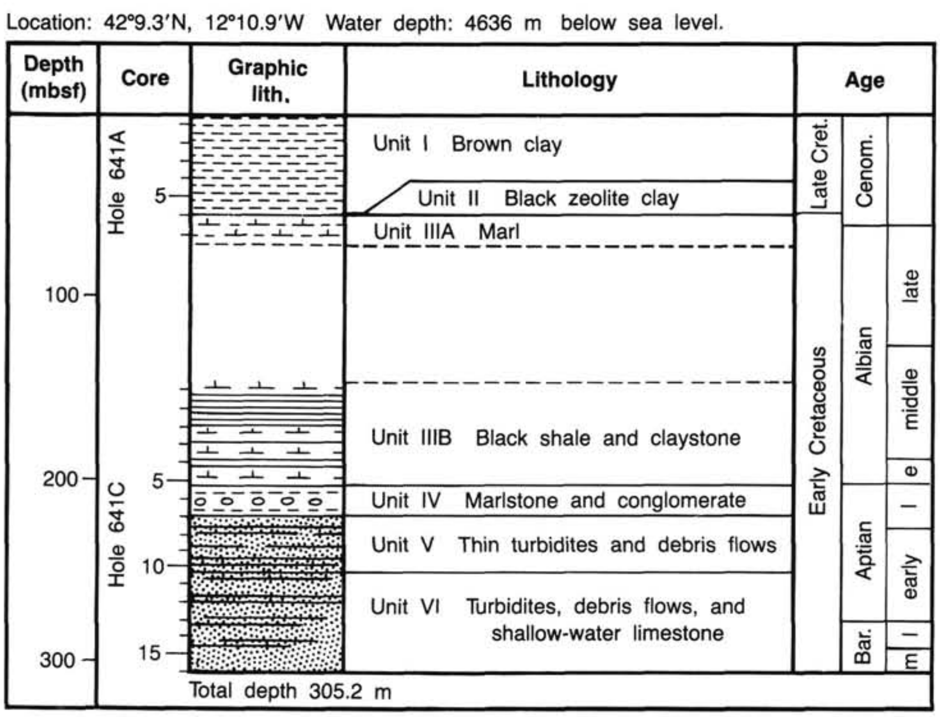

Figure 2. Stratigraphic summary log, Site 641 (Holes 641A and 641C).

Lithologic Unit II, 53.6–53.9 m: Black zeolitic clay having an organic carbon content of approximately 10% Type II (marine) organic matter. This clay lies a few cm above lower Cenomanian marl and about 20 m below clay beds having fossils that range from Coniacian to Maestrichtian.

Lithologic Unit III, 53.9–202.6 m: Albian to Cenomanian. Black and dark-green laminated claystone (151–202.6 m) overlain by upper Albian and Cenomanian calcareous clay and marl (53.9–64 m). The two sections are separated by an unsampled interval.

Lithologic Unit IV, 202.6–218.4 m: upper Aptian. Greenish gray marlstone with conglomerate of granule-sized clasts of shallow-water limestone.

Lithologic Unit V, 218.4–250.6 m: lower Aptian. Thin calcarenite turbidites, black claystone, and gray marlstone; debris flows with pelagic clay pebbles and shallow-water limestone clasts.

Lithologic Unit VI, 250.6–305.2 m: middle/upper Barremian to lower Aptian. Marlstone, thin silt turbidites, debris flows, shallow-water limestone, and sand turbidites.

Unstable hole conditions limited logging to about 66 m of Hole 641C, which was logged with density and natural-gamma tools.

We think that the break-up unconformity is near the Aptian/Albian boundary, at the contact between black claystone and underlying black claystone, debris-flow units, and turbidites. Remarkably, no hiatus could be detected in the biostratigraphy across this contact.

The results from Site 641 combine with those from Sites 638 and 639 to form a composite column about 1200 m thick, extending from the basement through the Upper Jurassic carbonate platform, the Lower Cretaceous syn-rift turbidites, and the post-rift sediments into the Upper Cretaceous.

BACKGROUND AND OBJECTIVES

Drilling Site 641 completed coring the upper part of the syn-rift sediments and cored the lower part of the post-rift sequence to supplement the cores from Site 638. At Site 638, we cored upper Barremian marlstone, directly underlying Neogene ooze infilling a Cenozoic valley, where we placed the site to ensure good stability for the reentry hole (see Site 638 chapter, this volume). Consequently, we missed part of the sequence, including the break-up unconformity that should mark the beginning of seafloor spreading to the west of Galicia.

Site 641 is on the lower slope of a hill east of the Cenozoic valley, about 1.2 km from Site 638, where the seismic record (Fig. 1) shows that reflectors correlated with the Upper Cretaceous sediments and Albian black shale are near the seafloor.

The main drilling objectives at Site 641 were

1. To date the break-up unconformity of the Galicia margin, correlated on the seismic line with reflector R2 (see "Seismic Stratigraphy" section, this chapter). According to the results of Leg 47B (Sibuet, Ryan, et al., 1979), this unconformity is latest Aptian in age. Micropaleontological control at Site 398 is poor near the Aptian/Albian boundary, and the dating of strata bracketing the unconformity is desirable. Note that the bracketing ages at the break-up unconformity could be somewhat different at Site 398 than at Site 641. To document the timing of rifting cessation is an important topical problem and was one of the main objectives of Leg 103.

2. To recover the Upper Cretaceous–Albian interval, correlated on the seismic line with the reflector R1 and underlying transparent layer between R1 and R2 (see "Seismic Stratigraphy" section, this chapter). This interval probably includes layers having high concentrations of organic matter, of both marine and continental origin. Paleoceanographers, sedimentologists, geochemists, and micropaleontologists are especially interested in the strata at the Cenomanian/Turonian boundary, where a layer exceptionally rich in marine organic matter occurs at many places in both deep and relatively shallow water, not only in the Atlantic and Tethyan regions but also in the Pacific, indicating a global paleoenvironmental event (Schlanger and Jenkyns, 1976; Arthur, 1979; de Graciansky et al., 1984). Albian–Cenomanian black shales are likewise of great interest because considerable disagreement still persists about their environmental significance.

OPERATIONS

Approach to Site 641

The ship moved slowly to Site 641 from Site 639, using thruster power, while pulling pipe to change the bit for drilling at the new site. The ship first headed to the Hole 638B acoustic beacon, which was still working, and then along a course of 80° from that beacon. This allowed us to follow the seismic profile and echo-sounding records made during and immediately after dropping the beacon at Site 638. When the ship had moved about 1250 m along this course from the beacon, we estimated that we had come far enough to ensure that the seafloor was a few tens of meters shallower than the seismic-reflector group in which we expected the Cenomanian/Turonian boundary to occur. This stratigraphic level is one at which organic-rich black clay occurs at many localities in both the Atlantic and Pacific Oceans and at outcrops on several continents; hence, we wanted to obtain cores through this interval.

Figure 3 shows the location of Site 641 with respect to the holes at Site 638 and to the track of *JOIDES Resolution*, where the seismic-reflection profile, discussed in the section on "Seismic Stratigraphy" (this chapter), was obtained.

Drilling and Coring Operations at Site 641

Three holes were drilled at Site 641, but in only two, Holes 641A and 641C, were any cores collected (see Table 1 for the details of the coring depths and recoveries). At Hole 641B, a technical problem, described in the following text, halted operations before coring began. Although the ship remained positioned directly over the acoustic beacon during the spudding of each of the three holes, the depth at which the driller felt firm bottom was different for each hole; Hole 641A spudded at 4646 m below the derrick floor, 641B at 4649 m, and 641C at 4650 m. Either a small-scale relief occurs on the seafloor or the ship moves from the beacon more than is recorded by the computer that registers the distance range of the four hydrophones listening to the beacon.

Hole 641A was planned to be continuously cored from the seafloor through all the post-rift sequence and to a stratigraphic level equivalent to that of the highest samples of Cretaceous sediments at Hole 638B. We estimated this depth to be about 300 mbsf. Coring began with a mishap, when the lower end of the core barrel of the advanced hydraulic piston corer (APC), parted from the upper end of the core barrel during coring. We changed to the extended core barrel (XCB), which features a retractable coring bit that extends about 30 cm ahead of the bit. Coring then proceeded normally to a depth of 63.6 mbsf, about 10 m deeper than a distinctive organic-rich black clay, which we had wanted to core and which we had recovered intact in Core 103-641A-6X. While coring for Core 103-641A-8X, the drill string suddenly lost about 23,000 lb of weight, indicating that a substantial part of the bottom-hole assembly (BHA) had broken off. A round trip ensued, and when the BHA began to emerge on deck, we saw that the bumper sub, located about 75 m above the bit, had broken. This bumper sub had taken a lot of abuse at Holes 639A, 639B, 639C, and 639D in coring through the hard and fractured carbonate rocks.

For Hole 641B, we decided to wash through the uppermost sediments just cored in Hole 641A and to begin coring again slightly above the level of the black clay to obtain additional material for analysis. When we reached a depth of 35 mbsf and tried to retrieve the center bit, it would not free itself, and a second round trip was thus required. Inspection of the core barrel after it arrived on deck revealed that when the core barrel and its attached center bit had dropped into the drill string, it broke the hinge that attaches the flapper valve in the lowest part of the BHA. Thus, the flapper valve broke away, allowing the lowest part of the core barrel assembly to shoot ahead and smash into the upper part of the center bit, cutting a deep notch and completely jamming the mechanism so that the barrel could not be freed by the overshot device.

For Hole 641C, because the remaining operational time for Leg 103 was diminishing, we elected to wash through the upper part of the sequence, down to about 150 mbsf, where we thought we would still be well within the Albian black shale formation and above the important regional unconformity that we were eager to sample. Coring began at 150.9 mbsf, using the standard rotary core barrel, and we began to achieve an outstanding recovery rate. Core after core recovered more than 8 m of excellent quality sediment—long unbroken cylinders, perfectly preserving

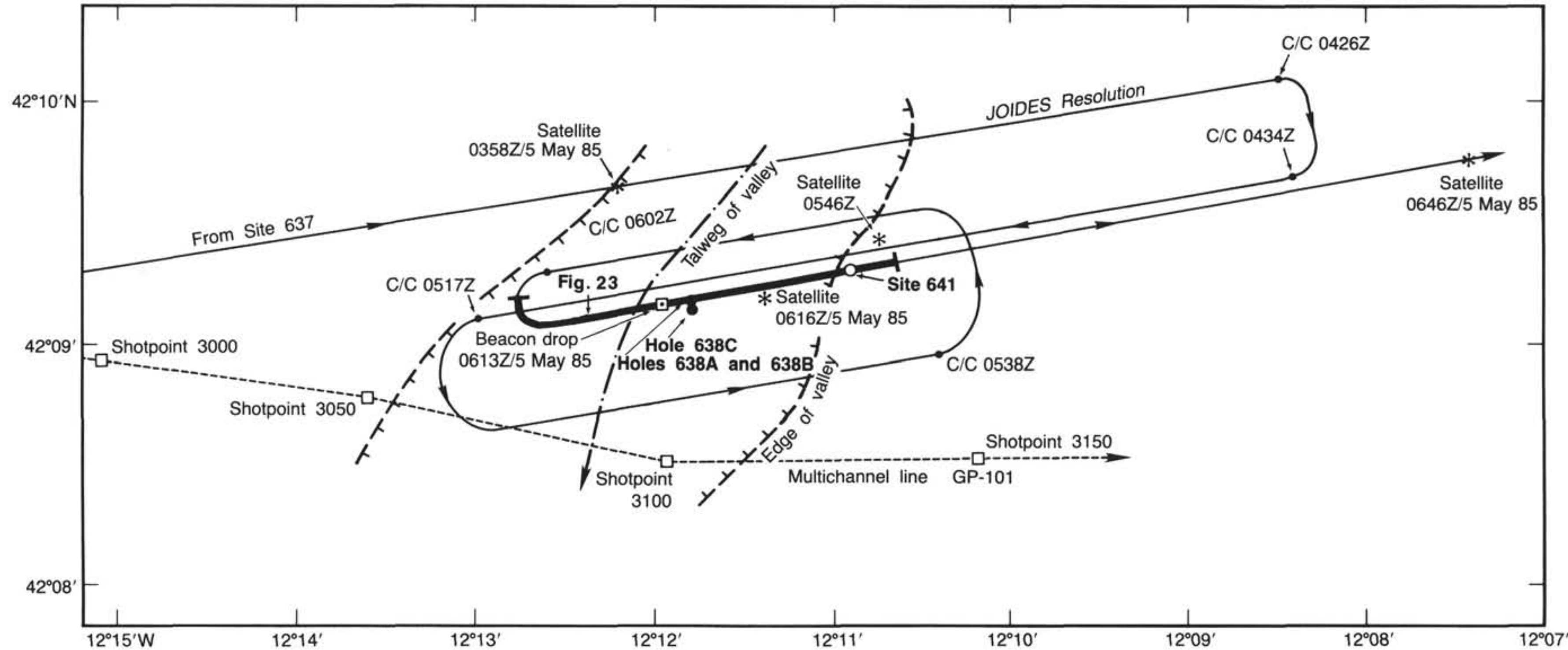

Figure 3. Chart showing the location of Site 641 and its relation to Site 638 and to the track of *JOIDES Resolution* along which a seismic profile was made. Location of IFP seismic line GP-101 is shown by dashed line. Location of *JOIDES Resolution* seismic profile shown in Figure 23 indicated by heavy solid line. Edge of valley, as delineated on *JOIDES Resolution* and IFP seismic lines, is indicated by hachured dashed line.

Table 1. Coring summary, Site 641.

Core no.	Date (mo./day) 1985	Time (hr)	Sub-bottom top (m)	Sub-bottom bottom (m)	Length cored (m)	Length recovered (m)	Percentage recovered
Hole 641A							
1X	06/09	0900	0.0	6.1	6.1	5.5	89.0
2X	06/09	1145	6.1	15.7	9.6	8.2	85.0
3X	06/09	1525	15.7	25.3	9.6	3.5	36.0
4X	06/09	1745	25.3	34.9	9.6	1.2	12.0
5X	06/09	1945	34.9	44.5	9.6	4.1	42.0
6X	06/09	2200	44.5	54.1	9.6	9.8	101.0
7X	06/10	0045	54.1	63.6	9.5	8.1	85.0
Hole 641C							
1R	06/12	1030	150.9	160.5	9.6	8.2	85.0
2R	06/12	1330	160.5	170.1	9.6	9.3	97.0
3R	06/12	1630	170.1	179.8	9.7	9.8	101.0
4R	06/12	1915	179.8	189.4	9.6	8.3	86.0
5R	06/12	2205	189.4	199.0	9.6	0.2	1.0
6R	06/13	0030	199.0	208.7	9.7	4.8	49.0
7R	06/13	0330	208.7	218.4	9.6	2.9	30.0
8R	06/13	0630	218.4	228.0	9.6	6.3	65.0
9R	06/13	0900	228.0	237.6	9.6	5.1	52.0
10R	06/13	1130	237.6	247.3	9.7	8.3	85.0
11R	06/13	1400	247.3	256.9	9.6	6.2	65.0
12R	06/13	1630	256.9	266.5	9.6	9.4	98.0
13R	06/13	2000	266.5	276.2	9.7	7.3	75.0
14R	06/13	2300	276.2	285.8	9.6	9.2	96.0
15R	06/14	0200	285.8	295.5	9.7	6.8	69.0
16R	06/14	0445	295.5	305.2	9.7	10.3	106.0

the *in-situ* sedimentary features. Recovery rates stayed acceptably high throughout the entire sequence, except one core (Core 103-641C-5R), which retrieved only a hard nubbin about 15 cm long. The final core, from a depth of 305.2 mbsf, delivered 10.32 m of core, which is about 0.5 m longer than the length of the core barrel. We asked the driller no questions and happily accepted this unexpected bounty.

Logging Operations in Hole 641C

Having decided that the combination of sedimentological and paleontological evidence showed that we were at or even slightly below the stratigraphic level of the highest Cretaceous strata at Hole 638B, we decided to log the hole. The alternative was to begin still another hole at this site to core the missed, upper part of the black shale and to obtain another sample of the organic-rich black clay. We were, however, mindful that this interval had been continuously cored at Site 398, about 90 km away. We also thought that logs would produce valuable new information, both about the seismic-impedance contrast associated with the unconformity at the top of the syn-rift sedimentary sequence and about the relations between the clay mineralogy and the uranium and organic-matter content of the black shale formation. We knew of no logs having been taken during the Deep Sea Drilling Project in the black shale and certainly of none with the tool that discriminates uranium, potassium, and thorium.

After retrieving the last core at about 0445 hr on 14 June, the hole was conditioned by making a wiper trip through the lower 155 m of the hole then sweeping the hole with 40 barrels of fresh-water mud. A go-devil was dropped, the bit released, and the pipe pulled back until the bottom of the BHA was at 110 mbsf. At 0945 hr, the logging team began to rig their equipment, and by noon the logging tools (gamma, sonic, and caliper) were lowered out of the end of the drill string into open hole. At a depth of only 127 mbsf the tools met an impassable bridge. Furthermore, the recorder electronics of the sonic tool proved faulty, and no sonic log could be made. Only a short segment of gamma log was obtained. We retrieved the tools, ending the first logging attempt.

For the next attempt, after a wiper trip to clean the hole, the drill pipe was then positioned at 128 mbsf, and the second group of tools (lithodensity, gamma-ray spectrometry, and neutron porosity) were lowered. A log was obtained from 160 to 196 mbsf and from 130 to 174 mbsf, making a composite log from 130 to 196 mbsf. Finally, the gamma-ray spectrometry tool was monitored all the way back up to the seafloor inside the drill collars and pipe. The tools were back on the derrick floor by 0630 hr on 15 June. By 1330 hr, the drilling equipment was secured for sea, and the *JOIDES Resolution* departed Site 641, heading for Bremerhaven, Federal Republic of Germany, at full speed.

The difficulties experienced in trying to log the hole at Site 641 are not unusual; in fact, similar problems arose at each hole that we tried to log during Leg 103. We do not think that these conditions are unusual for continental-margin settings, as past experience demonstrates (e.g., Leg 50 on the northwest African margin off Morocco). The basic problem is hole instability and insufficient means to deal with this inherent condition. We drill with salt water and cannot build up a mud cake on the wall of the hole to stabilize it; the little mud we do use is for flushing the hole and for slowing the descent of cuttings. Because the mud is mixed with fresh water, it probably reacts with the clay minerals in the muddy formations—omnipresent on most continental margins—and may leave them less stable than before mud application.

Downhole logs are definitely valuable. They provide data unobtainable in any other way, and nearly every scientific team sailing on the drilling ship is eager to log their holes. Downhole logging is valuable not only for the holes that penetrate deep into oceanic basement but also, perhaps even more so, for holes drilled on the continental margins, where detailed correlations to seismic-reflection data are a necessity and indeed commonly a major reason for drilling. Given good logs, we can tie in with commercially logged wells. Until practical means are developed to overcome the problems of unstable hole conditions, however, many scientists may be unwilling to invest the large expenditures of ship time required for what might be paltry results.

SEDIMENT LITHOLOGY

Drilling penetrated the uppermost 305 m of the sedimentary sequence at Site 641. The sedimentary section sampled (Table 2) can be divided into two parts, corresponding to Holes 641A and 641C, separated by an unsampled interval of approximately 90 m. The sequence sampled in Hole 641A consists of brown clay (lithologic Unit I), presumed to be Late Cretaceous or Paleogene, overlying a sequence of early Late Cretaceous claystone and marlstone (lithologic Units II and III). Lithologic Subunit IIIB is characterized by abundant black, organic-rich claystone. Lithologic Unit IV consists of greenish gray marlstone with characteristic interbeds of limestone conglomerate and calcarenite. Lithologic Units V and VI consist of rhythmically alternating intervals of thin-bedded calcareous claystone and marlstone, bioturbated and faintly laminated marlstone, and bioturbated, massive clayey limestone. Lithologic Unit VI is distinguished from Unit V by being richer in carbonate. The bottom of Unit VI was not drilled.

Lithologic Unit I: Brown Clay, Marl, and Calcareous Ooze (0–53.6 m; Core 103-641A-1X through Sample 103-641A-6X-7, 27 cm)

Subunit IA: 0–15.7 m; Cores 103-641A-1X and 103-641A-2X

Subunit IA consists of slumped brown clay, marl, and calcareous ooze. The uppermost 62 cm of Core 103-641A-1X consists of light yellowish brown and gray clayey nannofossil ooze. Below this, in the rest of Core 103-641A-1X and the upper part of Core 103-641A-2X, grayish brown and more reddish brown clay are interbedded on a scale of 10–20 cm. Boundaries between the two types of clay are gradational. The gray-brown clay is diffusely banded with 0.5–2.0-cm bands of darker gray-brown clay, possibly richer in iron-manganese oxides and/or organic matter, and the whole sequence is mottled with tiny black blebs of black manganese oxide. Both brown and reddish brown clays show irregular light yellowish brown bands as thick as 1.0 cm. The upper part of the clay is slightly calcareous, but the brown clay seems to be devoid of calcareous fossils. Smear slide studies suggest that the clay particles in the brown clays have not been extensively recrystallized.

The middle part of Core 103-641A-2X consists of a chaotic mixture of brown, bluish gray, and black clay, nannofossil marl and calcareous clay, and white nannofossil ooze. Individual clasts are as much as several centimeters across and appear to have been mixed by drilling and/or to have been part of a slump.

The lower part of Core 103-641A-2X consists of bedded, though highly disturbed, homogeneous olive-gray calcareous clay, light-gray mottled nannofossil marl, and brown clay. The lower boundary of Subunit IA falls between Cores 103-641A-2X and 103-641A-3X.

Because of the variety of lithologies, the chaotic nature of the cores, and the mixture of ages revealed by the calcareous sediments (see "Biostratigraphy" section, this chapter), Subunit IA is interpreted as being a slumped unit.

Subunit IB: 15.7–53.6 m; Core 103-641A-3X through Sample 103-641A-6X-7, 27 cm

Subunit IB consists almost entirely of uniform, structureless brown and dark grayish brown clay. The brown and the dark-brown clay alternate on a scale of 10–30 cm and are banded on a scale of 0.5–5.0 cm. Dark grayish brown spots of manganese-oxide-rich clay as much as 2 cm across are seen in the upper part of the subunit. The clay becomes redder and brighter colored downward. Apart from a slight suggestion of mottling, no internal structures or lamination are evident. Subunit IB is devoid of carbonate, and smear slides suggest that the clays are extensively recrystallized (cf. Subunit IA). Fine silt-sized detrital quartz is conspicuous in amounts as great as 10% in smear slides taken from the lower part of Subunit IB (Cores 103-641A-5X and 103-641A-6X).

The lowermost 10 cm of Subunit IB consists of greenish gray clay, which darkens downward. Under the microscope, this clay appears identical to the brown clay above. The color is attributed to the effect of the immediately underlying, highly reduced black clay of Unit II. The boundary between Subunit IB and Unit II is sharp and has no indication of erosion or hiatus.

Subunit IB is interpreted as being a pelagic clay, accumulating slowly in an oxygenated environment below the carbonate compensation depth (CCD). The sequence possibly contains significant accumulation hiatuses.

Table 2. Lithologic units sampled at Site 641.

Lithologic unit/subunit	Lithology	Cores	Sub-bottom depth (m)
IA	Slumped brown clay, marl, and calcareous ooze	103-641A-1X-1, 0 cm, to 103-641A-2X, CC	0–15.7
IB	Brown and gray clay	103-641A-3X-1, 0 cm, to 103-641A-6X-7, 27 cm	15.7–[a]53.6
II	Black zeolitic clay	103-641A-6X-7, 27 cm, to 103-641A-6X, CC, 20 cm	[a]53.6–[a]53.9
IIIA	Greenish gray calcareous clay and marl	103-641A-6X, CC, 20 cm, to 103-641A-7X, CC	[a]53.9–>63.6
Unsampled interval			
IIIB	Greenish gray and black homogeneous and laminated claystone	103-641C-1R-1, 0 cm, to 103-641C-6R-3, 58 cm	<150.9–202.6
IV	Greenish gray marlstone and limestone conglomerate	103-641C-6R-3, 58 cm, to 103-641C-7R, CC	202.6–218.4
V	Greenish gray microturbidites and marlstone	103-641C-8R-1, 0 cm, to 103-641C-11R-3, 26 cm	218.4–250.6
VI	Gray marlstone, microturbidites, debris flows, and limestone sand turbidites	103-641C-11R-3, 26 cm, to 103-641C-16R, CC	250.6–305.2

[a] These depths were derived by subtraction from the depth of the bottom of the cored interval because the total recovery slightly exceeded interval cored.

Lithologic Unit II: Black Zeolitic Clay (53.6–53.9 m; Samples 103-641A-6X-7, 27 cm, to 103-641A-6X, CC, 20 cm)

Lithologic Unit II consists of a uniform, structureless, dark-black zeolitic clay. The upper and lower boundaries of lithologic Unit II are sharp and have no evidence of erosion or hiatus in accumulation (Figs. 4 and 5). The clay is devoid of carbonate. Smear slides show that, in addition to recrystallized clay, the sediment contains as much as 10% zeolite mineral, tentatively identified as clinoptilolite, 10% organic matter, and a lesser amount of detrital quartz.

Although only 25 cm thick, the unique lithology of this clay layer merits its status as a lithologic unit. It clearly accumulated in a special environment favorable to the preservation of organic material.

Lithologic Unit III: Greenish Gray and Black Claystone, Calcareous Clay, and Marl (53.9–202.6 m; Sample 103-641A-6X, CC, 20 cm, to Sample 103-641C-6R-3, 58 cm)

Subunit IIIA: 53.9–>63.6 m; Sample 103-641A-6X, CC, 20 cm, through Core 103-641A-7X).

Subunit IIIA is composed of greenish gray and gray nannofossil marl and calcareous clay, badly disturbed by drilling. There is some suggestion of mottling and lamination, but otherwise internal structure is not evident. Smear slides show that the sediment consists principally of clay and nannofossils, with small amounts of detrital quartz and foraminifers and trace amounts of zeolite minerals. The carbonate content of the sediment ranges from 20% to 50%. Smear slides show that the sediments are calcareous, even immediately beneath the black clay of lithologic Unit II. The sharp boundary at the top of Subunit IIIA indicates that the depositional environment changed abruptly after the accumulation of Subunit IIIA.

Hole 641A was terminated before the lower boundary of Subunit IIIA was reached, so the thickness of the unit and its relationship to the underlying sediments could not be determined from actual samples. The logging results may give an indication of its thickness.

Subunit IIIA is interpreted as being a pelagic sediment accumulated in moderate water depths, i.e., above the CCD.

Subunit IIIB: <150.9–202.6 m; Sample 103-641C-1R-1, 0 cm, to Sample 103-641C-6R-3, 58 cm)

Subunit IIIB consists of lithologic alternations on the scale of 10–80 cm of (1) massive black claystone, (2) black claystone laminated on a scale of 1–10 mm, (3) black and dark greenish gray claystone interbedded on a scale of 1–15 mm, (4) greenish gray claystone, lightly bioturbated and faintly laminated, and (5) grayish green massive claystone. Lamination in lithology 3 is irregular and discontinuous, probably owing to weak bioturbation. The proportion of green and black claystone varies in lithology 3, and most commonly the black claystone forms the lamination. Lithologies 1, 2, and 3 predominate, and lithologies 4 and 5 are more common at the top of the subunit. Greenish gray marlstone is present in the uppermost part of the subunit (Sections 103-641C-1R-1 to 103-641C-1R-5), and the marlstone resembles that of Subunit IIIA. Minor lithologies in Subunit IIIB include very fine-grained sandstone and siltstone laminae and siderite micronodules and laminae.

The carbonate content of the claystone is less than 11% and generally less than 4% (see "Inorganic Geochemistry" section, this chapter). No differences between the black and greenish claystone are observed in smear slides. The claystone is composed primarily of clay minerals and trace amounts of zeolites, pyrit-

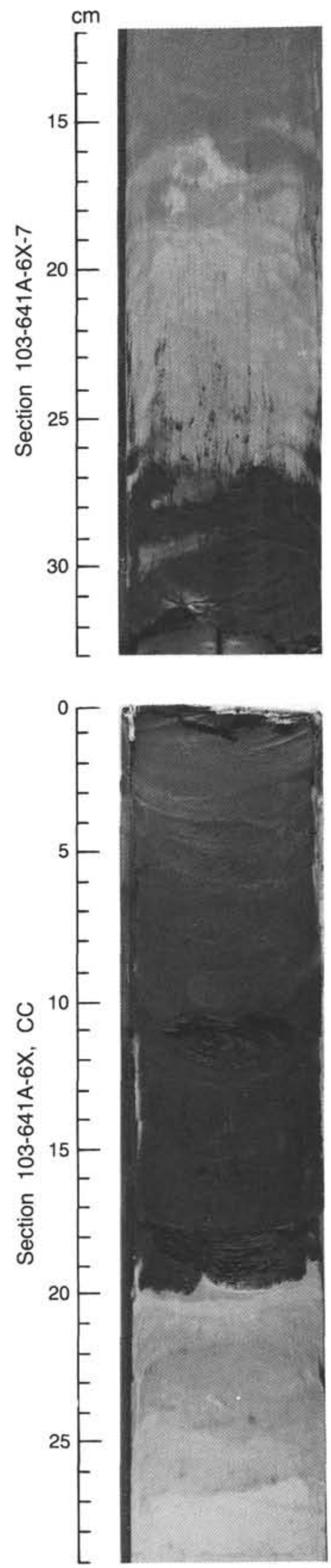

Figure 4. Black zeolitic clay of Unit II (Sample 103-641A-6X-7, 27 cm, through 103-641A-6X, CC, 20 cm), in contact with overlying gray and brown clay of Unit I and underlying greenish gray marl of Subunit IIIA.

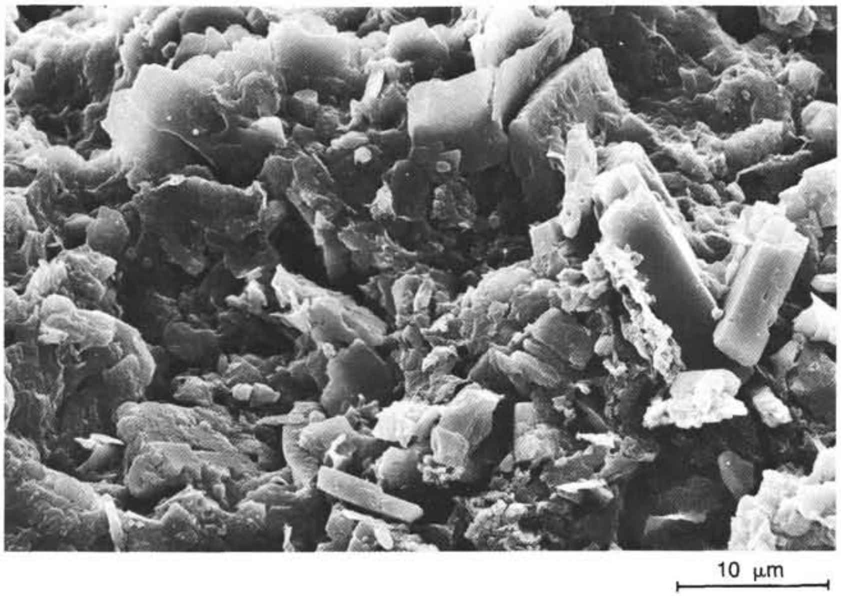

Figure 5. SEM photograph of the black zeolitic clay of lithologic Unit II (Sample 103-641A-6X, CC, 0-3 cm). The sediment is composed almost exclusively of zeolites (altered radiolarians) and clay minerals.

ized radiolarians, fish debris, and heavy minerals (zircon and rutile). Oxidized organic matter primarily of terrestrial origin constitutes 1%-2% of the claystone. Pyritized sponge spicules and Gorgonian spicules were found in a single patch of pyrite.

Planolites, Chondrites, and large, unidentified 3 × 20 mm burrows occur. Burrows are black and thus are most apparent in the greenish claystone. The black color may be due to downward reworking of overlying black claystone, but more likely it is due to diagenesis in a chemical microenvironment within the burrow itself.

A 208-cm-thick debris flow containing clasts of marlstone and claystone occurs in Sections 103-641C-1R-3 to 103-641C-1R-4. Maximum clast size is 7 cm. The claystone clasts consist of clay with variable amounts of nannofossils, rare foraminifers, zeolites, dolomite rhombs, pyrite, and organic debris. Marlstone clasts contain the same constituents but are richer in nannofossils. At the base of the debris flow, sand-sized quartz grains, dolomite rhombs, and fragments of *Inoceramus* are mixed with the claystone clasts.

Lithologic Unit IV: Greenish Gray Marlstone and Limestone Conglomerate (202.6-218.4 m; Sample 103-641C-6R-3, 58 cm, to Sample 103-641C-7R, CC)

Lithologic Unit IV consists of light greenish gray, light brownish gray, and light-gray marlstone and calcareous claystone with several interbeds of carbonate-granule conglomerate and coarse-grained calcarenite as thick as 20 cm. The coarse beds have sharp bases and gradational tops, and the upper part of each bed is normally graded and laminated. The beds were probably deposited as turbidites. Overall, lithologic Unit IV is greener and more calcareous than lithologic Unit III, and it contains coarse-grained beds, which are not present in lithologic Unit III. The contact between the two units is placed at the top of the uppermost carbonate-granule conglomerate bed (Fig. 6).

The calcarenite, or carbonate sandstone, is friable and cemented by only a thin isopachous rim of microspar calcite. Thin sections show that the carbonate grains are highly micritized. Nonetheless, skeletal debris of echinoderms, mollusks, orbitolinids, and rudists were identified. Trace amounts of quartz, sandstone rock fragments, and glauconite are also present. Inter- and intragrain porosity is as great as 30%.

The light greenish gray marlstone is slightly bioturbated. The dark greenish gray calcareous claystone is moderately laminated, and 1-3-mm-thick laminae of silt-sized material occur locally. Several thin slumps, less than 50 cm thick, are present in lithologic Unit IV. Bedding dips average about 10° throughout the unit.

Lithologic Unit V: Greenish Gray Calcareous Microturbidites and Marlstone (218.4-250.6 m; Sample 103-641C-8R-1, 0 cm, to Sample 103-641C-11R-3, 26 cm)

Lithologic Unit V consists of lithologic alternations on the scale of 10-50 cm of (1) massive black claystone, (2) laminated black claystone, (3) black and greenish gray claystone interbedded on a scale of 10-15 mm having irregular and discontinuous lamination and slight to moderate bioturbation, (4) greenish gray and grayish green claystone with weak bioturbation and rare to absent lamination, (5) dark-olive-gray laminated marlstone occurring as thin beds (microturbidites), (6) greenish gray and gray lightly to moderately bioturbated marlstone having diffuse banding on a scale of 0.3-2.0 cm, reflecting variations in the clay percentage, and (7) light greenish gray and light-gray clayey limestone that is slightly to moderately bioturbated and massive. Bioturbation is characteristically much more abundant in the greenish rocks than in the black claystone. Lithologies 1-4 are similar to the rocks in Subunit IIIB. Lithologies 2 and 3 dominate Cores 103-641C-8R and 103-641C-9R, and lithologies 5 and 6 dominate the rest of Unit V. Lithology 1 is present only in the upper part of Unit V, whereas lithology 7 is present only in the lowermost part. Contacts between the various lithologies are gradational over 1-3 cm. Bedding dips 13°.

The contact between lithologic Units IV and V is placed between Cores 103-641C-7R and 103-641C-8R, on the basis of a striking color change from mainly grayish and light brownish claystone in Core 103-641C-7R and alternating greenish gray, dark gray, and black in Core 103-641C-8R. Overall, lithologic Unit V becomes more calcareous in its lower part, and the abundance of black carbonaceous claystone decreases dramatically. The contact between lithologic Unit V and VI is entirely gradational and is placed at the top of the uppermost thick (> 10 cm) clayey limestone of lithology 7. Below this, marlstone and clay-

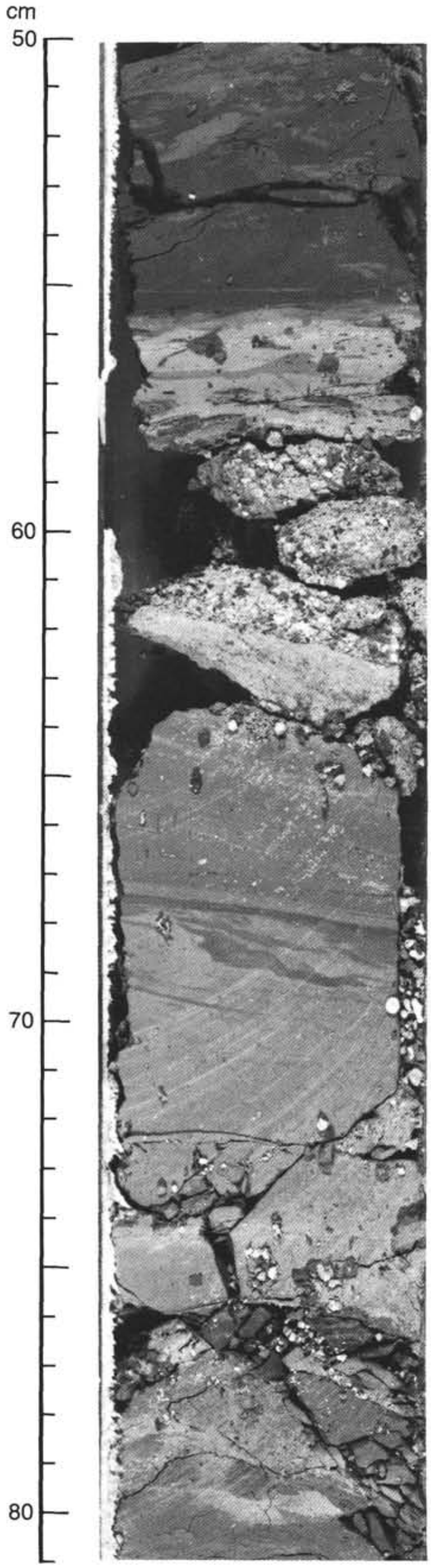

Figure 6. Sample 103-641C-6R-3, 50–81 cm. Contact between lithologic Subunit IIIB and lithologic Unit IV is placed at the top of the uppermost carbonate granule conglomerate at Sample 103-641C-6R-3, 58 cm.

ey limestone compose more than 50% of the recovered material, whereas above, they compose less than 50%.

The slightly calcareous microturbidites (lithology 5) are characteristically 5–30 mm thick and have sharp bases and tops. The lower part of the microturbidite is a laminated silty calcareous claystone slightly enriched in plant debris, which grades upward to homogeneous calcareous claystone, commonly overlain by a 0.5–1-mm-thick laminae of light-gray marlstone (Fig. 7). Normally, the lower laminated silty claystone is capped by a single quartz silt lamina.

Minor interbedded lithologies include calcarenite turbidites of a similar style and composition to those in lithologic Unit IV and debris-flow deposits composed principally of limestone and marlstone clasts. Bedding thickness in these two lithologies varies from 5–20 cm. Very fine-grained sandstone and siltstone laminae occur throughout, and pyritized radiolarians are commonly concentrated at the base of these laminae. The radiolarians also commonly have chalcedonic walls and interiors filled by zeolites. Small slumps are present in Cores 103-641C-8R and 103-641C-10R.

Five pieces of partly silicified coarse-grained skeletal packstone/grainstone are present in the core catcher of Core 103-641C-8R and in the uppermost 10 cm of Core 103-641C-9R. The rock consists of worn debris of rudists, hydrozoans, and echinoderms cemented by several generations of silica cement. The constituents are clearly derived from shallow water.

Lithologic Unit VI: Limestone and Marlstone (250.6–305.2 m; Sample 103-641C-11R-3, 26 cm, through 103-641C-16R, CC, 22 cm).

Lithologic Unit VI consists principally of (1) alternating light-gray bioturbated limestone and clayey limestone, (2) light greenish gray bioturbated marlstone, and (3) faintly laminated marlstone and calcareous microturbidites. Slumped beds and debris-flow deposits occur at several levels (Fig. 8). The lower boundary of this lithologic unit was not penetrated in Hole 641C. Lithologic Unit VI broadly corresponds to lithologic Subunit IIA at Site 638.

Light-gray and greenish limestone and clayey limestone is generally massive, only locally showing faint banding. Banding is produced by subtle changes in clay content, generally marked by a color change to more greenish shades. Bioturbation is extensive and is dominated by *Planolites* and by large 3 × 10–40 mm, unidentified burrows. Pyrite micronodules as large as 1 cm across are present as well as purplish and blue-gray staining from finely disseminated iron/manganese oxides.

Interbedded light-gray clayey limestone and greenish marlstone are moderately bioturbated. Interbedding is on the scale of 0.5–3 cm. The bedding surfaces are not sharply defined and are locally crenulated. These irregularities are attributed to bioturbation and/or syn-sedimentary downslope creep. The increase in clay content from lithology 1 to 2 is accompanied by a decrease in the intensity of bioturbation, probably related to an increase in sedimentation rate.

Dark-gray to gray, slightly greenish, laminated marlstone is bedded on a scale of 1–7 cm, averaging 2 cm. Laminated marlstone generally grades upward to structureless, gray to light-gray marlstone or calcareous claystone. Calcareous and quartz silt-sized material locally occurs at the base of the laminated marlstone layer as well as in concentrations at the boundary between laminated and massive intervals. Each layer is capped by a lamina, less than 1 mm thick, of white nannofossil micrite. Bioturbation is nearly absent; only two examples of *Chondrites* were found. Thin-section observation shows that the laminated marlstone consists dominantly of clay and nannofossil micrite, with small amounts of plant debris (5%), radiolarians (as much as 10%), quartz (as much as 3%), and trace amounts of mica. The

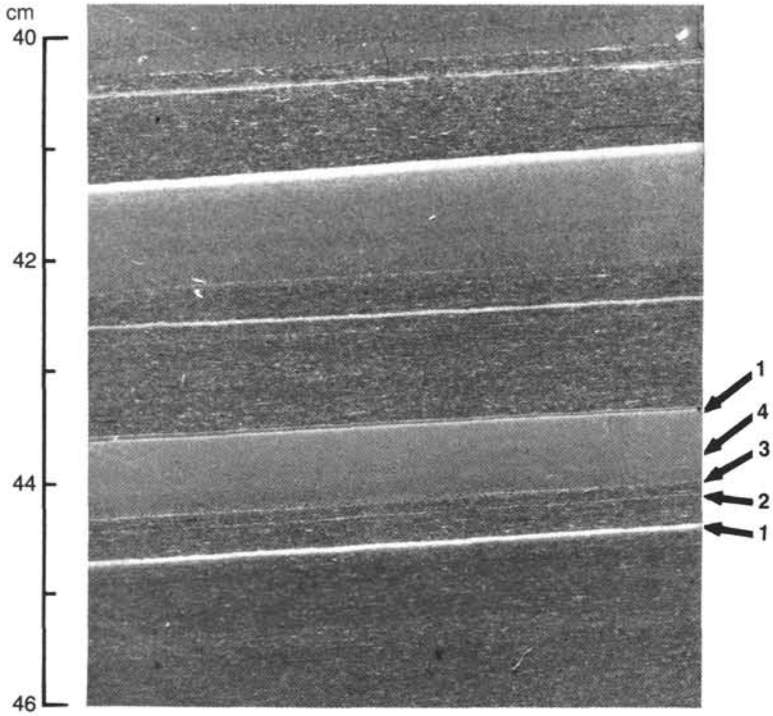

Figure 7. Sample 103-641C-11R-1, 40–46 cm. Typical microturbidites of lithologic Units V and VI. Silty calcareous clay grades upward to massive claystone, which is capped by a thin, light-colored marl lamina. 1, white marlstone lamina at top of microturbidite; 2, laminated silty claystone interval; 3, quartz silt lamina; 4, homogeneous claystone interval.

lamination is produced by the orientation of wood flakes and by the concentration of opaque minerals and radiolarians along laminae; subtle changes in the amount of clay are associated with the laminae. Syn-sedimentary deformation such as slumping and microfaulting is common.

Lithologies 1, 2, and 3 are similar to lithologies 7, 6, and 5, respectively, of lithologic Unit V. The microturbidites of lithology 3 of Unit VI are more calcareous than are the microturbidites of lithology 5 of Unit V. The contact between these lithologies is gradational over 1-3 cm. Bedding dips 13°.

Several layers, less than 1 mm thick, of grayish green, waxy-looking (smectite?) clay occur scattered throughout the succession. These thin layers contain glass shards and may be highly altered ash layers (e.g., Sample 103-641C-12-4, 136–142 cm).

Marlstone layers of lithology 3 are interpreted as being thin, distal microturbidite beds, composed of a mixture of pelagic and terrigenous material. The vaguely cyclic alternation of these three lithologies is probably related to fluctuations in the supply of clayey sediment, transported as a suspended load by very dilute turbidity currents.

Two types of coarse-grained gravity-flow deposits are interbedded in Unit VI. The first is poorly cemented medium- and coarse-grained sandstone and granule conglomerate, occurring sporadically in beds 3–40 cm thick at intervals of 2–10 m. These rocks are poorly sorted and compose light-gray, pale-tan, and pinkish limestone intraclasts, quartz (5%–7%, as much as 20%), skeletal debris (algae, bivalve shells, crinoids, corals, large benthic foraminifers, rudists, and *Inoceramus* fragments, in amounts as great as 40%), and minor amounts of mica, feldspar, plant debris, and rock fragments (proto- and metaquartzite, low-grade metamorphosed sandstones, biotitic granite, and schist). Glauconite, pyrite, opaque minerals, and chalcedony are present in trace amounts. The total terrigenous component is variable and ranges from 7%–20%. Rip-up clasts of all three major lithologies are present in the coarser fraction.

Beds are crudely graded and commonly show parallel lamination. Even though thin ripple-laminated intervals are only rarely present at the top of a sandstone bed, these are probably turbidite deposits partly fed by an active carbonate platform. The thinnest sandstone beds (5–6 cm) are fine grained, moderately well sorted, and parallel laminated throughout. The sandstone is commonly capped by a thin interval, not exceeding 1–2 cm, of white, light-olive-gray, and olive-gray massive marlstone.

The second type of coarse-grained gravity-flow deposit is matrix-supported, disorganized conglomerate and slumped beds as thick as 2 m. These beds are composed of clasts of white bioturbated limestone and light-gray and greenish marlstone, much like lithologies 1 and 2, embedded in a plastically deformed dark-gray marlstone matrix. White limestone clasts are well rounded and as much as 15 cm across. Marlstone clasts, either rounded or elongated and typically flattened and plastically deformed, are most common in Cores 103-641C-14R to 103-641C-16R. These slumps and debris flows appear to be mass wasting of pelagic material only.

BIOSTRATIGRAPHY

Holes 641A and 641C were drilled to sample the younger part of the post- and syn-rift series not sampled at Site 638. Foraminifers, nannofossils, and radiolarians were examined from core catcher and specific intervals allowing recognition of middle to Late Cretaceous sediments.

A rare to common, moderately well-preserved planktonic and benthic foraminiferal fauna and an abundant, moderately to well-preserved (preservation and abundance depending upon lithology) nannofossil flora occurs in Hole 641A. The brown pelagic clay of lithologic Unit I (see "Sediment Lithology" section, this

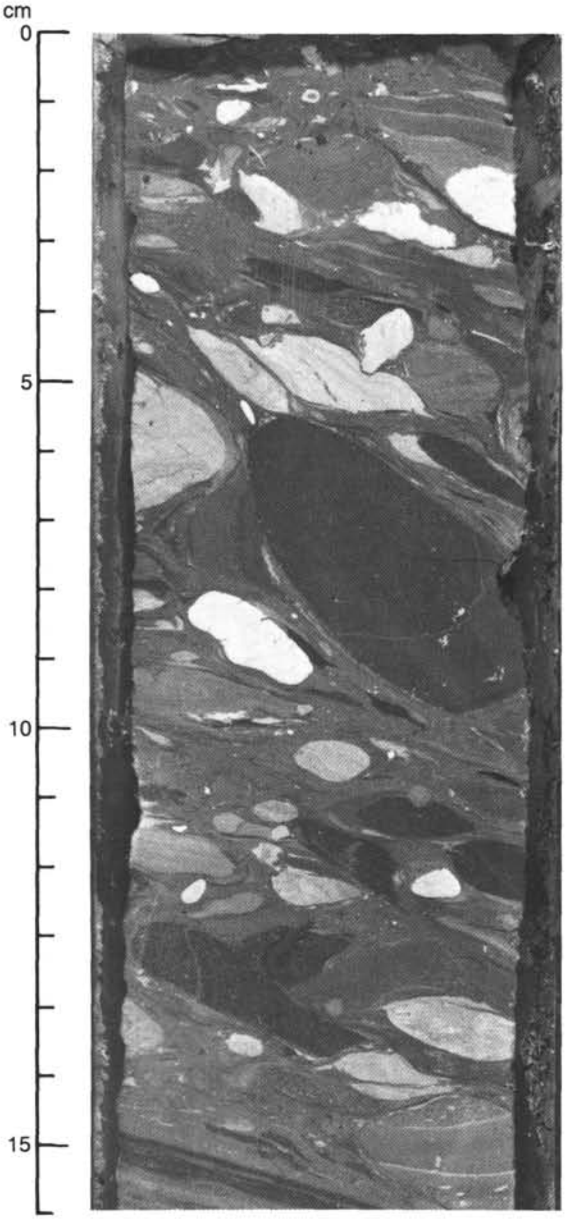

Figure 8. Sample 103-641C-15R-3, 0–17 cm. Typical debris-flow deposit in lithologic Unit VI.

chapter) in Sections 103-641A-1X-1 to 103-641A-6X-7 along with associated layers of gray clay do not contain nannofossils. Foraminifers, however, indicate a Santonian to Maestrichtian age, consisting entirely of agglutinated forms. Lower Pleistocene sediments of varied nannofossil content occur in the top 60 cm of Cores 103-641A-1X and are interbedded and intermixed with brown clay in Sections 103-641A-2X-2 to 103-641A-2X-6. Isolated clasts of upper Miocene to lower Pliocene nannofossil ooze, stringers of upper Campanian to lower Maestrichtian nannofossil marl, and a layer of uppermost Maestrichtian ooze are also present in the first two cores. Foraminifers from Sample 103-641A-2X, CC, similarly indicate an early Pleistocene age and are the result of contamination or slumping. Cores 103-641A-3X and 103-641A-4X are barren of nannofossils (in brown clay) but contain Santonian to Maestrichtian agglutinated foraminiferal assemblages.

A distinct layer of black clay (lithologic Unit II) in the bottom of Section 103-641A-6X-7 and in the top of Sample 103-641A-6X, CC, is barren of nannofossils. Planktonic foraminifers from just below the black layer indicate an early Cenomanian age. Similarly, nannofossils from below the black layer denote an early to middle Cenomanian age. Gray and greenish gray clay of Core 103-641A-7X is dated as latest Albian–earliest Cenomanian by the presence of nannofossils and as latest Albian by that of foraminifers. Hole 641A is devoid of radiolarians.

Rare to common and poorly to well-preserved foraminifers occur throughout Hole 641C. Agglutinated foraminifers are the main components of Cores 103-641C-1R to 103-641C-5R, whereas Cores 103-641C-6R to 103-641C-16R contain predominantly calcareous forms. Black clays of Subunit IIIB contain rare, poorly preserved Lower Cretaceous agglutinated benthics of early-middle Albian age. In Section 103-641C-6R-3 the foraminifers are indicative of the basal Albian (subzone C19a). The boundary between Subunit IIIB and Unit IV lies within this subzone. Samples from 103-641C-6R-3, 138–140 cm, to 103-641C-6R, CC, contain planktonics indicating an uppermost late Aptian age. Cores 103-641C-9R to 103-641C-12R contain a predominantly early Aptian foraminiferal fauna. A change to a middle to late Barremian-type fauna occurs in Sample 103-641C-15R, CC.

Late Barremian to middle Albian nannofossil assemblages occur in Hole 641C. The black claystone of lithologic Unit IIIB is mostly barren but sometimes contains a monospecific assemblage of the solution-resistant species *Watznaureria barnesae*. The coloring of the green claystone within this lithologic unit is directly related to nannofossil content. The nannofossils occur only in the lighter colored claystones of Core 103-641C-1R through Section 103-641C-2R-1 and in Sections 103-641C-3R-2 and 103-641C-3R-3. Nannofossils are common and moderately well preserved in the greenish gray marlstone of lithologic Unit IV of Sections 103-641C-6R-3 to 103-641C-7R, CC. Dark-green claystone present in the upper part of Unit V in Cores 103-641C-8R and 103-641C-9R does not contain nannofossils. Nannofossils do occur, however, in the gray marlstone of Unit V and in both the gray marlstone and limestone of Unit VI. Preservation is generally poorer in limestone than in the gray marlstone.

Moderately well-preserved radiolarians dominated by Albian types occur in Hole 641C. Samples from Cores 103-641C-3R to 103-641C-8R contain common but very poorly preserved Albian-type assemblages. The rest of the hole to Core 103-641C-15R contains a poorly preserved and as yet unidentifiable fauna.

Foraminifers

Hole 641A

Sample 103-641A-1X, CC, from the brown clay, marl, and calcareous ooze of lithologic Subunit IA (see "Sediment Lithology" section, this chapter) contains a completely agglutinated, *Rhabdammina*-like foraminiferal fauna including *Labrospira inflata, Hormosina ovulum, H. ovulum crassa, Haplophragmoides* sp., *Glomospira corona, Gaudryina pyramidata*, and *Bathysiphon* sp. This fauna is generally indicative of a Santonian to Maestrichtian age. Below this, slumping and/or contamination result in a Quaternary age for Sample 103-641A-2X, CC. Samples 103-641A-3X, CC, and 103-641A-4X, CC, of the brown and gray clays (Subunit IB) contain a fauna similar to the *Rhabdammina*-type assemblage. In addition, *Pseudobolivina cuneata, Uvigerammina jankoi*, and *Haplophragmoides* cf. *linki* are found, indicating a Coniacian to Maestrichtian age. Sample 103-641A-5X, CC, contains only a rare and poorly preserved agglutinated fauna having no particularly age-diagnostic forms.

A 30-m-thick, black zeolitic clay of Unit II occurs between Samples 103-641A-6X-7, 27 cm, and 103-641A-6X, CC, 20 cm. Planktonic foraminifers recovered from Sample 103-641A-6X, CC, just below this black layer, include *Hedbergella delrioensis, H. planispira, Globigerinelloides caseyi*, and *Schackoina cenomana* and indicate sediments of late Vraconian (late Albian) to

Cenomanian age. Sample 103-641A-7X-1, 77–79 cm, contains *H. delrioensis, S. cenomana, H. almadenensis, G. caseyi, H. planispira*, and *Rotalipora appenninica* together with the benthic foraminifers *Osangularia* cf. *utaturensis, O. californica*, and *Gyroidinoides crassa*. The former two samples are thought to indicate early Cenomanian age, latest Albian being represented in Sample 103-641A-7X-6, 19–21 cm, and below. This age determination is based on the common occurrence in Sample 103-641A-7X-3, 19–21 cm, of *Rotalipora brotzeni-greenhornensis* together with *R.* cf. *reicheli, Praeglobotruncana delrioensis, P. stephani*, and *R. appenninica*. Similar faunas but lacking the Cenomanian markers (*R. brotzeni*) are present in Samples 103-641A-7X-6, 19–21 cm, and 103-641A-7X, CC; additional taxa observed include *Dorothia oxycona, Tritaxia pyramidata, Pleurostomella obtusa, Gyroidinoides lenticula, G. crassa*, and *Gavelinella* cf. *complanata*.

Hole 641C

Rare to common and poorly to well-preserved foraminifers occur throughout Hole 641C. Cores 103-641C-1R to 103-641C-5R contain rare and dominantly agglutinated assemblages, whereas Cores 103-641C-6R to 103-641C-16R contain a significant, sometimes dominant proportion of calcareous specimens, with highly diversified but often partly dissolved planktonic forms at a few levels. The vertical distribution of selected planktonic and calcareous benthic foraminiferal species is shown in Figure 9.

Core-catcher samples taken from the black claystone of lithologic Subunit IIIB (see "Sediment Lithology" section, this chapter) contain rare and poorly to moderately well-preserved Lower Cretaceous agglutinated benthics, including various trochamminids (e.g., *Trochammina vocontiana, Ammodiscus cretaceus, Glomospirella gaultina, Verneuilinoides neocomiensis, Reophax* sp., and *Bathysiphon* sp.). Moreover, Sample 103-641C-1, CC, contains *Dorothia plummeri* and a calcareous benthic form, *Osangularia* sp. aff. *brotzeni* (*sensu* Moullade), which defines an early/middle Albian age.

Sample 103-641C-6R-1, 63–65 cm, contains an exclusively agglutinated assemblage, dominated by ammodiscids (*A. cretaceus* and *Glomospirella gaultina*), whereas from Section 3 of Core 103-641C-6R down to the bottom of the Hole 641C, planktonic and calcareous benthic foraminifers enable a more precise zonal assignment. Three samples (103-641C-6R-3, 53–55 cm, 103-641C-6R-3, 56–58 cm, and 103-641C-6R-3, 65–67 cm) contain *Hedbergella trocoidea, Ticinella bejaouaensis, Gavelinella flandrini, G. intermedia*, and *Osangularia* sp. aff. *brotzeni*, indicative of the C19a Subzone (basal Albian). Thus, the boundary between lithologic Units III and IV (103-641C-6R-3, 58 cm; see "Sediment Lithology" section, this chapter) is within this short basal Albian subzone. From Sample 103-641C-6R-3, 138–140 cm, down to the core catcher of Core 103-641C-6R, *H. trocoidea* and *Planomalina cheniourensis* co-occur, indicating the presence of the C17 Zone. To determine whether the uppermost late Aptian C18 Zone is represented within the 70-cm-thick interval between Sample 103-641C-6R-3, 67 cm, and Sample 103-641C-6R-3, 138 cm, would require further investigations based on a denser sampling. Samples taken from Core 103-641C-7R contain *Globigerinelloides ferreolensis, Hedbergella trocoidea*, and (in Sample 103-641C-7R-1, 124–125 cm, only) *G. algerianus*. Therefore, Section 103-641C-7R-2 and the core catcher of Core 103-641C-7R are attributed to Zone C15 (basal late Aptian), and Section 103-641C-7R-1 to Zone C16.

Age	Zone	Sample	*Ticinella bejaouaensis*	*Hedbergella trocoidea*	*Gavelinella intermedia*	*Gavelinella flandrini*	*Osangularia* sp. aff. *brotzeni*	*Hedbergella infracretacea*	*Saracenaria spinosa*	*Planomalina cheniourensis*	*Globigerinelloides ferreolensis*	*Globigerinelloides algerianus*	*Globorotalites rumanus*	*Globigerinelloides blowi*	*Hedbergella sigali*	*Hedbergella* sp. aff. *planispira*	*Globigerinelloides gottisi*	*Globorotalites aptiensis*	*Lenticulina ouachensis*	*Gavelinella barremiana*	*Clavihedbergella eocretacea*
basal Albian	C19a	103-641C-6R-3, 53–55cm	●	●	●	●															
		103-641C-6R-3, 56–58cm	●	●	●																
		103-641C-6R-3, 65–67cm	●	●		●	●														
late Aptian	C17	103-641C-6R-3, 138–140cm		●		●		●													
		103-641C-6R-4, 10–13cm		●	●	●		●													
		103-641C-6R, CC		●	●	●		●	●	●											
		103-641C-7R-1, 124–125cm		●				●	●		●	●	●								
	C15–16	103-641C-7R-2, 39–43cm		●	●	●		●			●			●							
		103-641C-7R, CC		●		●					●										
- - -		103-641C-8R, CC																			
early Aptian	C12–13	103-641C-9R, CC				●		●							●	●	●				
		103-641C-10R, CC						●							●	●					
		103-641C-11R, CC				●		●							●		●	●			
- - -		103-641C-12R, CC						●							●		●				
middle–late Barrem.		103-641C-13R, CC													●				●		
		103-641C-14R, CC													●						
	C10–11	103-641C-15R, CC						●							●					●	●

Figure 9. Vertical distribution of planktonic and selected calcareous benthic foraminiferal species, Hole 641C.

The best preservation and highest diversity of planktonic foraminifers occurs in the upper part of Core 103-641C-7R. Below and above this level, signs of dissolution are observed among planktonics, and assemblages lack a significant number of the species commonly found in various deep-water (but not affected by CCD) Tethyan areas.

Sample 103-641C-8R, CC, contains only the uppermost Aptian/lowermost Albian specimens, as *H. trocoidea* and *T. bejaouaensis*, resulting from downhole contamination. From Core 103-641C-9R to 103-641C-12R, rare and poorly preserved assemblages, chiefly composed of tiny planktonics (*Hedbergella sigali, H. infracretacea, H.* sp. aff. *planispira, Globigerinelloides gottisi*), and a few calcareous and agglutinated benthics are found. They indicate an early Aptian (C12–13 Zones) age. Cores 103-641C-13R and 103-641C-14R contain *H. sigali* and are devoid of *H.* sp. aff. *planispira*. Finally, Sample 103-641C-15R, CC, yields a more diverse foraminiferal microfauna, including *H. sigali, H. infracretacea, Clavihedbergella eocretacea, Gavelinella barremiana*, and *Lenticulina* spp., indicating a middle/late Barremian (C10–11 Zones) age.

The composition of the foraminiferal assemblages in Hole 641C suggests at least a bathyal (infrabathyal?) environment of deposition for lithologic Units IV and V, just above or near the CCD during the late Aptian (= Unit IV) (cf. Guerin, 1981). The rarity of calcareous foraminifers in Subunit IIIB might result from a shallowing of the CCD and/or increasing paleodepth or from peculiar environmental conditions (not necessarily linked to the paleodepth) that affect the deposition of black claystone. Rare and poorly preserved shallow-water foraminifers (trocholines, larger orbitolinids), which are mainly found in Cores 103-641C-6R down to 103-641C-9R, are thought to have been transported at much greater depths by strong turbidity currents (see also "Sediment Lithology" section, this chapter). Calcareous impoverished assemblages (essentially composed of tiny hedbergellids) in the lower Aptian and upper Barremian (lithologic Unit V) are not thought to represent an *in-situ* microfauna and might have also been transported and redeposited through distal turbidites.

Nannofossils

Hole 641A

The upper 37 cm of Section 103-641A-1X-1 contains common and moderately preserved nannofossil assemblages of early Pleistocene age (*Pseudoemiliania lacunosa* Zone; Gartner, 1977) in light-brown and dark-gray marl. Five centimeters of upper Miocene nannofossil ooze (*Amaurolithus primus* Subzone, CN-9b) containing abundant and moderately preserved nannofossils occurs below this. From Sample 103-641A-1X-1, 42–60 cm, light- and dark-gray layers of lower Pleistocene (*Helicosphaera selli* Zone) nannofossil ooze occur. Assemblages are better preserved within the light-gray layers. These layers also contain fewer reworked nannofossils and less clastic material.

Section 103-641A-1X-2 contains isolated stringers of nannofossil marl within barren brown clay at the following intervals: 6–7 cm, 30–35 cm, 40–44 cm, 55–58 cm, 79–92 cm, and 108-109 cm. These stringers contain common and poorly preserved nannofossils of late Campanian–early Maestrichtian age (NC-20, Roth, 1983). Only brown pelagic clay is present in Section 103-641A-1X-3 to Sample 103-641A-2X-2, 65 cm. The rest of Core 103-641A-2X is mostly a mixture of barren brown clay and lower Pleistocene nannofossil-bearing sediment similar to that in Sample 103-641A-1X-1. Within this mixed interval are a clast of lower Pliocene (*Discoaster asymmetricus* Subzone, CN-11b) nannofossil ooze in Sample 103-641A-2X-3, 119–122 cm, a clast of upper Miocene (*Amaurolithus primus*, CN-9b) nannofossil ooze in Sample 103-641A-2X-3, 130–132 cm, and a layer of uppermost Maestrichtian (*Micula prinsii* Zone) nannofossil ooze in Sample 103-641A-2X-5, 60–73 cm.

Section 103-641A-3X-1 through Section 103-641A-6X-7, 27 cm (lithologic Unit IB; see "Sediment Lithology" section, this chapter), is barren.

The black zeolitic clay of lithologic Unit II does not contain nannofossils. Two samples taken from the greenish gray clay immediately beneath the black clay (Samples 103-641A-6X, CC, 20 cm, and 103-641A-6X, CC, 22 cm) are rich in zeolites and do not contain nannofossils. Samples 103-641A-6X, CC, 24.5 cm, and 103-641A-6X, CC, 27 cm, contain common, but very poorly preserved nannofossils. *Darwinilithus pentarhethum*, described only from middle Cenomanian sediment at Site 540, is the only age-diagnostic form present in these samples. Abundant and moderately well-preserved nannofossil assemblages occur from Sample 103-641A-6X, CC, 27 cm, to the bottom of Core 103-641A-7X, CC. The occurrence of *Lithraphidites alatus, L. acutum*, and *Microstaurus chiastus* from Sample 103-641A-6X, CC, 29 cm, to the bottom of Sample 103-641A-6X, CC, indicates an early to middle Cenomanian age for this interval, which is assigned to the *Lithraphidites acutum* Zone (Manivit et al., 1977). *L. acutum* is not present in Core 103-641A-7X, an indication of a late Albian to early Cenomanian age. This core is assigned to the *Eiffellithus turriseiffeli* Zone (CC-9; Sissingh, 1977).

Hole 641C

The interval from Samples 103-641C-1R-1, 18 cm, through 103-641C-6R-3, 55 cm, is placed within the *Prediscosphaera columnata* Zone of late early to early late Albian age (CC-8; Sissingh, 1977). *Prediscosphaera columnata* is present in all assemblages from this interval, whereas *Eiffellithus turriseifelli, Corollithion signum, Tranolithus exiguus*, and *Cruciribrum anglicum*, which are present higher in the section in Hole 641A, are not. *Podorhabdus albianus*, found only in Sample 103-641C-1R-1, 52 cm, has its earliest occurrence in the middle Albian (Thierstein, 1976) and is evidence that these cores are no younger than middle Albian. *Hayesites albiensis* and *Eprolithus floralis* occur in many samples from these cores.

Samples 103-641C-6R, CC, through 103-641C-8R-4, 76 cm, contain *Eprolithus floralis* but not *Prediscosphaera columnata*. This interval is placed within the *Rhagodiscus angustus* Zone (CC-7b; Sissingh, 1977) of late Aptian to early Albian age.

Samples 103-641C-8R-4, 121 cm, through 103-641C-12R-2, 44–45 cm, contain *Rucinolithus irregularis* but not *Lithastrinus floralis* and are placed within the lower to middle Aptian *Chiastozygus litterarius* Zone (CC-7a; Sissingh, 1977). The occurrence of *Conusphaera mexicana, Micrantholithus obtusus*, and *Nannoconus steinmannii* throughout this interval denotes an age no younger than early Aptian (Perch-Nielsen, 1979). Samples 103-641C-12R-3, 103 cm, through 103-641C-16R, CC, lack the Aptian marker *Rucinolithus irregularis* and are placed within the *Micrantholithus hoschulzii* Zone (CC-6) of late Barremian age (Sissingh, 1977). *Chiastozygus litterarius*, a species having a reported lowest occurrence at the Aptian/Barremian boundary (Thierstein, 1973), is present to the bottom of Hole 641C. However, it has been reported from the Hauterivian (S. Wise and M. Covington, pers. comm., 1985), and its utility as an Aptian marker is doubtful. *Haysites radiatus* and *Chiastozygus tenuis*, which have not been reported from sediment younger than late Barremian, are also present in this interval. The nannofossil assemblages in this interval are similar to those in the upper part of the Lower Cretaceous section at Hole 638B.

Radiolarians

Hole 641A

Radiolarian preparations made for all core-catcher samples from Hole 641A and for an additional 20 samples were barren of radiolarians and other siliceous microfossils.

Hole 641C

Radiolarian preparations were made for all core-catcher samples from Hole 641C, together with an additional 65 samples from 103-641C-1R-1, 73-82 cm, to 103-641C-16R, CC, 12-15 cm. Samples 103-641C-1R, CC, and 103-641C-2R, CC, contain a moderately well-preserved radiolarian assemblage. The faunas are dominated by large, poorly preserved non-diagnostic Spumellarids, *Patellula* ssp., and *Orbiculiforma* ssp. Both genera are represented in Hole 641C by different species that have not been described but are known to characterize the Albian. *Halesium quadratum, Hexapyramis cretaceous, Alievum antiguum, Crucella messinae, Patulibracchium* ssp., and *Holocryptocanium barbui* characterize upper Albian/lower Cenomanian radiolarian assemblages of California. Furthermore, several undescribed genera/species known from Albian/lower Cenomanian in Oman do occur. However, the common surface dissolution of the silica-preserved radiolarian tests precludes precise determinations with on-board facilities. Cores 103-641C-3R to 103-641C-8R contain common, but mainly very poorly preserved radiolarian assemblages of Albian type. Again, a pronounced dissolution of the silica-preserved radiolarian tests obscures the taxa-characteristic surface patterns of the radiolarian tests.

Samples from lithologic Units V (except Core 103-641C-8R) and VI are barren or contain only a few, poorly preserved radiolarians (preserved in silica/pyrite). The occurrence of *Sethocapsa orca*, preserved in pyrite in Sample 103-641C-12R-5, 38-41 cm, indicates an early Aptian (or older) age. However, the rough preparation methods necessary to extract radiolarians from these samples may have obscured or destroyed large parts of the faunas.

PALEOMAGNETICS

Shipboard paleomagnetic sampling consisted of 38 minicores of Upper Cretaceous brown clay and greenish gray calcareous clay at Hole 641A and 122 minicores of Aptian-Barremian marlstone at Hole 641C. These discrete samples were analyzed on a cryogenic magnetometer at the University of Wyoming, as described in the paleomagnetics report of Site 638 (see Site 638 chapter, this volume). Shipboard studies consisted mainly of an orientation study of the direction of small-scale syn-sedimentary folding.

Shipboard Analysis of Orientation of Sedimentary Structures

At Hole 641C, a few blocks of Aptian-Barremian laminated marlstone were analyzed on board to obtain orientations of structures. The direction of initial magnetization (NRM) in all samples is of apparent normal polarity. This NRM direction is interpreted as being an overprint of the present-day field upon the weaker primary magnetization, an interpretation that will be tested in later shore-based paleomagnetic analysis. However, the NRM of Early Cretaceous pelagic marls typically shows this magnetic behavior (Ogg, in press). The declination of NRM, therefore, can be considered as the approximate orientation of present-day north. By comparing the relative direction of structural features in the samples to the NRM declination, the actual direction of these features at the site can be estimated.

Several cut blocks (portions of the archive half of cores) displaying uniform lamination dips were analyzed with the cryogenic magnetometer. The direction of dip relative to NRM or the assumed "north" is variable but is generally "southeast" to "east" (mean relative declination is 110°-140°). Later analysis of discrete samples taken from these cores indicated that the lamination dip direction is oriented toward the south-southeast. This is consistent with the apparent dip of reflectors in the seismic-reflection profiles across this site, although a much more eastwardly orientation was expected.

The Aptian-Barremian section contains many intervals of slumped beds and intraclast debris flows. One cut block (Sample 103-641C-16R-6, 0-10 cm) contains a limb of a small fold with a horizontal fold axis (Fig. 10). The folded sediments contain several fine-grained turbidites. Such turbidites in undistorted intervals display a uniform color grading, with a light-gray part at the top of each turbidite; this grading was used to determine the orientation of the beds in the slump. The center of the slump contains the oldest sediments. If this feature is part of a

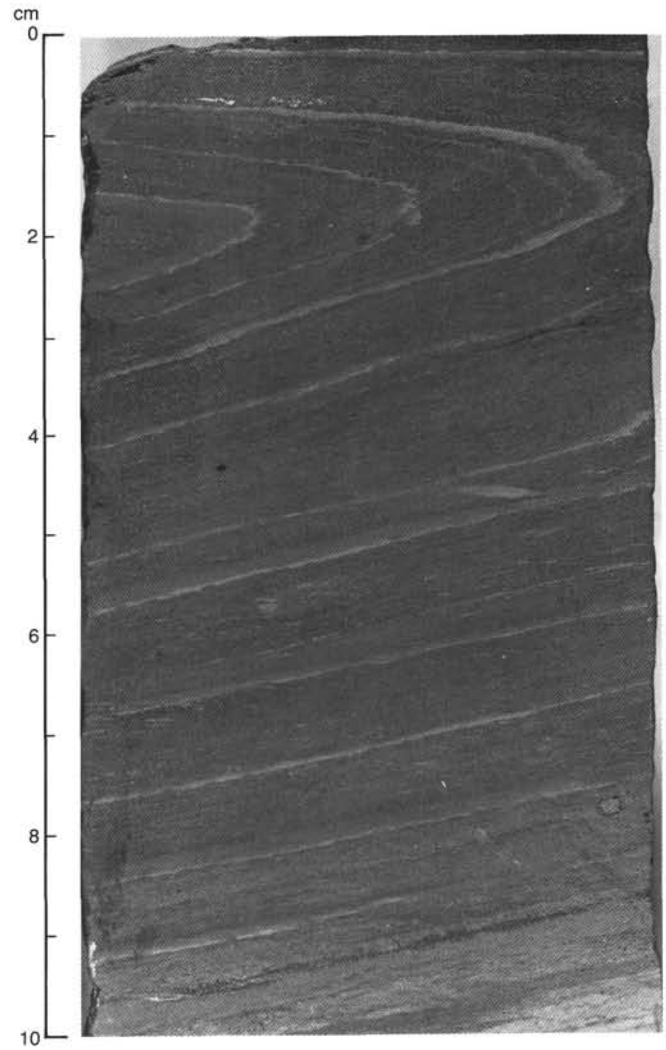

Figure 10. Slump feature in Sample 103-641C-16R-6, 0-10 cm, of Barremian age. The color grading of the thin, fine-grained turbidites in the laminated marl implies that this is an anticlinal limb of the slump. The direction of plunge is 50° clockwise with respect to a normal plane into the cut surface; the direction of NRM magnetization is 120° clockwise. Therefore, the relative declination of the plunge with respect to NRM (assumed to be dominated by the present-day normal field overprint, hence towards geographic north) is 290°, or approximately westward. If the slump represents downslope sediment creep, then the paleoslope at this site dipped westward during the Barremian.

simple slump fold formed by syn-sedimentary compression or downslope movement, then the direction of the plunge of this anticlinal limb is the direction of movement of the slump. The declination of the plunge relative to NRM of the block is 290° which is assumed to be the direction of slump transport relative to present-day north. Downslope creep probably generated the slump. If all these assumptions are true and a conclusion can be based on only one data point, then the dip direction of the paleoslope at this site was toward the west.

Rapid determinations of such structural orientations directly from the cut blocks of cores without having to collect discrete samples is one of the advantages of an on-board large-bore cryogenic magnetometer.

Brown and Gray Clay (Late Cretaceous; Cores 103-641A-1X through 103-641A-7X)

The brown clay samples have strong magnetizations; NRM intensities average about 6×10^{-5} emu/cm^3 (= 6×10^{-2} A/m). Stable characteristic directions were generally obtained above 400°C. Characteristic magnetization is probably carried by hematite. The greenish gray calcareous clay of Core 103-641A-7X has much weaker magnetization (average NRM intensity is 1×10^{-7} emu/cm^3); characteristic magnetization was displayed between 180°C and 300°C, and unstable or viscous magnetization above 350°C.

Most of Cores 103-641A-1X and 103-641A-2X are allochthonous; therefore, the apparent polarity pattern (Fig. 11) may not be a reliable indicator of the original magnetostratigraphy. Cores 103-641A-3X through 103-641A-6X are poorly dated as Maestrichtian to Coniacian or older. The mixed polarity is consistent with the late Late Cretaceous age (polarity chrons 34 through 29), but assignment of specific polarity chrons is not possible.

Gray Marlstone (Barremian–Aptian; Cores 103-641C-7R through 103-641C-16R)

An extensive suite of 122 samples was taken in the Aptian–Barremian marls (lithologic Units IV–VI; Cores 103-641C-7R to 103-641C-16R). All these samples were oriented with respect to the 10°–15° dip direction of the laminated sediments. This relative orientation enables the use of declination data in determining polarity and in computing the actual direction of dip of the laminations. The relative declination control aided in identifying reversed-polarity chron M0. This apparent dip was thought to be mainly the result of a regional post-rift structural tilt toward the east. However, the NRM declinations of normal-polarity samples imply that the apparent dip is primarily south-southeast. Details of these results will be given in a paleomagnetics paper in the Leg 103 Part B volume. A component of this apparent dip laminae in the cores may be caused by a deviation of the hole from vertical.

The intensity of NRM averages about 1×10^{-7} emu/cm^3 (= 1×10^{-4} A/m). Progressive thermal demagnetization resulted in a rapid decrease in intensity to an average of about 3×10^{-8} emu/cm^3 at 250°C. Characteristic magnetization was generally attained between 180°C and 300°C.

Polarities are all normal, except a distinct reversed-polarity interval (seven samples) in Samples 103-641C-10R-2, 72 cm, to 103-641C-10R-4, 59 cm (Fig. 12). The early Aptian age of this reversed-polarity zone implies that it is polarity chron M0, according to the magnetic polarity time scale of Ogg (in press). Hole 641C did not penetrate to polarity chron M1 or older; therefore, the oldest sediment recovered is probably late middle Barremian. The sharply delimited chron M0 may enable future precise biostratigraphic correlation of the top of the M sequence of magnetic anomalies and a determination of its exact duration, which is currently estimated as being 0.62 m.y. by Ogg and Lowrie (1986).

ORGANIC GEOCHEMISTRY

Introduction

Occurrences of dark-colored layers of Cretaceous rocks having relatively high concentrations of organic matter have been found in numerous locations studied as part of the Deep Sea Drilling Project. The distribution of such occurrences in the North Atlantic Ocean was discussed by Arthur (1979), Waples (1983), and Meyers et al. (in press), among others, attempting to identify the paleoceanographic conditions involved in the formation of these unusual strata, commonly called "black shales." Improved preservation of organic matter, increased contribution of continental organic matter to oceanic basins, and enhanced production of marine organic matter are some of the suggested conditions. Because these three possibilities affect the character of the organic content of black shales, investigations have been made of the type of organic matter in North Atlantic examples and are summarized by Summerhayes (1981) and Katz and Pheifer (1982). Varying proportions of marine and terrigenous organic constituents are found in sediments deposited at different times and locations in the Cretaceous Atlantic Ocean. Comparison of the organic matter contained within black shales to that of the adjacent organic-carbon-poor lithologies further contributes to this information (Dunham et al., in press).

Organic Carbon Analysis

Sixty-six sediment samples were taken at Site 641 for organic carbon and nitrogen determination using the Perkin Elmer elemental analyzer. Results of the organic carbon percentage on a dry-sediment weight basis and percentage of carbonate are plotted vs. depth in Figure 13. Because of technical problems, reliable determination of elemental nitrogen was not possible. Because atomic carbon-to-nitrogen ratios were unavailable, determination of the type of organic matter (marine vs. terrestrial) was based solely on Rock-Eval interpretation.

From 0 to 53.6 m sub-bottom depth, preservation of organic matter is poor, averaging 0.12%, which is below the 0.3% average for ancient deep-ocean sediments (McIver, 1975). This 53.6 m of organic-carbon-lean sediment corresponds to lithologic Unit I (see "Sediment Lithology" section, this chapter). From 53.6 to 53.9 m sub-bottom depth, a Cenomanian or younger black clay occurs (see "Sediment Lithology" and "Biostratigraphy" sections, this chapter). This black clay averages 10.6% organic carbon. Below 151.42 m sub-bottom depth, organic carbon concentrations become cyclic, exhibiting alternating organic-carbon-rich and -lean layers. Within lithologic Subunit IIIB, black claystones contain about 2.5% organic carbon, and bioturbated green claystones have about 1% organic carbon.

In lithologic Units IV, V, and VI, high organic carbon concentrations are associated with greenish gray marlstones. Microturbidites rich in detrital plant remains are also common in these lithologic units.

Rock-Eval Analysis

Thirty-seven samples from green and black claystones recovered at Site 641 were analyzed using the Rock-Eval. Results are shown in Figure 14, using a van Krevelan diagram. The organic matter at Site 641 is composed of marine (Type II) and terrigenous (Type III) kerogen. The Cenomanian black shale has an average hydrogen index (HI) of 491 and an average oxygen index (OI) of 8. These values are typically associated with marine organic matter. The Albian black and green shales have average HI and OI values of 66 and 23, respectively, which are typically associated with terrestrial organic matter. The temperature of the S2 peak maximum (T_{max}) indicates the maturation level of the organic matter (Espitalie et al., 1977). T_{max} values of the Cenomanian black shale and Albian black and green claystones

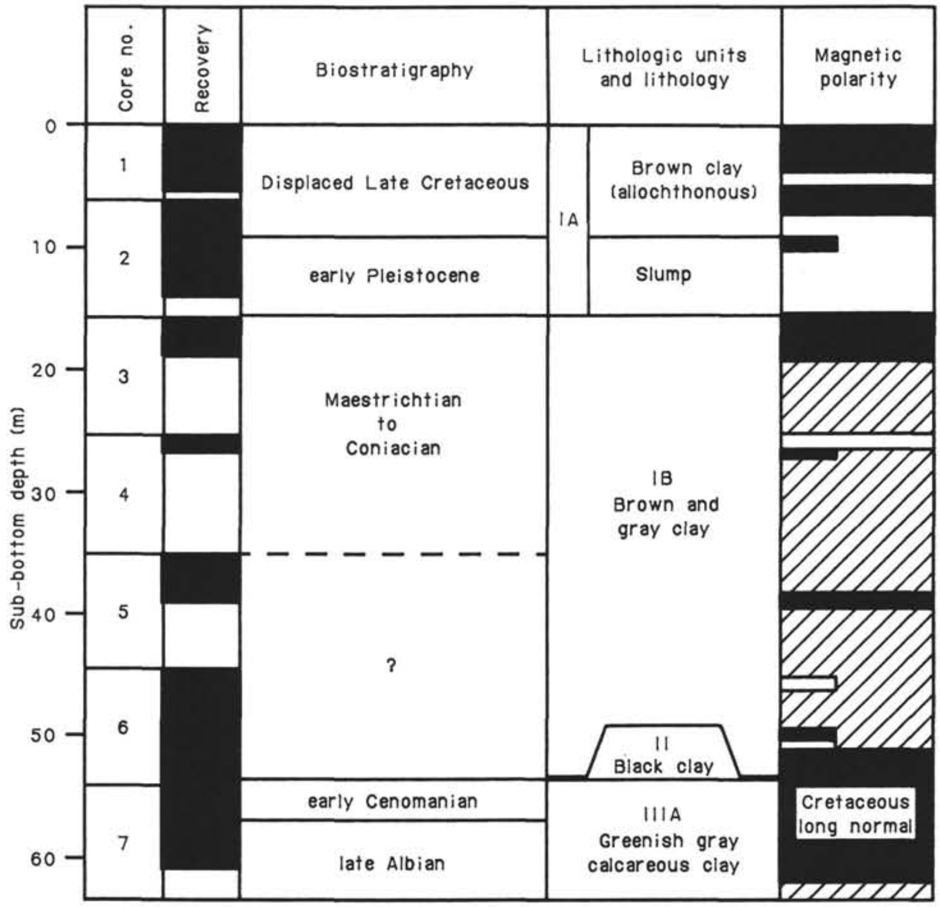

Figure 11. Magnetostratigraphy and tentative assignment of polarity chrons of Hole 641A. Black shading is normal-polarity zones; white is reversed polarity. Diagonal pattern indicates gaps in recovery or intervals of indeterminant or unreliable polarity. Half bar represents a single sample having a polarity interpretation opposite that of the adjacent samples or indicates that only one sample was available from the core. Assignment of magnetic polarity chrons is the best current guess based upon the biostratigraphy given in this site chapter and in published magnetic polarity time scales. Complete tables of the paleomagnetic data and polarity interpretations will be given in Part B of the Leg 103 volumes.

average 404°C and 420°C, respectively. These low values indicate a history of low-thermal conditions in the preserved kerogen.

Organic Carbon Isotope Analysis

Organic carbon isotope values are listed in Table 3. Isotope interpretation will be discussed in a chapter in the Leg 103 Part B volume.

INORGANIC GEOCHEMISTRY

Interstitial-Water Chemistry

Ten sediment samples were taken from rotary-drilled cores recovered at Site 641. Of these ten samples, eight samples were taken immediately from the core while on deck as whole rounds of the core, whereas the other two sediment samples were obtained from a 10-cm interval of the working half of the core immediately after the designated core section was split (Table 4). The cores from Hole 641A were drilled using an extended core barrel to obtain sediments with less drilling disturbance than in typical rotary drilled cores. Five samples were taken from the sediments cored in the upper 60 m of Hole 641A for interstitial-water analysis. The sampling strategy was to obtain one sample from each core in the upper 50 m of Hole 641A and in decreasing frequency below 50 m. In Hole 641C, samples were taken from approximately every third core, the first sample being from 169.4 m sub-bottom depth (Sample 103-641C-2R-6, 140–150 cm) because the hole was washed to 150.9 m sub-bottom depth before coring. This strategy was followed if at least 1.5 m of sediment was recovered in the designated core.

The ten sediment samples were squeezed aboard ship to obtain the interstitial water from the sediment. The water samples were analyzed for pH, alkalinity, chlorinity, salinity, calcium, and magnesium. The same analytical methods used at the previous sites on Leg 103 were employed for the samples recovered at Site 641. The primary standard used for calibration of the water analysis is IAPSO standard seawater, and surface-seawater samples retrieved by a bucket overboard were used for comparison with the interstitial-water samples from each drill hole.

The results, listed in Table 4 and graphed in Figure 15, show little variation in the values with increasing depth. Alkalinity and pH slightly decrease in Hole 641A and more rapidly decrease in Hole 641C. The highest alkalinity and pH values are from the uppermost sample from Hole 641C (Sample 103-641C-2R-6, 140–150 cm; 169.4 m sub-bottom depth), taken from the greenish gray and black homogeneous and laminated claystone of lithologic Subunit IIIB. The high organic carbon content in these interbedded "black shales" may have influenced these pH and alkalinity values.

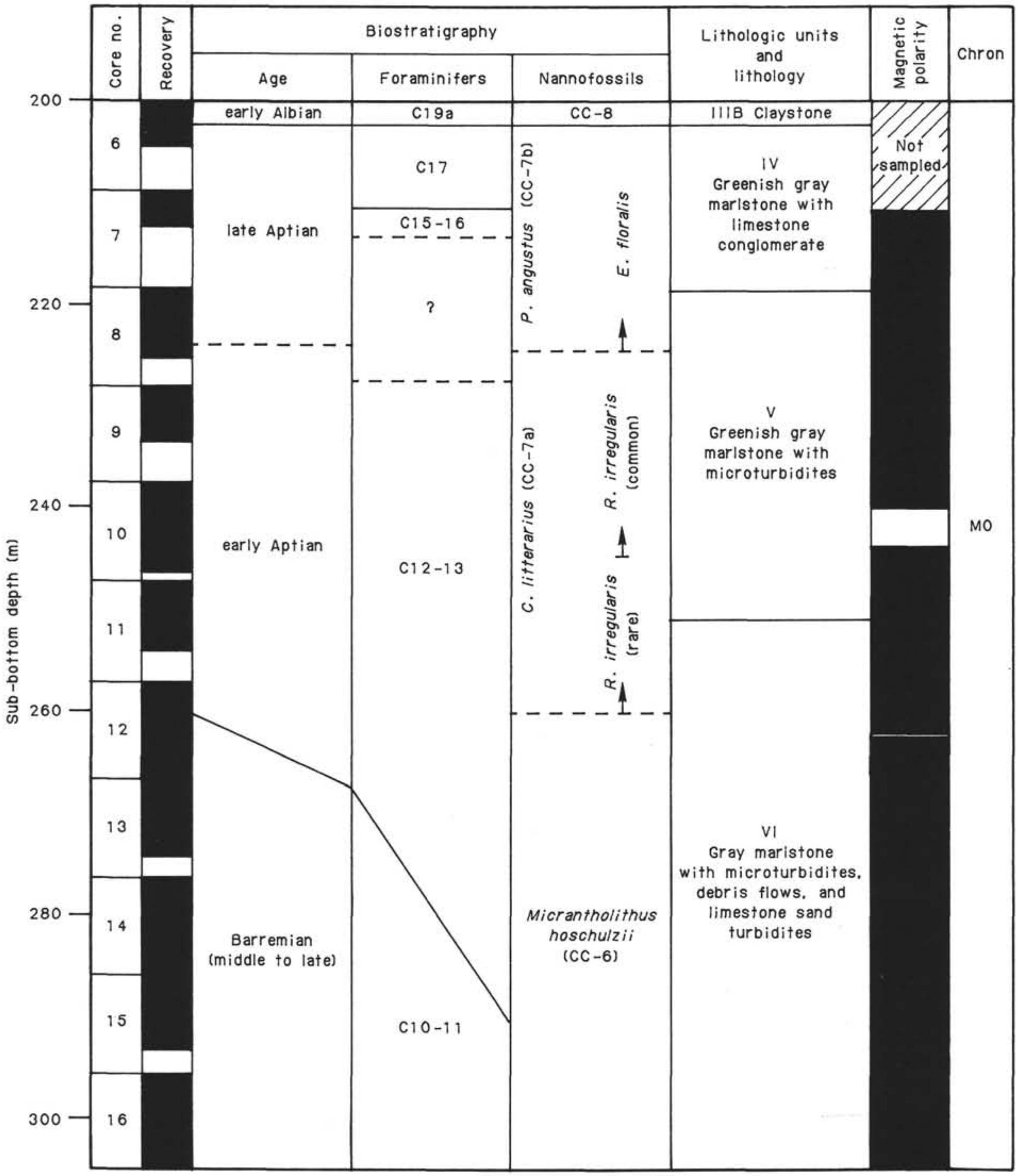

Figure 12. Magnetostratigraphy and tentative assignment of polarity chrons of Hole 641C. Black shading is normal-polarity zones; white is reversed polarity. Diagonal pattern indicates gaps in recovery or intervals of indeterminant or unreliable polarity. Half bar represents a single sample having a polarity interpretation opposite that of the adjacent samples or indicates that only one sample was available from the core. Assignment of magnetic polarity chrons is the best current guess based upon the biostratigraphy given in this site chapter and in published magnetic polarity time scales. Complete tables of the paleomagnetic data and polarity interpretations will be given in Part B of the Leg 103 volumes.

Salinity and chlorinity values show a slight decrease in Hole 641A but do not show a clear trend in Hole 641C. Calcium and magnesium values at Site 641 show weak but significant trends downhole. The calcium values generally increase and the magnesium values generally decrease with increasing sub-bottom depth (Fig. 16). A one-to-one relationship does not exist because the decrease in the magnesium concentration is not equal to the increase in the calcium concentration. The changes in the calcium values may relate to calcium carbonate dissolution and reprecipitation as calcite cements or zeolites. The decrease in magnesium downhole may result from its uptake in detrital clay minerals.

Calcium Carbonate

Approximately 100 samples were analyzed for percentage of carbonate; the results are listed in Table 5 and graphed in Figure

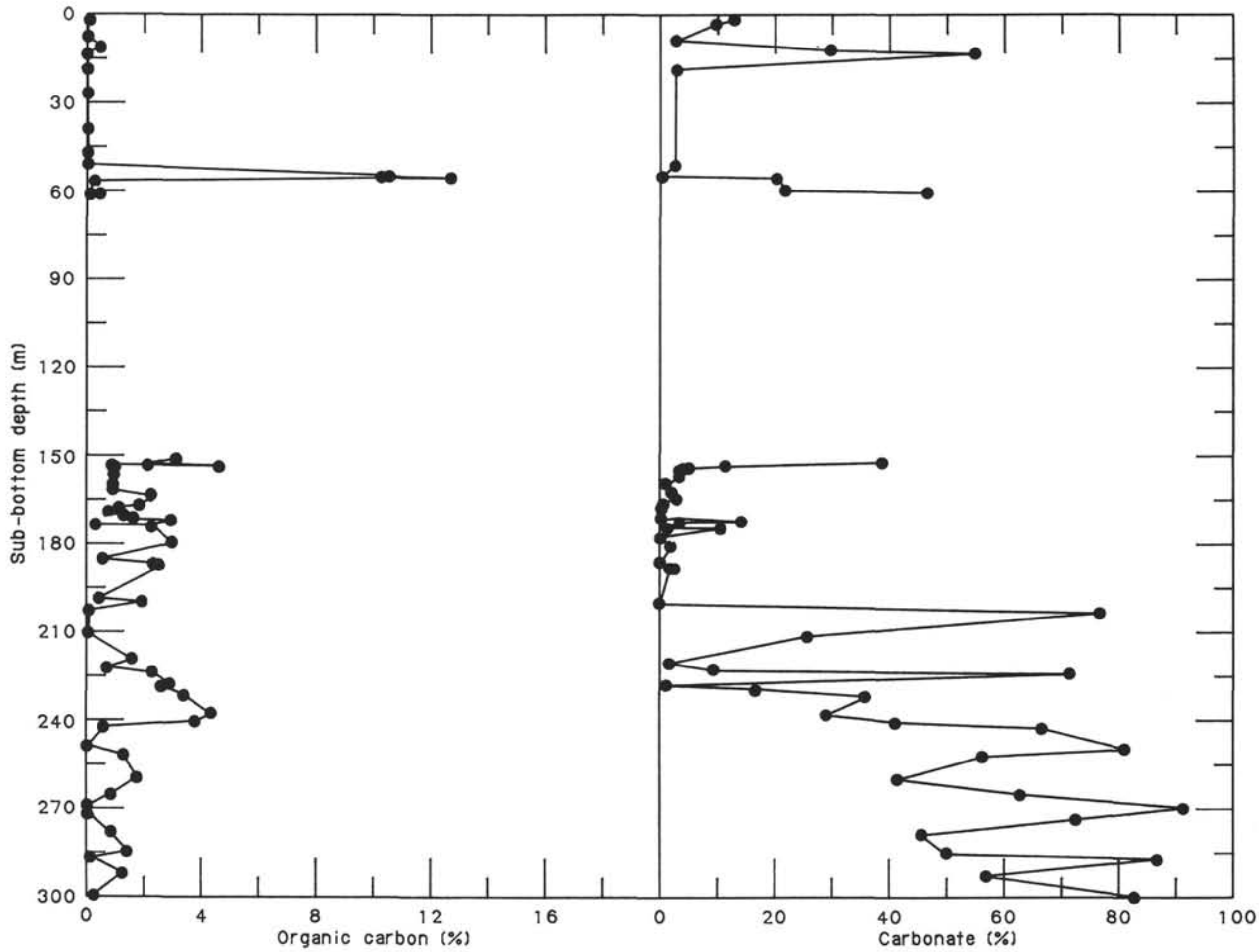

Figure 13. Organic carbon percentage and percent carbonate vs. depth, Site 641.

17. The results reflect the differences between the assigned lithologic units (see "Sediment Lithology" section, this chapter).

In lithologic Subunit IA (Samples 103-641A-1X-1, 0 cm, to 103-641A-2X, CC; 0–15.7 m sub-bottom depth), composed of slumped brown clay, marl, and calcareous ooze, the carbonate ranges from 1% to 55% of the dried-sediment weight. Lithologic Subunit IB (Core 103-641A-3X-1, 0 cm, to Sample 103-641A-6X-7, 27 cm; 15.7–53.6 m sub-bottom depth) contains brown and gray clay having carbonate contents near zero. The carbonate content remains near zero in the zeolitic clay of lithologic Unit II. The greenish gray calcareous clay and marl of Subunit IIIA has carbonate values ranging from 17% to 47% of the dried-sediment weight.

In Hole 641C, we recovered greenish gray and black homogeneous and laminated claystone (lithologic Subunit IIIB; Core 103-641C-1R-1 to Sample 103-641C-6R-3, 58 cm; 150.9–202.6 m sub-bottom depth), the carbonate content ranging from 0% to 11% of the dried-sediment weight. A minor lithology of marlstone, represented by Sample 103-641C-1R-1, 52–53 cm, having 39% carbonate in the dried sediment, was recovered in the upper strata of this subunit.

Lithologic Unit IV (Samples 103-641C-6R-3, 58 cm, to 103-641C-7R, CC; 202.6–218.4 m sub-bottom depth) is composed of marlstone and limestone conglomerate. The carbonate values range from 26% to 94% of the dried-sediment weight in three samples analyzed from Unit IV. Lithologic Unit V (Core 103-641C-8R to Sample 103-641C-11R-3, 26 cm; 218.4–250.6 m sub-bottom depth) is characterized by microturbidites and marlstone having wide-ranging carbonate values from 2% to 82% of the dried-sediment weight. In lithologic Unit VI, turbidites are also present, but the sediment types change to marlstone, debris flows, and limestone sand turbidites (Samples 103-641C-11R-3, 26 cm, to 103-641C-16R, CC; 250.6–305.2 m sub-bottom depth). The pattern of carbonate values (Fig. 17) reflects the rapid input of the carbonate-rich turbidites. The carbonate contents of the samples from lithologic Unit VI are typically higher than those of the overlying units and range from 42% to 92% of the dried-sediment weight.

PHYSICAL PROPERTIES

Physical-property measurements were made on sediments and sedimentary rocks from Site 641 according to the procedure outlined in previous site chapters, except as noted in the following text. Unsplit sediment cores were analyzed on the Gamma Ray Attenuation Porosity Evaluator (GRAPE) for bulk-density measurement and then allowed to warm to room temperature for 4 hr for thermal-conductivity measurement. After the sections were split, samples were taken for compressional seismic-velocity measurement on the Hamilton Frame velocimeter. The same samples were analyzed gravimetrically for index properties (bulk density, porosity, and water content). Bulk density of these discrete samples was also measured by 2-min GRAPE analysis. After physical-property measurements were completed, the carbonate content of the samples was analyzed using the carbonate bomb (Müller and Gastner, 1971; see "Inorganic Geochemistry" section, this chapter). Sediment at the sediment/water in-

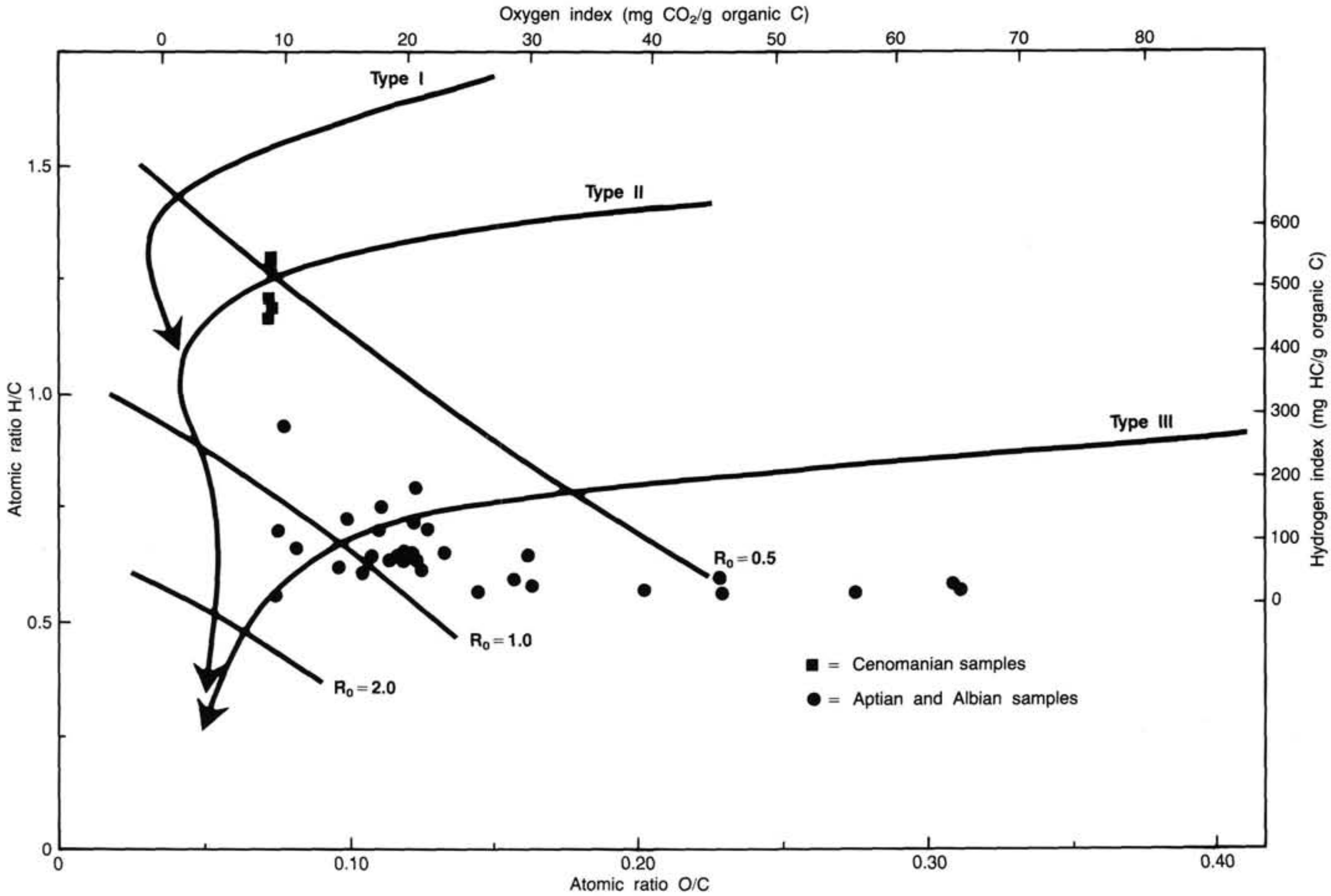

Figure 14. Rock-Eval diagram, Site 641.

Table 3. Organic carbon isotope values, Site 641. HI = hydrogen index; OI = oxygen index.

Sample (interval in cm)	Sub-bottom depth (m)	Age	Organic carbon (%)	$CaCO_3$ (%)	$\delta^{13}C$	HI	OI
103-641A-1X-2, 100-102	2.5	Pleistocene	0.05	10	−25.3	[a]na	na
103-641A-2X-5, 69-70	12.79	Maestrichtian	0.03	55	−26.2	na	na
103-641A-4X-1, 80-82	26.1	?	0.07	3	−25	na	na
103-641A-6X-7, 31	53.81	Cenomanian	10.66	0.7	−24.1	522	8
103-641A-6X, CC, 3-6	53.88	Cenomanian	10.34	0.5	−23.9	529	8
103-641A-6X, CC, 11	53.96	Cenomanian	10.55	0.4	−24.4	483	8
103-641A-6X, CC, 16	54.01	Cenomanian	10.78	0.9	−23.9	454	7
103-641A-6X, CC, 20	54.05	Cenomanian	12.78	0.9	−23.9	465	8
103-641A-7X-1, 100-103	55.1	Cenomanian	0.28	21	−27.6	na	na
103-641A-7X-5, 19-21	60.29	Cenomanian	0.49	47	−30.3	na	na
103-641C-1R-1, 51-52	151.42	Albian	3.07	39	−26	6	26
103-641C-1R-2, 13-14	152.53	Albian	2.18	11.3	−26.3	19	30
103-641C-1R-2, 61-62	153.02	Albian	4.66	5.5	−27.8	191	22
103-641C-1R-2, 95-96	153.35	Albian	0.87	4.4	−24.3	12	65
103-641C-2R-3, 148-149	164.98	Albian	2.26	1.2	−27.7	86	21
103-641C-2R-4, 3-6	165.03	Albian	4.38	1	−31.7	na	na
103-641C-2R-5, 57-60	167.07	Albian	0.15	1	−25.1	na	na
103-641C-3R-2, 4-5	171.64	Albian	1.67	14.5	−24.4	8	38
103-641C-3R-2, 6-7	171.66	Albian	2.96	3.6	−25	121	21
103-641C-3R-5, 55-56	176.65	Albian	19.74	0.6	−23.6	108	9
103-641C-4R-4, 127-129	185.57	Albian	0.55	0.6	−23.5	38	27
103-641C-6R-1, 63-66	196.03	Albian	1.38	2	−23	na	na
103-641C-8R-4, 116-119	224.06	Aptian	3.46	52	−27.3	na	na
103-641C-9R-1, 30-32	228.3	Aptian	2.97	1.6	−25.7	290	10

[a] n.a. = not available.

Table 4. Shipboard interstitial-water analyses, Site 641.

Sample (interval in cm)	Sub-bottom depth (m)	pH	Alkalinity meq/kg	Salinity ‰	Chlorinity ‰	Ca^{++} mmol/L	Mg^{++} mmol/L
103-641A-1X-2, 140-150	2.9-3.0	7.51	3.28	34.0	18.54	11.05	50.99
[a]103-641A-2X-3, 140-150	10.5-10.6	7.63	2.50	34.6	19.01	10.25	50.72
[a]103-641A-3X-1, 140-150	17.1-17.2	7.43	3.18	34.5	18.92	10.76	50.65
103-641A-5X-2, 140-150	37.8-37.9	7.42	3.40	34.0	18.40	12.71	52.63
103-641A-7X-4, 140-150	60.0-60.1	7.39	3.34	34.1	17.24	12.85	50.27
103-641C-2R-6, 140-150	169.4-169.5	7.87	5.07	33.0	18.20	15.71	47.65
103-641C-6R-2, 140-150	207.9-208.0	7.67	2.99	34.1	18.95	15.43	48.96
103-641C-8R-1, 140-150	219.8-219.9	7.47	2.46	34.8	17.72	14.69	48.24
103-641C-11R-4, 140-150	253.2-253.3	7.49	3.63	34.5	15.59	16.52	44.08
103-641C-14R-2, 140-150	279.1-279.2	7.07	2.98	34.0	19.19	16.60	43.73

[a] Sediment sample taken from working half of core immediately after section was split.

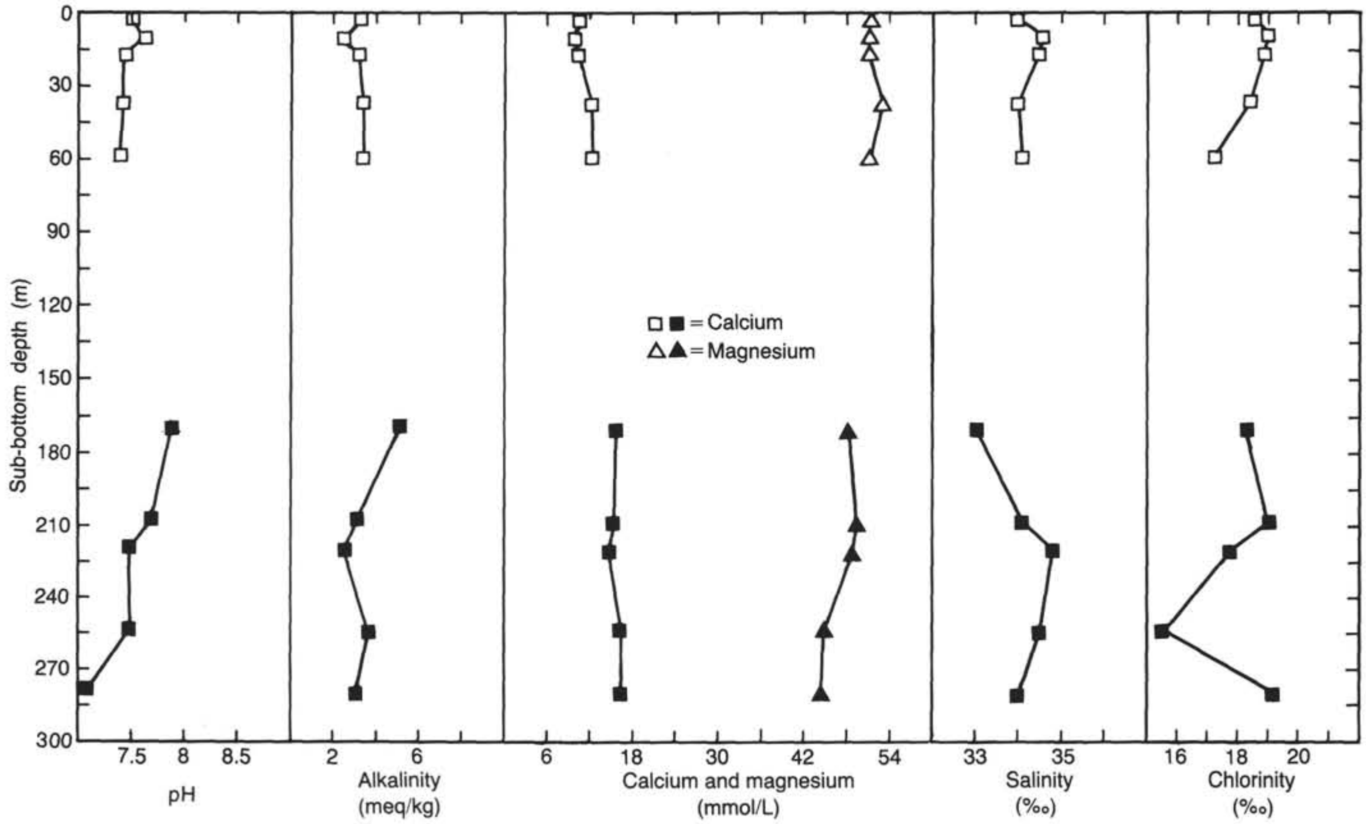

Figure 15. Summary of interstitial-water data, Site 641. Data are given in Table 4. Data from Hole 641A are plotted as open symbols, whereas data from Hole 641C are plotted as solid symbols.

terface was stiff, and vane-shear-strength measurements were not made at this site.

Thermal Conductivity

Thermal-conductivity measurements were made on sediments from Cores 103-641A-1X through 103-641A-7X (0-64 m sub-bottom depth) and Cores 103-641C-1R through 103-641C-6R (151-209 m sub-bottom); the data are plotted in Figure 18A. Below Core 103-641C-6R, sediment was too firm for needle-probe insertion. Thermal conductivity is fairly low throughout Hole 641A, ranging from 2.04 to 2.66 $\times 10^{-3}$ cal $\times °C^{-1} \times cm^{-1} \times s^{-1}$ (calories/degree Celsius-centimeter-second) without an apparent trend. Thermal-conductivity values do not appear to trend with depth at Hole 641C; values range from 2.30 to 2.61 $\times 10^{-3}$ cal $\times °C^{-1} \times cm^{-1} \times s^{-1}$, and two high values of 4.35 and 4.70 $\times 10^{-3}$ cal $\times °C^{-1} \times cm^{-1} \times s^{-1}$ occur in Samples 103-641C-3R-2, 60 cm, and 103-641C-3R-4, 102 cm, respectively.

Compressional Seismic Velocity

Seismic velocity (Fig. 18B) is remarkably uniform throughout Hole 641A (lithologic Units IA, IB, II, and IIIA; see "Sediment Lithology" section, this chapter). Measured velocity in the brown and gray clay, marl, and calcareous clay ranges from 1.44 to 1.58 km/s, averaging 1.52 km/s. No clear velocity distinction corresponding to the lithologic units appears. Velocities reported in the visual core descriptions reflect a precision of ± 0.03 km/s in the upper four cores of Hole 641A and ± 0.02 km/s throughout the rest of Holes 641A and 641C.

Lithologic Subunit IIIB in the top of Hole 641C (Samples 103-641C-1R-1, 0 cm, through 103-641C-6R-3, 58 cm; 150.9-202.6 m sub-bottom) shows a slight increase in seismic velocity

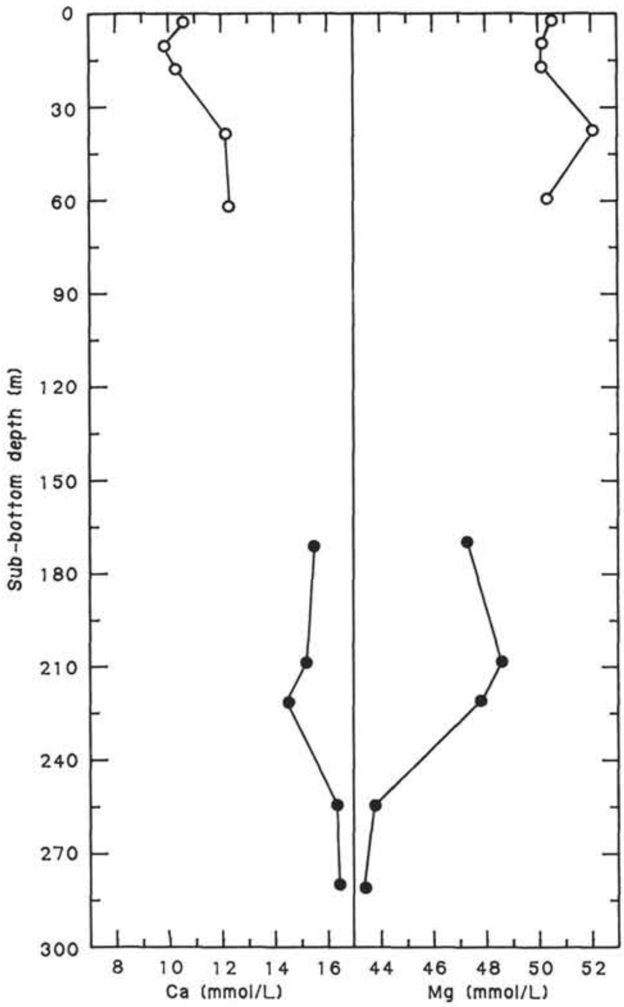

Figure 16. Calcium and magnesium cation concentrations in interstitial-water samples, Site 641. Data are given in Table 4. Data from Hole 641A are plotted as open symbols, whereas data from Hole 641C are plotted as solid symbols.

with depth, averaging about 1.83 km/s. The seismic velocity of the greenish calcareous component of Subunit IIIB is generally a few hundred meters per second greater than that of the dark mudstone of Subunit IIIB.

The green marlstone of lithologic Unit IV (Samples 103-641C-6R-3, 58 cm, through 103-641C-7R, CC; 202.6–218.4 m sub-bottom) has a seismic velocity within the range of values of lithologic Unit III, averaging 1.77 km/s. Two layers of loosely cemented, redeposited carbonate-platform sandstone in Unit IV yielded an average seismic velocity of 2.61 km/s. Recovery was only 49% and 30% in Cores 103-641C-6R and 103-641C-7R, respectively, and much of the unrecovered material may consist of loosely cemented sand, which crumbles easily and could have been disrupted during drilling. Attributing a carbonate sandstone composition to the unrecovered material would raise the average velocity of Unit IV from 1.94 km/s (calculated by assuming marl composition of unrecovered sediment) to 2.52 km/s (calculated by assuming carbonate sandstone composition of unrecovered material). The average velocity probably lies between these values, but we expect it to be nearer the high value because of generally high recovery during coring of marl sediment at Site 641. For calculating acoustic impedance, we will assign an average seismic velocity of 2.4 km/s to lithologic Unit IV.

The green and black marlstone and microturbidites of lithologic Unit V show a slight increase in seismic velocity with depth. Measured values range from about 1.75 to 2.17 km/s, averaging 1.90 km/s. A calcite-cemented sandstone layer (Sample 103-641C-9R-1, 7–9 cm) yields a seismic velocity of 4.3 km/s, and silicified redeposited coarse carbonate-platform sandstone (Sample 103-641C-8R, CC, 15–17 cm) yields a velocity of 5.74 km/s.

In lithologic Unit VI (Samples 103-641C-11R-3, 26 cm, through 103-641C-16R, CC; 250.6–305.2 m sub-bottom), bioturbated limestone and limestone-sand turbidites compose a significant proportion of the section. The marlstone of lithologic Unit VI ranges in seismic velocity from 1.85 to 2.17 km/s, lower values corresponding to darker, less calcareous samples. Average marlstone velocity is 1.95 km/s. The average of seismic velocities of bioturbated limestone is 2.65 km/s. Measured seismic velocities of two sandy limestone turbidite layers from Core 103-641C-13R average 5.0 km/s, whereas a more loosely cemented sandy layer from Core 103-641C-12R yields a seismic velocity of 2.70 km/s. Recovery in lithologic Units V and VI was good, allowing calculation of average seismic velocity through tabulation of thicknesses of the different sediment types from core photographs and shipboard visual core descriptions. The average seismic velocity of Unit VI calculated by this means is 2.08 km/s. Results of this core-by-core average are plotted against sub-bottom depth in Figure 19, which also includes the base of Unit III and Unit IV, where core velocity is calculated as described in the previous text.

Examination of Figure 18B marlstone velocities in Subunit IIIB and Units V and VI reveals a small but consistent velocity anisotropy in the layered microturbidites; seismic velocity measured in the plane of the core diameter (triangular and square data points; b- and c-directions, respectively) ranges from 30 to 180 m/s greater than that measured perpendicular to the plane of the core diameter (circular data points; a-direction). We attribute this to vertical compaction and horizontal alignment of clay minerals in the bedding plane of the turbidite layers.

Index Properties

Bulk-density and porosity values are plotted against sub-bottom depth in Figures 18C and 18D, respectively. In Hole 641A, bulk density of lithologic Subunits IA and IB ranges from 1.66 to 1.80 g/cm^3 and averages 1.75 g/cm^3. Porosity ranges from 57% to 66%. Bulk density of lithologic Subunit IIIA (Samples 103-641A-6X, CC, 20 cm, through 103-641A-7X, CC; 53.9–63.6 m sub-bottom) ranges from 1.64 to 1.71 g/cm^3, averaging 1.68 g/cm^3, and porosity averages 65%.

The range of bulk-density and porosity values measured on samples of lithologic Subunit IIIB (Samples 103-641C-1R-1, 0 cm, through 103-641C-6R-3, 58 cm; 150.9–202.6 m sub-bottom) is 1.74–1.88 g/cm^3, averaging 1.81 g/cm^3, and 54%–60%, averaging 57%. No trend with depth is apparent.

Two sandstone samples from lithologic Unit IV average a bulk density and porosity of 2.3 g/cm^3 and 44%, respectively. A single sample of marlstone from lithologic Unit IV has a bulk density of 1.92 g/cm^3 and a porosity of 55%, similar to that of the Subunit IIIB marlstone. Calculating a bulk density for Unit IV on the assumption that the unrecovered material consists of loosely cemented carbonate sandstone, yields an average bulk density of 2.07 g/cm^3.

The bulk density of microturbidites and marlstone from lithologic Unit V (Samples 103-641C-8R-1, 0 cm, through 103-641C-11R-3, 26 cm; 218.4–250.6 m sub-bottom) ranges from 1.77 to 2.08 g/cm^3, averaging 1.93 g/cm^3 and increasing slightly with depth. Porosity ranges from 33% to 62%, generally decreasing with depth.

Table 5. Carbonate-bomb data, Site 641.

Sample (interval in cm)	Sub-bottom depth (m)	Carbonate (%)	Lithology[a]
103-641A-1X-1, 100-102	1.00	13	Calcareous clay
103-641A-1X-2, 100-102	2.50	10	Clay
103-641A-2X-2, 9-10	7.69	1	Clay
103-641A-2X-2, 18-20	7.78	<3	Clay
103-641A-2X-3, 3-4	9.13	55	Marl
103-641A-2X-4, 53-55	11.13	30	Calcareous clay
103-641A-2X-4, 90-91	11.50	23	Calcareous clay
103-641A-2X-5, 45-46	12.55	29	Calcareous clay
103-641A-2X-5, 69-70	12.79	55	Marl
103-641A-3X-2, 60-62	17.80	<3	Clay
103-641A-4X-1, 35-37	25.65	<3	Clay
103-641A-4X-1, 80-82	26.10	<3	Clay
103-641A-5X-2, 100-102	37.40	<3	Clay
103-641A-6X-1, 71-73	45.21	<3	Clay
103-641A-6X-1, 100-102	45.50	<3	Clay
103-641A-6X-4, 100-102	50.00	<3	Clay
103-641A-6X-6, 100-102	53.00	<3	Clay
103-641A-6X-7, 31	53.81	<1	Clay
103-641A-6X-CC, 5	53.90	<1	Clay
103-641A-6X-CC, 11	53.96	<1	Clay
103-641A-6X-CC, 16	54.01	<1	Clay
103-641A-6X-CC, 20	54.05	<1	Clay
103-641A-7X-1, 100-103	55.10	21	Calcareous clay
103-641A-7X-2, 60-62	56.20	17	Calcareous clay
103-641A-7X-3, 36-37	57.46	38	Marl
103-641A-7X-4, 56-58	59.16	22	Calcareous clay
103-641A-7X-5, 19-21	60.29	47	Marl
103-641C-1R-1, 52-53	151.42	39	Marlstone
103-641C-1R-2, 13-14	152.53	11	Claystone
103-641C-1R-2, 47-49	152.87	9	Claystone
103-641C-1R-2, 61-62	153.02	5	Claystone
103-641C-1R-2, 95-96	153.35	4	Claystone
103-641C-1R-2, 147-148	153.87	4	Claystone
103-641C-1R-4, 53-55	155.93	1	Claystone
103-641C-1R-4, 105-107	156.45	4	Claystone
103-641C-1R-6, 23-25	158.63	1	Claystone
103-641C-1R-6, 56-58	158.96	4	Claystone
103-641C-2R-1, 132-134	161.82	2	Claystone
103-641C-2R-2, 127-128	163.27	3	Claystone
103-641C-2R-3, 148-149	164.98	1	Claystone
103-641C-2R-5, 28-30	166.78	<1	Claystone
103-641C-2R-5, 50-52	167.02	1	Claystone
103-641C-2R-5, 138-140	167.88	<1	Claystone
103-641C-2R-6, 52-54	168.52	<1	Claystone
103-641C-2R-7, 8-9	169.58	<1	Claystone
103-641C-3R-1, 20-21	170.30	1	Claystone
103-641C-3R-2, 4-5	171.64	15	Calcareous claystone
103-641C-3R-2, 6-7	171.66	4	Claystone
103-641C-3R-3, 16-17	173.26	2	Claystone
103-641C-3R-3, 68-70	173.78	11	Claystone
103-641C-3R-5, 55-56	176.65	<1	Claystone
103-641C-3R-6, 115-117	178.75	1	Claystone
103-641C-3R-7, 49-51	179.59	2	Claystone
103-641C-4R-1, 61-63	180.41	1	Claystone
103-641C-4R-3, 3-5	182.83	1	Claystone
103-641C-4R-4, 127-129	185.57	<1	Claystone
103-641C-4R-5, 110-119	186.90	3	Claystone
103-641C-4R-5, 145-147	187.25	3	Claystone
103-641C-4R-CC, 12-13	188.06	2	Claystone
103-641C-6R-1, 40-41	199.4	<1	Claystone
103-641C-6R-1, 133-134	200.33	<1	Claystone
103-641C-6R-3, 146-148	203.46	77	Carbonate conglomerate
103-641C-7R-1, 143-145	210.13	94	Carbonate conglomerate
103-641C-7R-2, 127-129	211.47	26	Calcareous claystone
103-641C-8R-2, 53-54	220.43	2	Claystone
103-641C-8R-3, 133-135	222.75	10	Claystone
103-641C-8R-34, 113-115	224.03	48	Marlstone
103-641C-8R-5, 7-8	224.47	72	Pebbly mudstone (with carbonate pebbles)
103-641C-8R-CC, 15-17	224.55	71	Carbonate conglomerate
103-641C-9R-1, 7-9	228.07	34	Carbonate sand
103-641C-9R-1, 30-32	228.30	2	Claystone
103-641C-9R-1, 93-95	228.93	18	Carbonate sand/clay
103-641C-9R-2, 29-31	229.79	2	Claystone
103-641C-9R-3, 80-82	231.80	37	Carbonate sand/clay
103-641C-10R-1, 66-68	238.26	47	Marlstone
103-641C-10R-1, 69-70	238.29	29	Calcareous claystone
103-641C-10R-2, 123-125	240.33	46	Marlstone
103-641C-10R-3, 2-3	240.62	42	Marlstone
103-641C-10R-4, 93-95	243.03	67	Marlstone
103-641C-11R-2, 75-77	249.55	82	Calcarenite
103-641C-11R-4, 60-62	252.40	57	Marlstone
103-641C-12R-2, 4-6	258.44	68	Clayey limestone
103-641C-12R-3, 40-42	260.30	42	Marlstone
103-641C-12R-6, 88-90	265.28	63	Marlstone
103-641C-13R-1, 133-135	267.83	60	Marlstone
103-641C-13R-3, 24-26	269.74	92	Carbonate turbidite
103-641C-13R-5, 93-95	273.43	73	Carbonate turbidite
103-641C-14R-2, 131-133	279.01	46	Marlstone
103-641C-14R-5, 145-147	283.65	43	Marlstone
103-641C-14R-6, 128-130	284.98	50	Marlstone
103-641C-15R-1, 128-130	287.08	87	Clayey chalk
103-641C-15R-3, 101-103	289.81	60	Marlstone
103-641C-15R-5, 50-52	292.30	57	Marlstone (slump)
103-641C-16R-2, 133-135	298.33	55	Marlstone
103-641C-16R-4, 133-135	301.33	83	Clayey limestone
103-641C-16R-7, 143-145	304.43	43	Marlstone

[a] Lithologic names are those used on visual core-description forms.

In lithologic Unit VI the marlstone bulk density ranges from 1.95 to 2.19 g/cm^3, averaging 2.06 g/cm^3; porosity ranges from 36% to 51%. The bioturbated limestone ranges in bulk density from 2.15 to 2.69 g/cm^3, averaging 2.32 g/cm^3, and porosity ranges from 23% to 40%. The average bulk density of two sandy limestone layers in lithologic Unit VI is 2.64 g/cm^3, and average porosity is 12%. Except in these two samples, a slight increase in bulk density and decrease in porosity can be seen in Figures 18C and 18D. The average bulk density of lithologic Unit VI calculated by tabulating recovered percentages of marlstone and limestone is 2.11 g/cm^3.

Acoustic Impedances and Possible Reflectors

Few persistent and pronounced changes occur in bulk density and seismic velocity in Holes 641A and 641C. The boundary between lithologic Units V and VI is the only interface where recovered material implies a significant contrast in acoustic impedance; Figure 18E shows low acoustic impedance of little variation with depth throughout Site 641. The occurrence of highly friable carbonate sandstone and the low recovery in Unit IV (202.6–218.4 m sub-bottom), however, suggest the presence of a reflector generated by the loosely cemented but higher impedance carbonate sandstones at the interface between Subunit IIIB and Unit IV. Using the aforementioned average bulk density and seismic-velocity values, we calculated the reflectivity R of these interfaces according to the equation

$$\frac{V_{p1}\rho_{b1} - V_{p2}\rho_{b2}}{V_{p1}\rho_{b1} + V_{p2}\rho_{b2}}$$

where V_p is compressional seismic velocity and ρ_b is bulk density. Table 6 lists the calculated acoustic impedance and reflectivity between lithologic Units V and VI; the reflection coefficient of 0.09 is extremely low and is not expected to generate a significant reflector. The calculated reflection coefficient between lithologic Subunit IIIB and Unit IV is 0.25 and may be the site of reflector R2 (see "Seismic Stratigraphy" section, this chapter).

Summary

Thermal-conductivity values ranging from 2.04 to 2.66 $\times 10^{-3}$ cal $\times$ °C^{-1} $\times$ cm^{-1} $\times$ s^{-1} persist without apparent trend throughout Site 641 materials; two high values of 4.35 and 4.70 $\times 10^{-3}$ cal $\times$ °C^{-1} $\times$ cm^{-1} $\times$ s^{-1} were measured in Core 103-641C-3R.

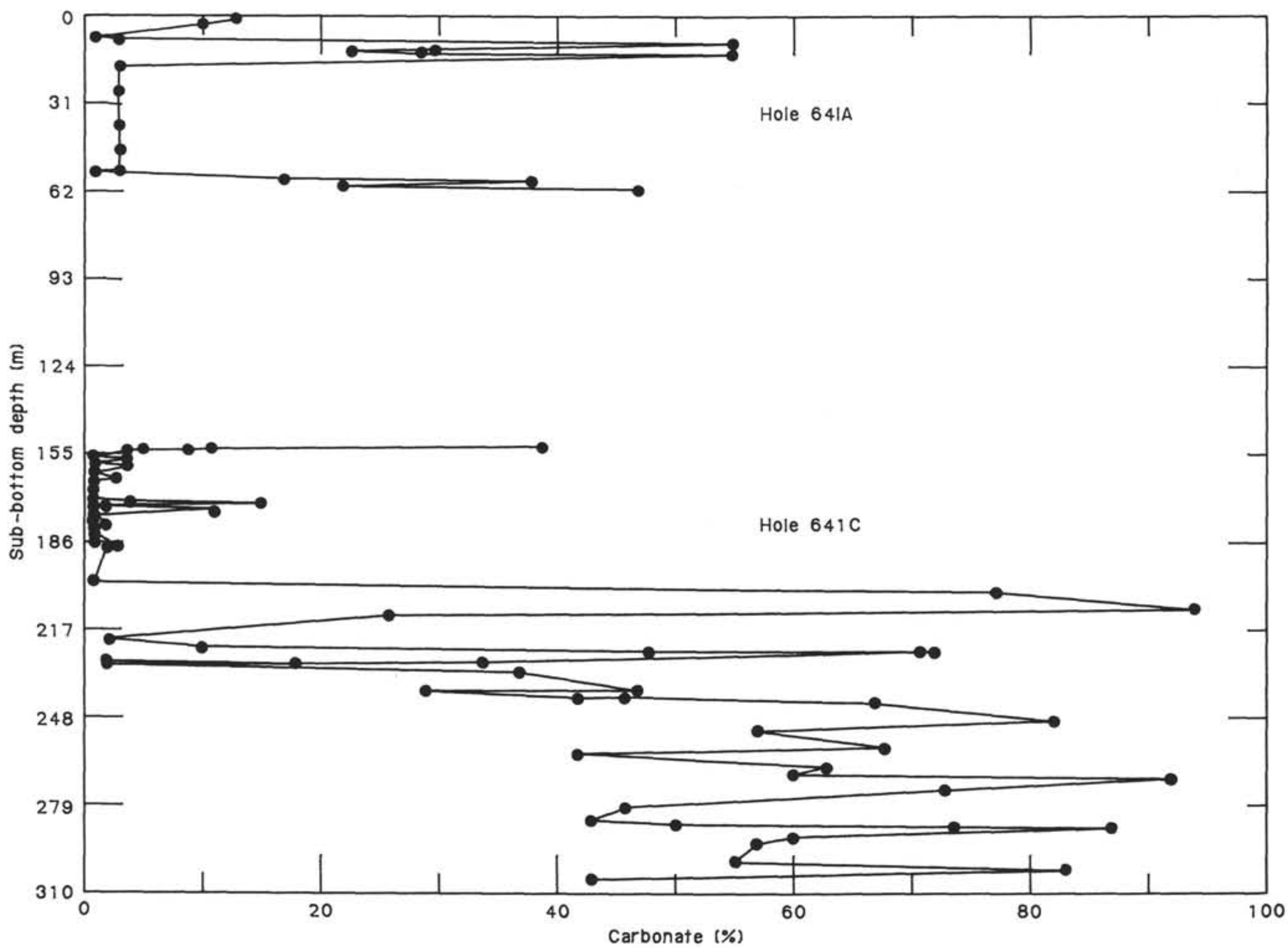

Figure 17. Percentage of carbonate in dried-sediment samples, Site 641. Data are given in Table 5.

Compressional seismic-velocity measurements change very little throughout Hole 641A and average 1.52 km/s through lithologic Subunits IA, IB, and IIIA. No measurements were made on the black zeolitic clay of lithologic Unit II. Lithologic Subunit IIIB at the top of Hole 641C shows a slight increase in seismic velocity with depth; the greenish calcareous component of this unit averages a few hundred meters per second higher velocity than does the darker claystone component, but measured velocities remain near the average of measured values of 1.83 km/s. The seismic velocity of green marlstone from lithologic Unit IV falls within the range of marlstone velocities in the overlying unit. Two poorly cemented carbonate sandstone layers in Unit IV yield an average velocity of 2.61 km/s. The green and the black marlstone of lithologic Unit V show a slight increase in seismic velocity with depth, ranging in value from 1.75 km/s to 2.17 km/s, averaging 1.90 km/s. A calcite-cemented sandstone layer yields a seismic velocity of 4.30 km/s, and a silicified carbonate-platform sandstone yields a seismic velocity of 5.74 km/s. In lithologic Unit VI, bioturbated marly limestone occurs in sufficient proportion to increase the average seismic velocity of the unit to 2.08 km/s, above typical marlstone values.

Marlstone samples in lithologic Units V and VI were measured both in the plane of the core diameter (parallel to the cut face of the core) and perpendicular to the plane of the core diameter; seismic velocity in the latter direction is consistently 30–180 m/s less than that measured in the former. We relate this to alignment of clay minerals in the bedding plane of the turbidite layers.

Bulk density and porosity are fairly constant with depth throughout lithologic Subunits IA and IB, averaging 1.75 g/cm^3 and 60%, respectively. The bulk density of lithologic Subunit IIIA is slightly less, averaging 1.68 g/cm^3. Lithologic Subunit IIIB bulk-density values remain near the measured average of 1.81 g/cm^3, and average porosity is 57%. Except for the presence of medium- to coarse-grained carbonate sandstone layers in lithologic Unit IV, having average measured bulk density of 2.60 g/cm^3 and porosity of 44%, the unit is similar in physical-property characteristics to Subunit IIIB. Bulk density of lithologic Unit V increases slightly with depth but remains near the average calculated value of 1.93 g/cm^3; porosity also decreases slightly with depth, but values are scattered over a range from 33% to 62%. The average bulk density of lithologic Unit VI is augmented by a significant amount of marly limestone to a value of 2.11 g/cm^3.

Calculations of acoustic impedances based on the assumption that unrecovered material from lithologic Unit IV consists largely of friable carbonate sandstone that crumbles during drilling suggest that a reflector may exist between lithologic Subunit IIIB and Unit IV.

AGE-VS.-DEPTH CURVE

The age-vs.-depth curve for the combined data from Holes 641A and 641C is shown in Figure 20. Biostratigraphic control in Hole 641A is poor, and the rates of sedimentation and accumulation cannot be estimated satisfactorily. However, sedimentation rates were slow, about 2–3 m/m.y., in the latest Albian

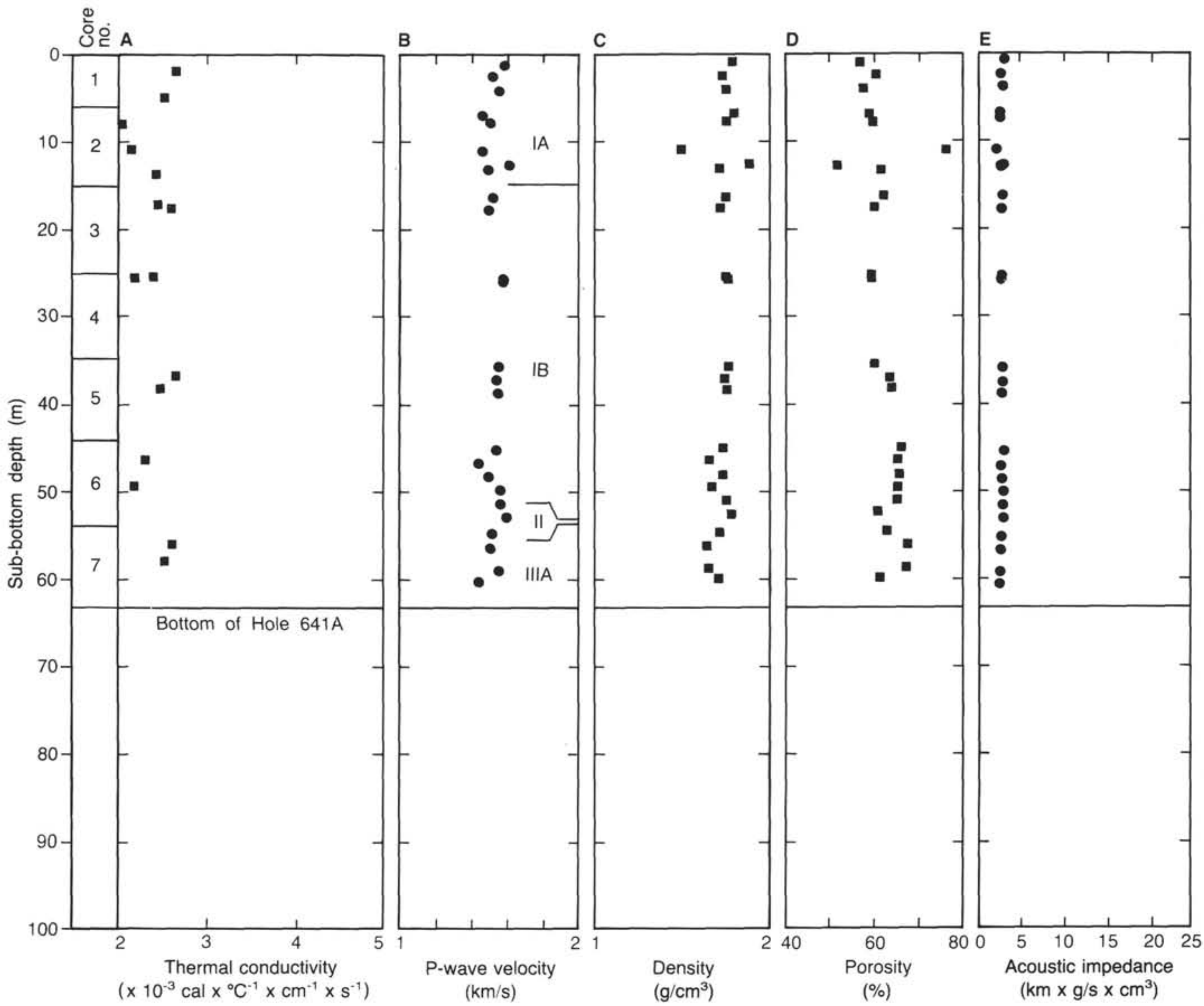

Figure 18. Physical-property measurements on sediments and sedimentary rocks from Site 641 plotted against sub-bottom depth. Lithologic units described in the "Sediment Lithology" section (this chapter) are indicated on the right side of the seismic-velocity column. A. Thermal-conductivity values ($\times 10^{-3}$ cal $\times$ °C^{-1} $\times$ cm^{-1} $\times$ s^{-1}). B. Compressional seismic velocity (kilometers per second). Square data points indicate velocities measured in the plane of the core diameter and parallel to the cut face of the core (c-direction), triangular data points indicate velocities measured in the plane of the core diameter and perpendicular to the cut face of the core (b-direction) and dots indicate velocities measured perpendicular to the plane of the core diameter (a-direction). Bioturbated limestone data points are encircled, and sandy limestone data points are enclosed by squares. Lithologic units are indicated on right side of the column. Possible reflector is indicated by R. Note different seismic velocity scales used for data from Hole 641A versus that from Hole 641C. C. Bulk density (grams per cubic centimeter). D. Porosity (percent). E. Acoustic impedance (compressional seismic velocity $\times$ bulk density; g-km/cm^3-s). Square data points indicate acoustic impedances calculated from velocities measured in the c-direction; triangular data points indicate acoustic impedance calculated from velocities measured in the b-direction; dots indicate impedances calculated from velocities measured in the a-direction.

and earliest Cenomanian. The interval from about 64 to 151 mbsf was not cored, but the Lower Cretaceous strata provide reasonably good biostratigraphic control for the lower part of the hole. The crowding of biostratigraphic zones in the uppermost Aptian indicates a rate of accumulation of only about 5 m/m.y., and the thin zones in the lower Cenomanian indicate a rate of about 2 m/m.y. An unconformity may occur at this level, but the data amassed from shipboard studies do not require this.

LOGGING RESULTS

Geophysical logging in Hole 641C used lithodensity, natural gamma-ray spectrometry, and neutron porosity tools run in two segments in the interval between 130 and 196 mbsf. Hole 641C was drilled with a 9.875-in. bit and, to avoid induced swelling of the clay-rich rock, was not filled with fresh-water mud. The 5-in. (outer diameter) drill pipe and 8.25-in. (outer diameter) drill collars were pulled up to 110 mbsf before the first logging run. The long-spaced sonic tool assembly stopped at an impassable bridge at 127 mbsf, and measurements were not obtained in open hole. The drill pipe was then positioned at 128 mbsf to clear this bridge, and the lithodensity, gamma-ray spectrometry, and neutron porosity tools were run to 174 mbsf, where a second bridge stopped penetration. After circulating in the hole for 20 minutes and lowering the pipe to 192 mbsf, the same tool was run and stopped at a bridge at 196 mbsf. The drill string was

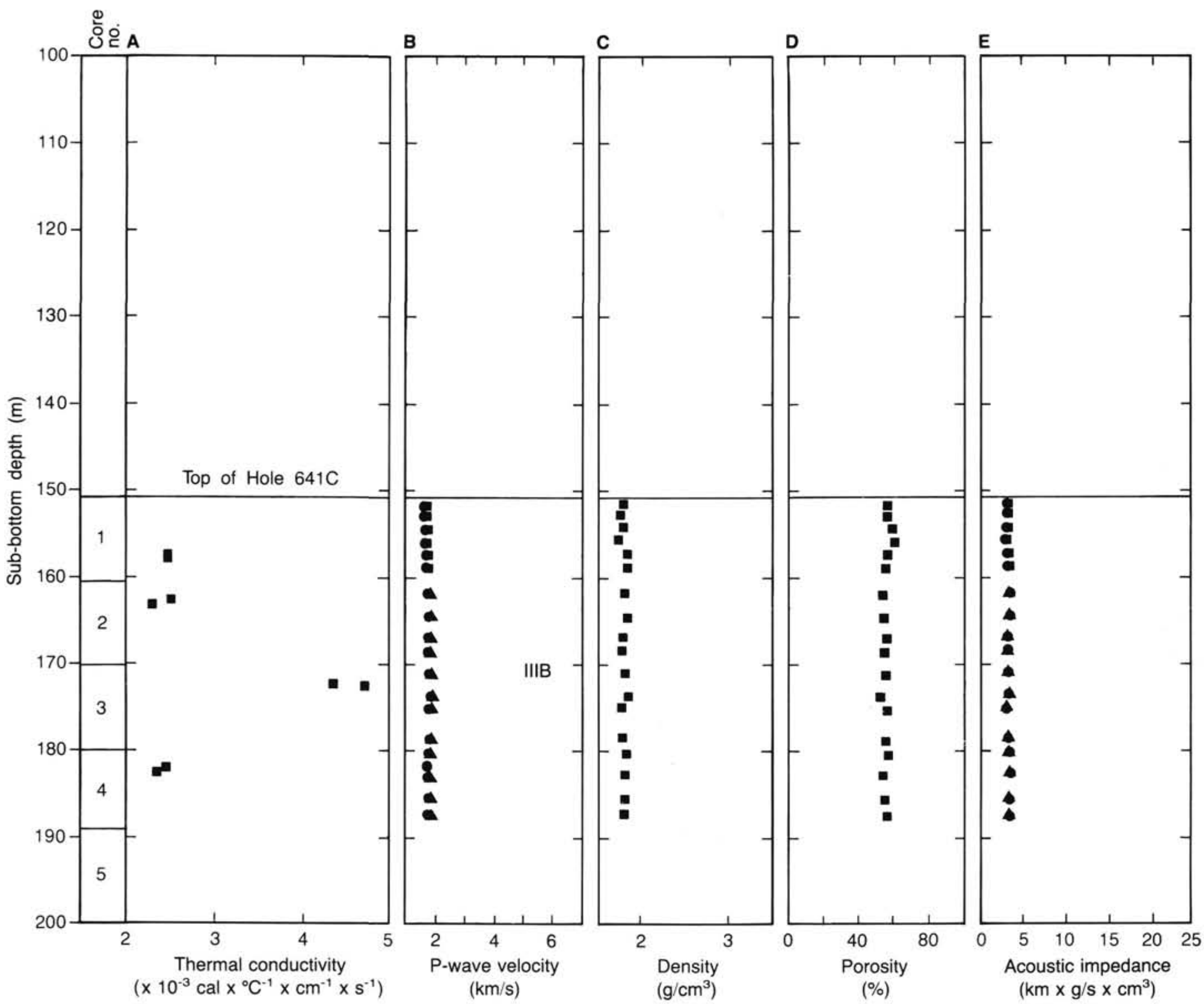

Figure 18 (continued).

pulled up 30 m, and open-hole measurements were obtained from 160 to 196 mbsf. The logs were recorded as the tools were pulled uphole at approximately 1000 ft/hr. The composite open-hole log spans from 130 to 196 mbsf.

The gamma-ray spectrometry tool was run in the BHA and drill pipe from the seafloor to 192 mbsf. Gamma-ray readings made in the drill pipe and BHA are suppressed owing to thickness of the pipe; therefore, BHA recordings are generally near zero. Caution is recommended in the interpretation of the gamma-ray log run in the drill pipe (0–95 mbsf) because of the suppressed readings and varying effects of pipe collars.

Log Analysis

In the open-hole interval, the tool responses show a single, relatively homogeneous log-lithologic unit of clay-rich sediments. The logs are shown in Figure 21, and the value ranges are summarized in Table 7. Borehole rugosity and wash-out were not directly measured by a caliper log, but the low density-correction values suggest that the data are reliable.

In this log-lithologic unit, gamma-ray readings generally vary between 40 and 88 API units, bulk density between 1.25 and 1.8 g/cm^3, and neutron porosity between 51% and 69% (Table 7). Relative changes in the uranium content between 0 and 3.5 ppm are shown by the difference between the total clay content (SGR) and potassium and thorium content (CGR) curves (Fig. 21). Variation apparent in the logs is probably due to relative changes in clay type in layers between 2 and 4 m thick. In the interval between 178 and 183 mbsf, the uranium content decreases sharply where the SGR increases to 88 API units.

In the interval logged through the drill pipe, the gamma-ray response shows considerable variation between 0 and 50 API units. The pipe collar locations (DPT) have suppressed gamma-ray values and are identified in Figure 22. The variation of the SGR and CGR curves suggests that the clay content generally decreases with depth. Sharp decreases in gamma-ray values occur at about 20 mbsf and about 52 mbsf. In addition, the uranium content, indicated by the difference between the SGR and CGR curves, increases significantly below 45 mbsf, peak values being at 46 and 52 mbsf.

Lithostratigraphic Correlation

The open-hole log responses show changes in clay type between greenish gray and black claystone intervals within lithologic Subunit IIIB, as described from the recovered cores (see

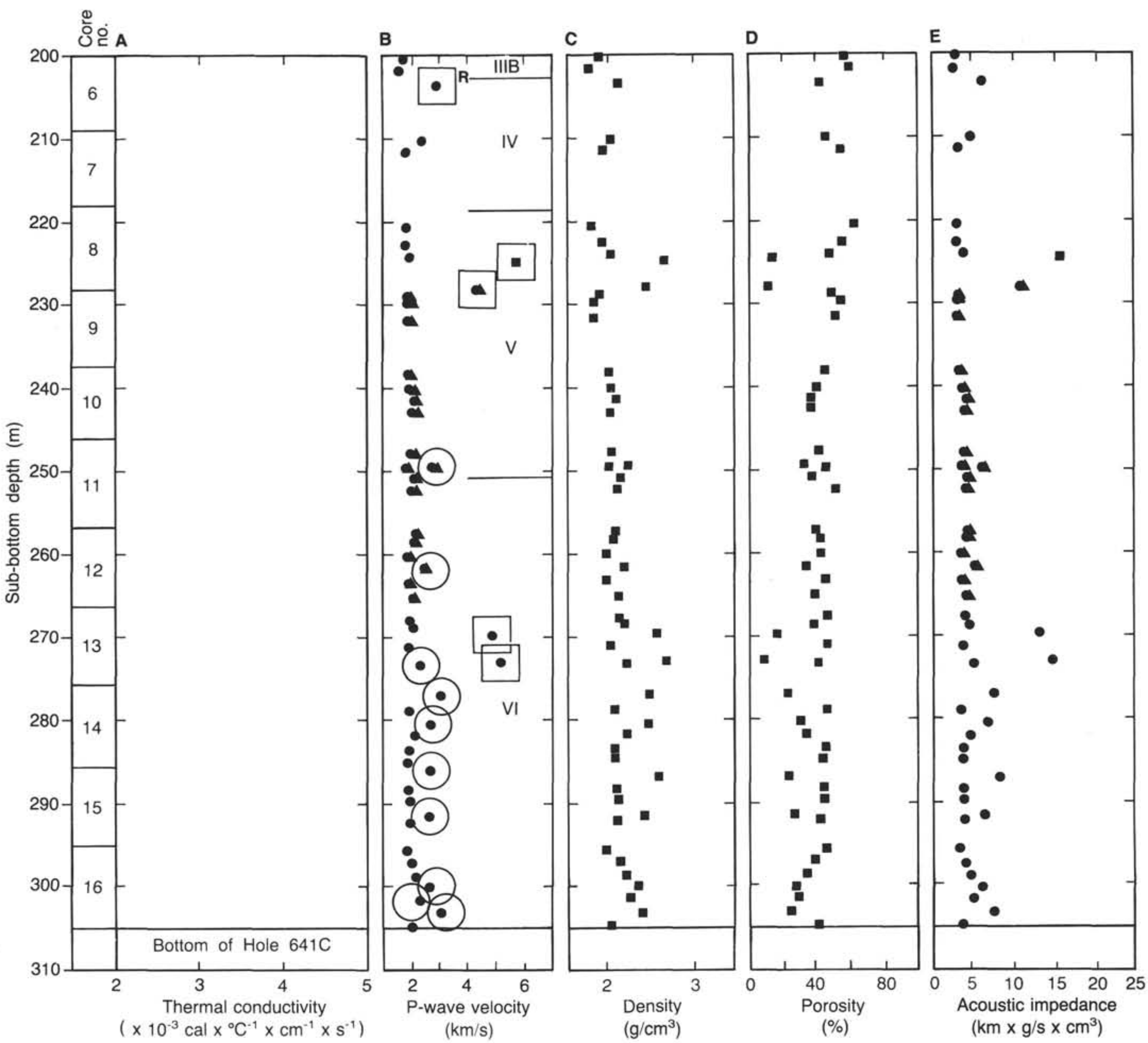

Figure 18 (continued).

"Sediment Lithology" section, this chapter). The lamination of the claystones observed in the cores contributes to the variation in the gamma-ray log response.

The effects of the drill pipe and collars on the gamma-ray response preclude an exact log interpretation. However, log boundaries determined by the gamma-ray response through the drill pipe can be "informally" correlated with lithologic Units IA, IB, II, and IIIA described from the recovered cores in Hole 641A (see "Sediment Lithology," this chapter). The brown clay and calcareous ooze of lithologic Subunit IA and the brown and gray clay of lithologic Subunit IB correspond to the upper log interval between the seafloor and about 52 mbsf. The boundary between Subunits IA and IB is approximately 20 mbsf, according to logging data (Fig. 22). The black zeolitic clay of lithologic Unit II probably corresponds to the 2-m-thick interval at 52 mbsf, where the gamma-ray log values are relatively high, although this correlation is uncertain due to the closeness of the pipe collar. Low gamma-ray values in the interval below 52 mbsf correspond to the underlying greenish gray calcareous clay and marl of lithologic Unit IIIA.

SEISMIC STRATIGRAPHY

Site 641 is on the seismic line recorded by the *JOIDES Resolution* when it surveyed Site 638 (Figs. 23A and B; see "Operations" section, Site 638 chapter, this volume). Site 641 is about 1.2 km N80°E from Site 638 (see "Operations," this chapter). At Site 641, the depth is about 20 m above the depth of the seafloor at Site 638, i.e., about 50 m deeper than expected from both the seismic line and the echo-sounding records. We interpret this discrepancy as being an effect of the seafloor morphology; we recorded strong side echos from the slope east of the site but only a faint echo of the seafloor exactly below the vessel. On Figure 23B, we deleted side echos to show the seismic stratigraphy more correctly. We tentatively correlate reflector R1 with the Upper Cretaceous pelagic sediments above the Albian–Cenomanian black shale and reflector R2 with the base of the

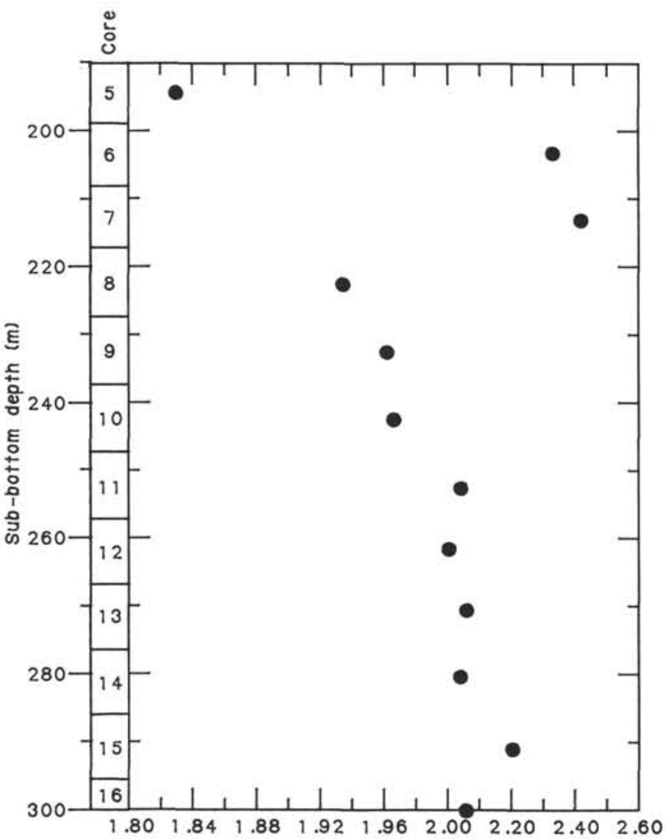

Figure 19. Average seismic velocity of Cores 103-641C-5R through 103-641C-16R plotted against sub-bottom depth (see text for discussion).

black shale, i.e., with the regional break-up unconformity near the Albian/Aptian boundary. R1 and R2 are located at 45 and 240 milliseconds below the seafloor, respectively. If Hole 638 is projected onto seismic line GP-101 (Fig. 23C), Hole 638 would coincide with the same reflectors at about the same reflection times (Fig. 23C).

Made from the velocities measured on board (see "Physical Properties," this chapter), the correlation between the seismic stratigraphy and the drilling data at Site 641 is given in Figure 24. R1 is correlated with Core 103-641A-5X, where Late Cretaceous pelagic sediments were sampled, above the black clay. R2 is correlated with Core 103-641C-6R, at the boundary between lithologic Units III and IV, which is a major change in the sedimentary sequence (see "Sediment Lithology," this chapter). We thus conclude that (1) the R2 reflector correlates with the boundary between black shale (Unit III) and underlying marlstone and turbidites, including limestone conglomerate (Unit IV), and (2) the break-up unconformity is latest Aptian in age, according to the micropaleontological data that place the Aptian/Albian boundary just above the top of Unit IV (see "Biostratigraphy," this chapter). This conclusion agrees with the results of Leg 47B, which placed the break-up unconformity at the same stratigraphic level (Sigal, 1979).

SUMMARY AND CONCLUSIONS

Objectives

Drilling at Site 641 completed the stratigraphic column we had been constructing from data at Sites 638 and 639 by coring the part of the Cretaceous section not present at Site 638. Two particular stratigraphic levels drew our interest: the Cenomanian/Turonian boundary, where organic-rich black clay occurs at many localities around the world, and the seismic-reflecting horizon between the syn-rift sediments and the post-rift sediments, generally termed the "break-up unconformity." We wanted samples of the black clay and adjacent beds for paleontological dating and for organic geochemical and paleoenvironmental studies. As for the seismic discontinuity, we wanted to know what lithologic changes produce the impedance contrast, and we needed samples across the reflector for paleontological dating.

Stratigraphy

Three holes were drilled at Site 641, but only from Holes 641A and 641C were cores recovered. Hole 641A cored from the seafloor to a depth of 63.6 mbsf, and Hole 641C from 150.9 to 305.2 mbsf.

The stratigraphy of the holes at Site 641 is summarized graphically in Figure 25 and described in the following paragraphs, from oldest to youngest.

Syn-rift Sediments—Upper Barremian to Uppermost Aptian

The section beneath the level of the seismic reflector at the top of the Aptian is about 103 m thick and comprises three lithologic units. Beds representing rapid sedimentation from debris flows, turbidity currents, and slumps characterize these syn-rift sediments. These "event" beds are within a rather monotonous background of greenish and grayish marlstone and claystone, commonly in the form of thin turbidite layers.

1. The lowest of the three lithologic units, from 305.2 to 250.6 mbsf in Hole 641C, consists of gray marlstone, thin turbidites, debris flows, and turbidites of resedimented shallow-water limestone sand. The thin turbidites commonly include silt-size quartz at the base, but the thicker turbidites and the debris flows contain little quartz or feldspar. The debris flows consist mainly of resedimented ovoid pebbles and cobbles of marlstone, limestone, and claystone of pelagic and hemipelagic facies and doubtless represent materials of intrabasinal, local derivation. The limestone-sand calcarenite turbidites contain abundant shallow-water molluscan debris, including rudist and *Inoceramus* fragments, plus large foraminifers, crinoids, and corals. An uncored thin interval might occur in the hole.

The age of the lowest samples in this lowest unit cored at Hole 641C is middle/late Barremian, according to the foraminifer evidence, and early Aptian, according to the nannofossil occurrences. Whichever the age, we are missing nothing essential

Table 6. Average compressional seismic velocities (V_p) and bulk densities (ρ_b) used to calculate lithologic unit acoustic impedance ($V_p\rho_b$) and reflectivity (R) between lithologic Subunit IIIB and Unit IV, and between Units V and VI.

		V_p	ρ_b	$V_p\rho_b$	R
Subunit IIIB	Black and green claystone	1.83	1.81	3.31	
Unit IV	Greenish gray marlstone and carbonate sands	2.40	2.30	5.52	0.25 IIIB/IV
Unit V	Marlstone and microturbidites	1.90	1.93	3.67	
Unit VI	Marlstone, microturbidites, bioturbated limestone, sandy limestone	2.08	2.11	4.38	0.09 V/VI

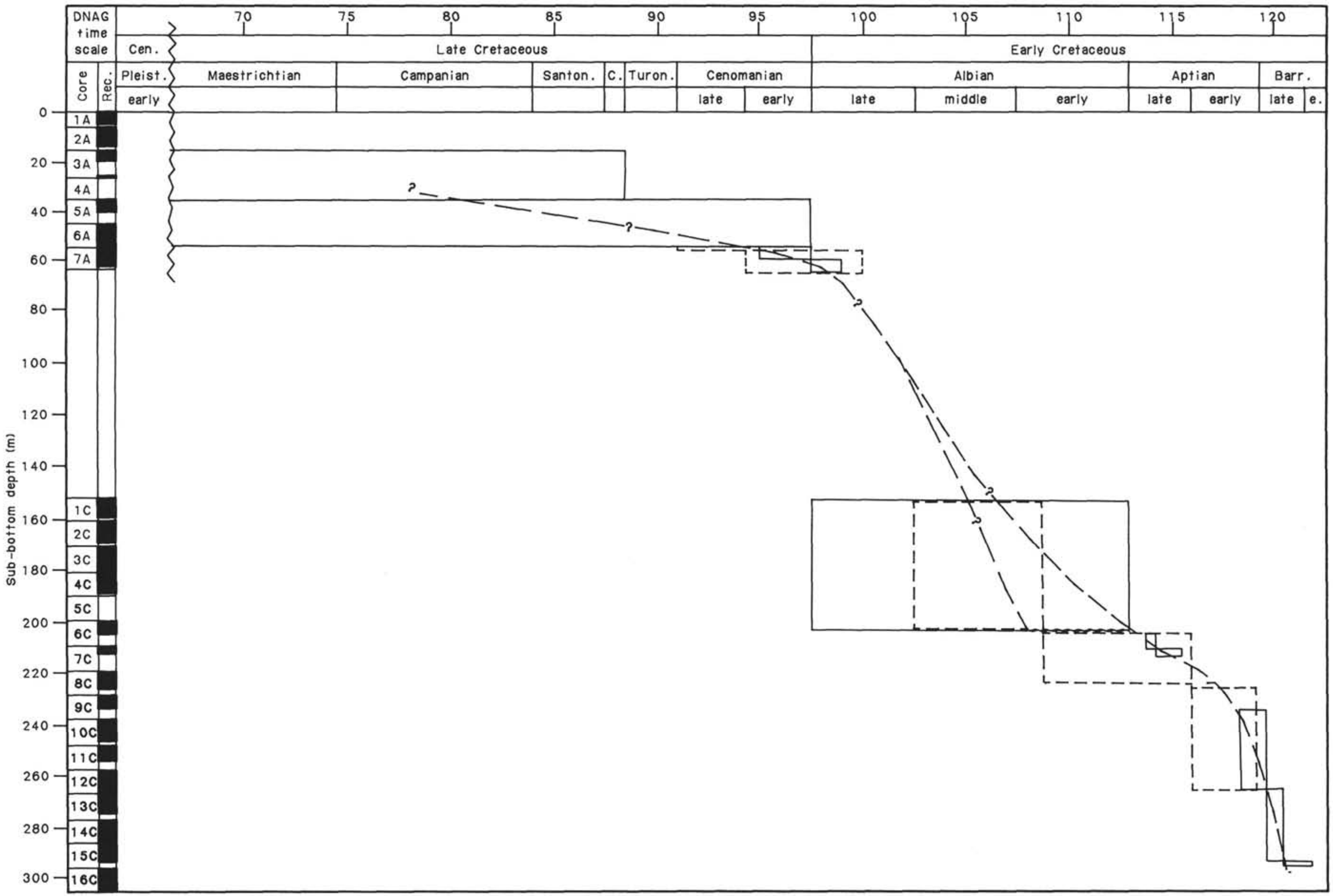

Figure 20. Age-vs.-depth curve, Holes 641A and 641C. Foraminiferal data are shown by solid-line boxes and nannofossil data by dotted-line boxes.

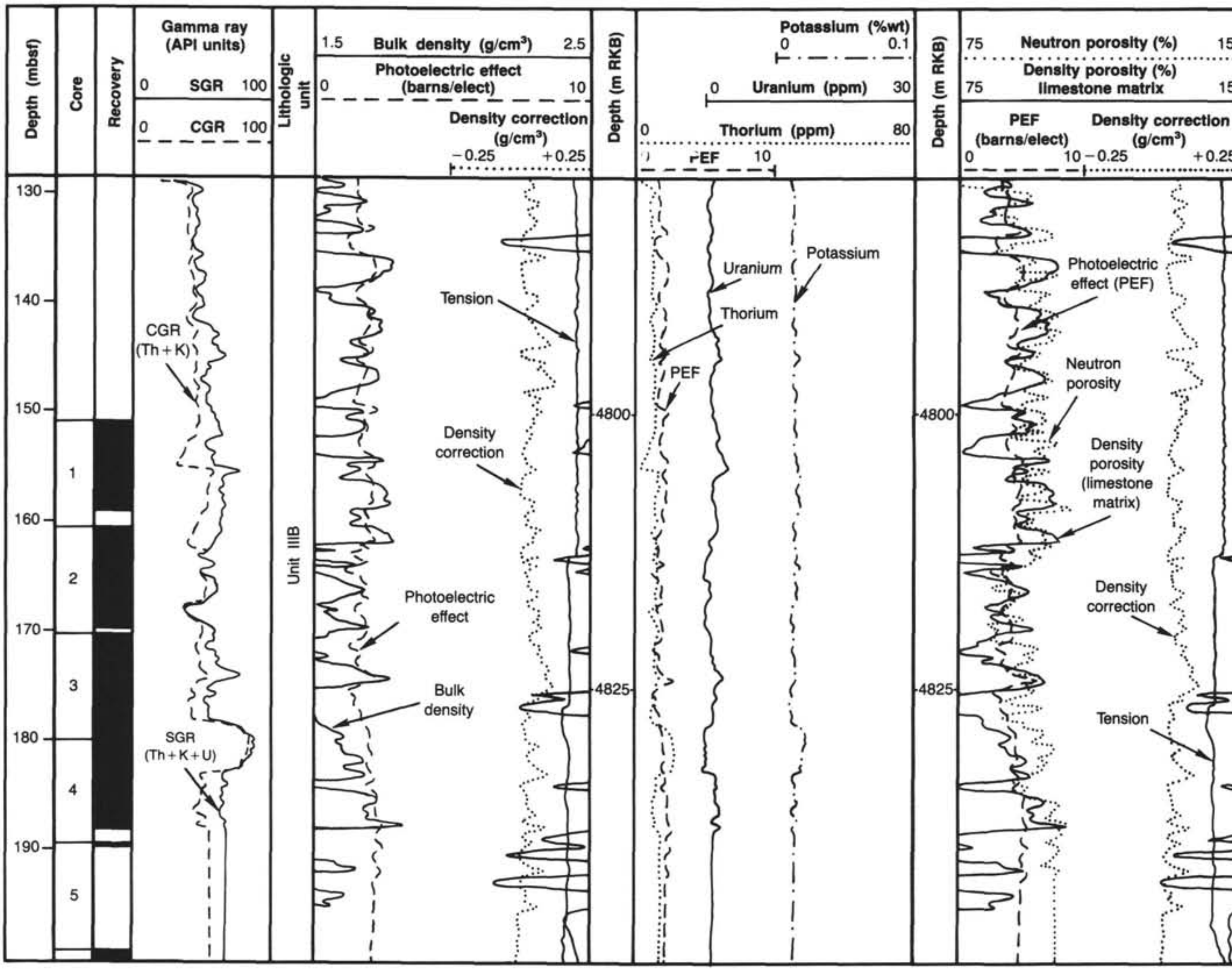

Figure 21. Composite log and core recovery, Hole 641C. See text for description of logs.

Table 7. Minimum/maximum log values in lithologic Unit IIIB, Hole 641C. GR = gamma ray, RHOB = bulk density, PEF = photoelectric effect, NPHI = neutron porosity, POTA = potassium content, URAN = uranium content, THOR = thorium content.

Log	Range
Depth (mbsf)	130–196
GR (API units)	40/88
RHOB (g/cm^3)	1.25/1.8
PEF (barns/elect.)	1.3/2.5
NPHI (%)	51/69
POTA (% wt)	0.01/0.023
URAN (ppm)	0/3.5
THOR (ppm)	1/12

between this level and the highest levels in the Cretaceous sampled in Hole 638B and can confidently reconstruct the stratigraphy from the Valanginian upward.

2. The next higher lithologic unit, from 250.6 to 218.4 mbsf, comprises lower Aptian black claystone, interbedded with greenish claystone and gray marlstone as the background sediments, and thin turbidite layers of olive-gray calcareous claystone and siltstone. Only a few calcarenite turbidites occur in this interval.

3. The highest lithologic unit in the syn-rift sequence, from 218.4 to 202.6 m, is of late Aptian age and extends to almost the end of the Aptian. The unit consists of greenish marlstone as the background sediment, intercalated with graded turbidite beds of coarse-grained calcarenite and limestone-granule conglomerate. The limestone grains comprise many types of skeletal components, all of shallow-water origin.

Post-rift Sediments—Albian to Coniacian-Maestrichtian

The syn-rift sequence of turbidites and debris flows is capped by the regional seismic reflector that follows the contact between the syn-rift sediments and the overlying black claystone. Average density and velocity of sediments change across this contact, mainly owing to the cemented calcarenite beds in the Apti-

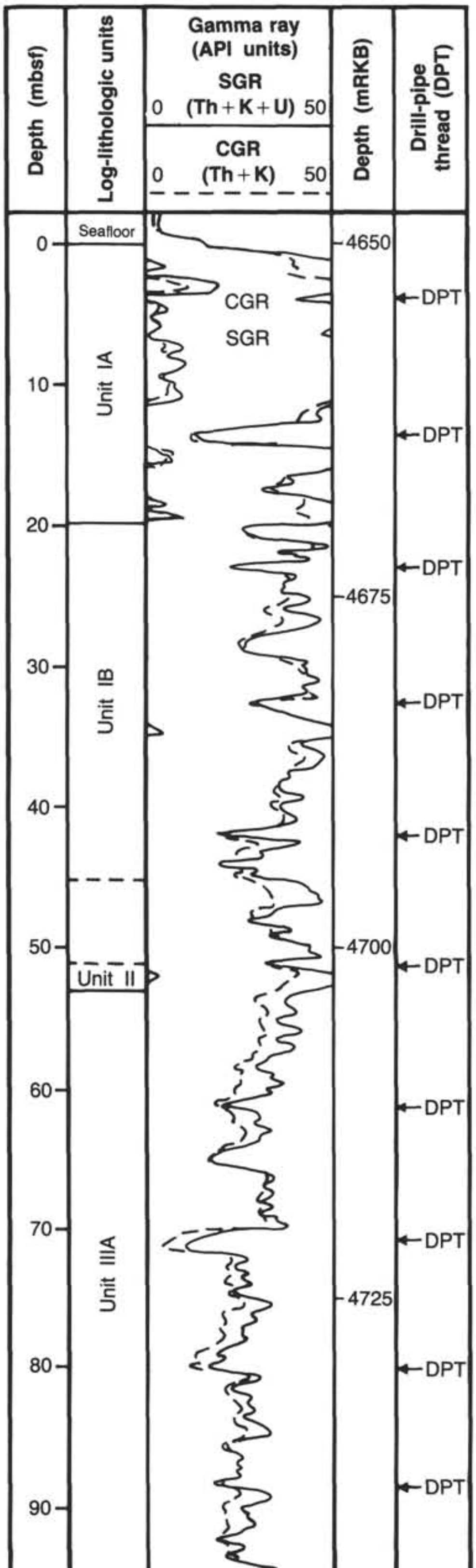

Figure 22. Preliminary correlation of gamma-ray spectrometry log, recorded through the drill pipe in Hole 641C, and lithologic units at Hole 641A. Boundaries of lithologic units are based on logging results and roughly correlate with lithologic units described from the recovered cores (see Table 2).

an that cause the impedance contrast that produces the reflector. Post-rift sediments at Site 641 include the following:

1. Black claystone occurs in Hole 641C in the interval from 202.6 to 150.9 m, but it probably continues upward almost to the lowest samples obtained in Hole 641A, at about 64 mbsf. The claystone is Albian in age, and consists, in the part sampled in Hole 641C, of massive and laminated black claystone and greenish claystone. The different color and lamination varieties are interbedded on a scale of decimeters. The black claystone is more generally laminated than are the green sediments. Minor thin beds of fine-grained sandstone and siltstone are scattered in the sequence, and diagenetic siderite micronodules and laminae occur in some places.

2. In the upper part of the sequence, sampled in Hole 641A, the lithology is different from that in the black claystone interval. At the bottom of the interval cored in Hole 641A, from 63.6 to 53.9 mbsf, the sediments consist of greenish gray nannofossil marl and calcareous clay, having only a suggestion of mottling or lamination. Foraminifer and nannofossil evidence date the interval as being late Albian and early Cenomanian.

3. A thin band, only about 25 cm thick, between 53.9 and 53.6 mbsf, is of special interest. It consists of uniform, structureless, dark-black zeolitic (clinoptilolite) clay, containing about 10% organic carbon. Rock-Eval analysis of a few samples showed Type II marine plant matter as being the source of the organic matter. The contacts with under- and overlying gray and greenish claystone are sharp, but these claystones are barren of fossils. Smear slides of the black clay, prepared for study of nannofossils, proved barren.

4. Above the black clay is a thickness of about 38 m of uniform, structureless brown and grayish brown clay. Only long-ranging foraminifers occur in the unit, and its age can be constrained only as Late Cretaceous.

5. Slumped beds of Pleistocene ooze mixed with clasts of a variety of sediment types, including black clay, nannofossil marl, and calcareous clay, occupy the upper 15.7 m of Hole 641A.

Discussion of Sedimentary Sequence at Site 641

Together with the data supplied by coring at Site 638, the cores from Site 641 complete the column for the syn-rift sediments. A few generalizations can be made about this sequence. First, an overall evolution occurs from quartzo-feldspathic, terrigenous turbidites in the lower part of the section to turbidites derived from a limestone platform (probably of about the same age as the turbidites themselves) to debris flows containing only clay and marlstone pebbles derived from sediments much like the host sediments in the upper part. In short, there is a change from extrabasinal sources of sediment to intrabasinal sources. This change may reflect an increasing compartmentalization of the margin, cutting off the terrigenous supply by growth of carbonate platforms on fault blocks, by steepening of local slopes owing to increased relief created by faulting, or by some combination of these. To judge whether these trends reflect more than merely local changes in paleogeography, Galicia margin stratigraphy must be compared with that on other contemporaneous margins around the North Atlantic.

The strata drilled at Site 641 have both similarities to and differences from synchronous sequences in the western North Atlantic (Jansa et al., 1979). The brown clay in the Upper Cretaceous lithologic Unit I is similar to the variegated clay of the Upper Cretaceous and Paleogene Plantagenet Formation (Jansa et al., 1979). The dark-gray and greenish gray, organic-rich, noncalcareous claystone fraction of lithologic Units III and V is similar to that of the middle Cretaceous Hatteras Formation. From only the clayey and marly fractions, lithologic Unit VI appears to have some features in common with the uppermost part of the Lower Cretaceous Blake–Bahama Formation, but Unit

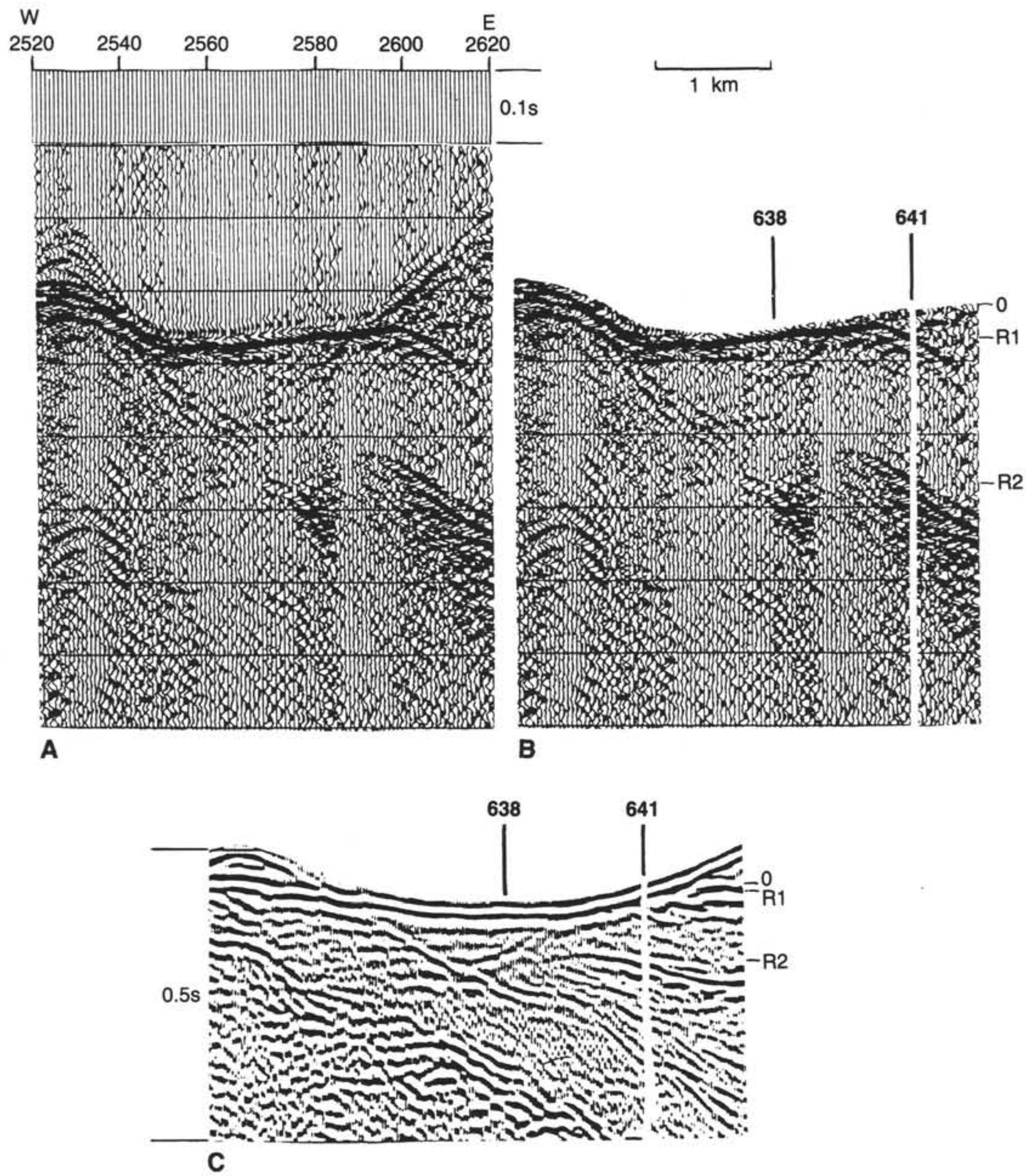

Figure 23. A. Seismic line recorded aboard *JOIDES Resolution*, when surveying the Sites 638 and 641 area. Location of line shown in Fig. 3. B. The same line, with side echos erased, showing the location of Sites 638 and 641. R1 and R2 are reflectors discussed in the text. C. IFP processed seismic line GP-101, onto which Sites 638 and 641 are projected. Location of line shown in Figure 3. Courtesy of L. Montadert.

VI has a relatively higher percentage of dark calcareous claystone. On the other hand, the sequence at Site 641 differs fundamentally from the central North Atlantic sequences in the occurrence of carbonate turbidites and debris flows in lithologic Units IV to VI and to a lesser degree in the occurrence of gray marlstone in Unit IV and greenish gray marlstone and calcareous claystone in Unit III.

The occurrence at Site 641 of a thin and conspicuous, black marine-organic-matter-rich zeolitic claystone (lithologic Unit II) is most important. This unit may correlate with the organic-matter maximum observed at the top of the middle Cretaceous Hatteras Formation in some of the Deep Sea Drilling Project sites in the central North Atlantic (Jansa et al., 1979).

A remaining problem is how the break-up unconformity relates to the inception of seafloor spreading on the adjacent seafloor. The clear delineation of magnetic anomaly M0 perhaps in Core 103-641C-10R, about 30 m (representing perhaps several million years) below the break-up unconformity, explains why this anomaly cannot be traced northward on the ocean floor to the Galicia margin: seafloor spreading did not begin at this latitude until after the formation of M0. This suggests that the earliest seafloor spreading propagated northward.

REFERENCES

Arthur, M. A., 1979. North Atlantic Cretaceous black shales: the record at Site 398 and a brief comparison with other occurrences. *In* Sibuet, J. C., Ryan, W. B. F., et al., *Init. Repts. DSDP*, 47B: Washington (U.S. Govt. Printing Office), 719-738.

de Graciansky, P. C., Deroo, G., Herbin, J. P., Montadert, L., Müller, C., Shaaf, A., and Sigal, J., 1984. Ocean-wide episode in the Late Cretaceous. *Nature*, 308:346-369.

Dunham, K. W., Meyers, P. A., and Dunham, P. L., in press. Organic geochemical comparison of Cretaceous black shales and adjacent strata from DSDP Site 603, Outer Hatteras Rise. *In* van Hinte, J. E., Wise, W. S., et al., *Init. Repts. DSDP*, 93: Washington (U.S. Govt. Printing Office).

Espitalie, J., Madec, M., and Tissot, B., 1977. Source rock characterization method for petroleum exploration. *Ninth Annual Offshore Technology Conference Proceedings*: 399-404.

Gartner, S., 1977. Calcareous nannofossil biostratigraphy and revised zonation of the Pleistocene. *Mar. Micropaleontol.*, 2:1-25.

Guerin, S., 1981. Utilisation des foraminifères planctoniques et benthiques dans l'étude des paleoenvironements océaniques au Crétacé moyen: application au materiel des forages D.S.D.P. de l'Atlantique Nord et Sud. Comparison avec la Tethys [Thesis]. Univ. of Nice, *Trav. Cent. Rech. Micropaleont. Jean.*

Jansa, L. F., Enos, P., Tucholke, B. E., Gradstein, F. M., and Sheridan, R. E., 1979. Mesozoic-Cenozoic sedimentary formations of the North American Basin, western North Atlantic. *In* Talwani, M., Hay, W. W., and Ryan, W. B. F. (Eds.), *Deep Drilling Results in the Atlantic Ocean: Continental Margins and Paleo-Environment:* Washington (Am. Geophys. Union), 3:1-57.

Katz, B. J., and Pheifer, R. N., 1982. Characteristics of Cretaceous organic matter in the Atlantic. *In* Watkins, J., and Drake, C. (Eds.), *Geology of Continental Margins. Am. Assoc. Pet. Geol., Mem.* 34: 617-628.

Manivit, J., Perch-Nielsen, K., Prins, B., and Verbeek, J. W., 1977. Mid-Cretaceous calcareous nannofossil biostratigraphy. *Kon. Nederl. Akad. Wet. B.*, 80(3):169-181.

McIver, R., 1975. Hydrocarbon occurrence from JOIDES Deep Sea Drilling Project. *Proceedings Ninth World Petroleum Congress*, 269-280.

Meyers, P. A., Dunham, K. W., and Dunham, P. L., in press. Organic geochemistry of Cretaceous organic-carbon-rich shales and limestones from the western North Atlantic Ocean. *Proc. North Atlantic Paleoceanography* meeting. Burlington House, London. 6-7 November 1984.

Müller, G., and Gastner, M., 1971. The "Karbonate-Bombe," a simple device for determination of the carbonate content in sediments, soils, and other materials. *Neues. Jahrb. Mineral. Monatsch.*, 10:466-469.

Ogg, J. G., in press. Early Cretaceous magnetostratigraphy, DSDP Sitres 534 and 603, western North Atlantic. *In* van Hinte, J., Wise, S., et al., *Init. Repts. DSDP*, 93: Washington (U.S. Govt. Printing Office).

Ogg, J. G., and Lowrie, W., 1986. Magnetostratigraphy of the Jurassic-Cretaceous boundary. *Geology*, 14:547-550.

Perch-Nielsen, K., 1979. Calcareous nannofossils from the Cretaceous between the North Sea and the Mediterranean. *In* Wiedmann, J. (Ed.), *Aspekte der Kreide Europas*. Int. Union. Geol. Sci. Ser. A, 6. Stuttgart (Schweizerbart): 223-272.

Roth, P. H., 1983. Jurassic and Lower Cretaceous calcareous nannofossils in the western North Atlantic (Site 534). Biostratigraphy, preservation, and some observations on biogeography and paleoceanography. *In* Sheridan, R. E., Gradstein, F. M., et al., *Init. Repts. DSDP.*, 76: Washington (U.S. Govt. Printing Office), 587-621.

Schlanger, S. O., and Jenkyns, H. C., 1976. Cretaceous anoxic events: causes and consequences: *Geol. Mijnbouw*, 55:179-184.

Sibuet, J. C., Ryan, W. B. F., et al., 1979. *Init. Repts. DSDP*, 47, Pt. 2: Washington (U.S. Govt. Printing Office).

Sigal, J., 1979. Chronostratigraphy and ecostratigraphy of the Cretaceous formations recovered on DSDP Leg 47B, Site 398. *In* Sibuet, J. C., Ryan, W. B. F., et al., *Init. Repts. DSDP*, 47B: Washington (U.S. Govt. Printing Office), 287-326.

Sissingh, W., 1977. Biostratigraphy of Cretaceous calcareous nannoplankton. *Geol. Mijnbouw*, 56:37-65.

Summerhayes, C. P., 1981. Organic facies of middle Cretaceous black shales in the deep North Atlantic. *Am. Assoc. Petrol. Geol. Bull.* 65:2364-2380.

Thierstein, H. R., 1973. Lower Cretaceous calcareous nannoplankton biostratigraphy. *Abh. Geol. Bundesanst.*, Wien, 29.

________, 1976. Mesozoic calcareous nannoplankton biostratigraphy of marine sediments. *Mar. Micropaleontol.*, 1:325-362.

Waples, D. W., 1983. Reappraisal of anoxia and organic richness, with emphasis on Cretaceous of North Atlantic. *Am. Assoc. Petrol. Geol. Bull.*, 67:963-978.

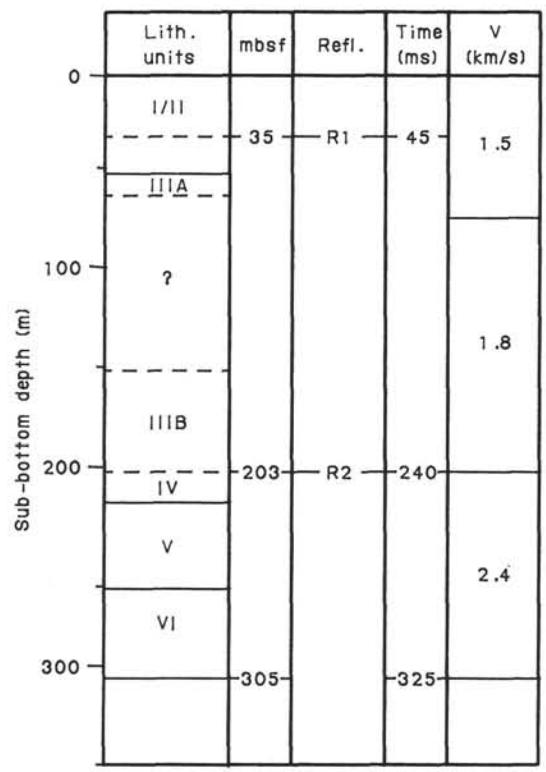

Figure 24. Correlation between lithologic units (see "Sediment Lithology," this chapter) and reflectors R1 and R2, according to the velocities measured on board (see "Physical Properties" section, this chapter).

Location: 42°09.3'N., 12°10.9'W
Water depth: Hole 641A: 4646.0 m below derrick floor (4636 m below sea level)
Hole 641C: 4649.0 m below derrick floor (4639 m below sea level)

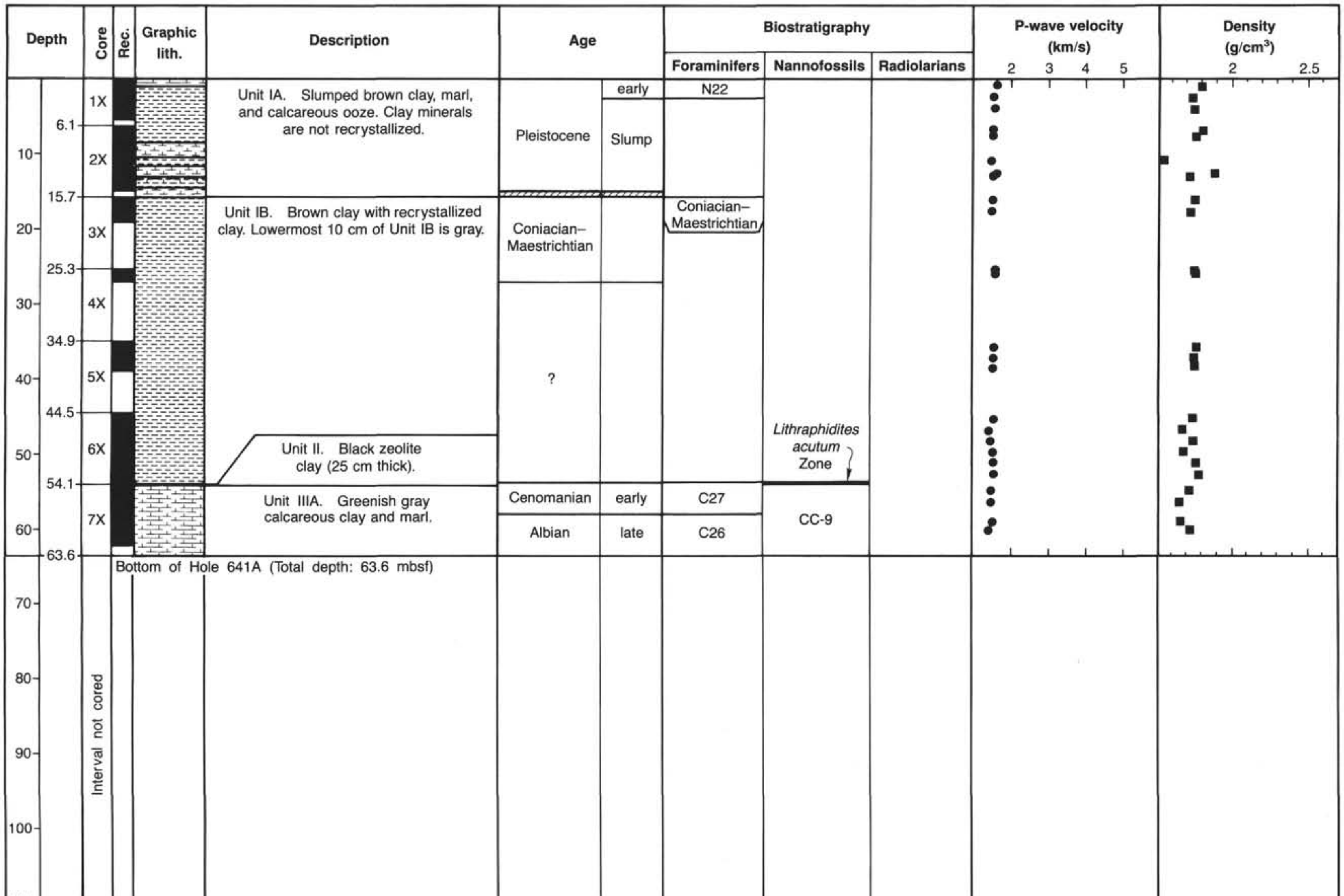

Figure 25. Site 641 summary logs. Explanation of symbols used in P-wave velocity and density columns given in Figure 18.

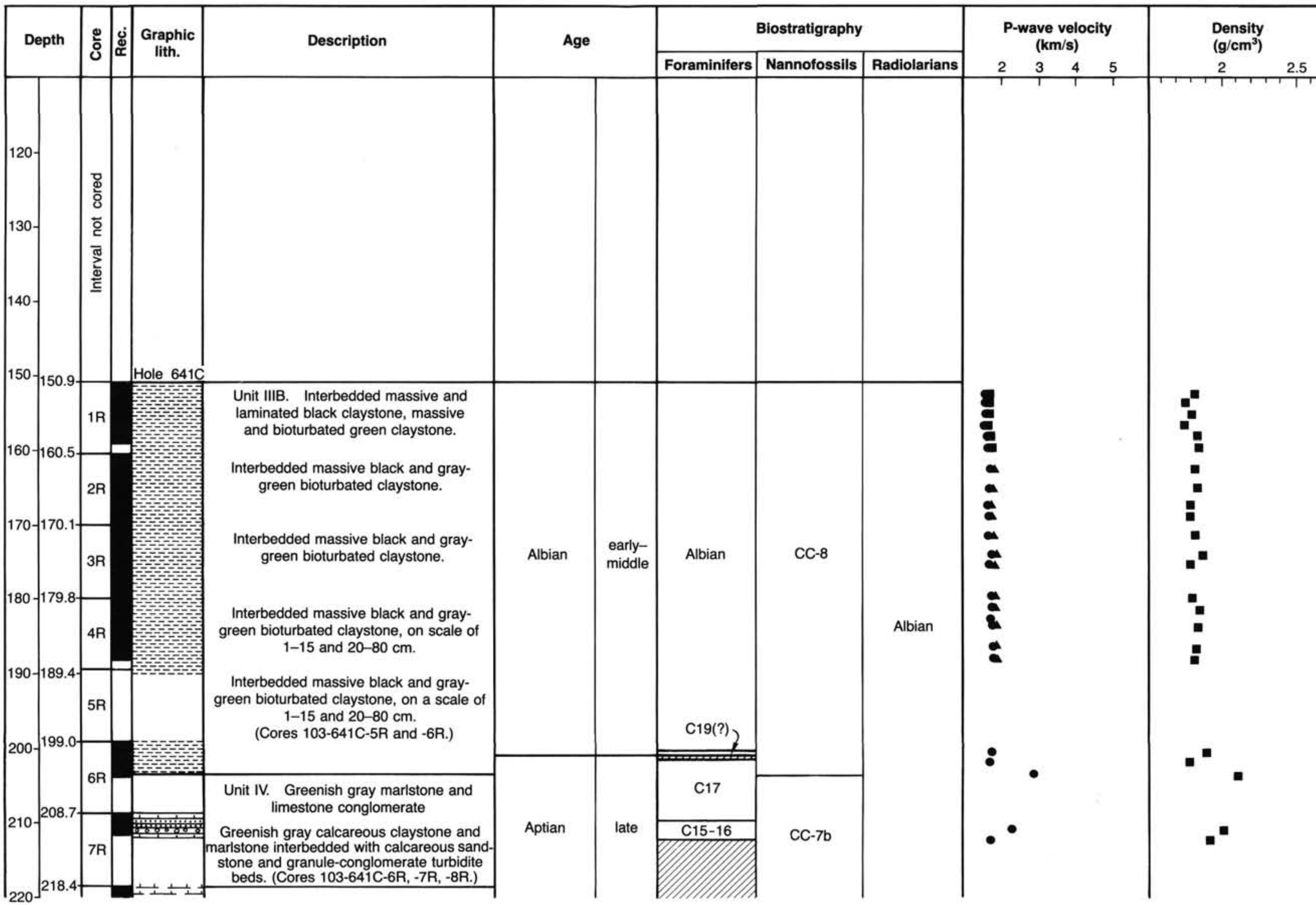
Depth
Core
Rec.
Graphic lith.
Description
Age
Biostratigraphy
Foraminifers
Nannofossils
Radiolarians
P-wave velocity (km/s)
2 3 4 5
Density (g/cm³)
2 2.5
120
130
140
150
160
170
180
190
200
210
220
Interval not cored
Hole 641C
150.9
160.5
170.1
179.8
189.4
199.0
208.7
218.4
1R
2R
3R
4R
5R
6R
7R
Unit IIIB. Interbedded massive and laminated black claystone, massive and bioturbated green claystone.
Interbedded massive black and gray-green bioturbated claystone.
Interbedded massive black and gray-green bioturbated claystone.
Interbedded massive black and gray-green bioturbated claystone, on scale of 1–15 and 20–80 cm.
Interbedded massive black and gray-green bioturbated claystone, on a scale of 1–15 and 20–80 cm. (Cores 103-641C-5R and -6R.)
Unit IV. Greenish gray marlstone and limestone conglomerate
Greenish gray calcareous claystone and marlstone interbedded with calcareous sandstone and granule-conglomerate turbidite beds. (Cores 103-641C-6R, -7R, -8R.)
Albian
early–middle
Albian
CC-8
Albian
C19(?)
Aptian
late
C17
C15-16
CC-7b

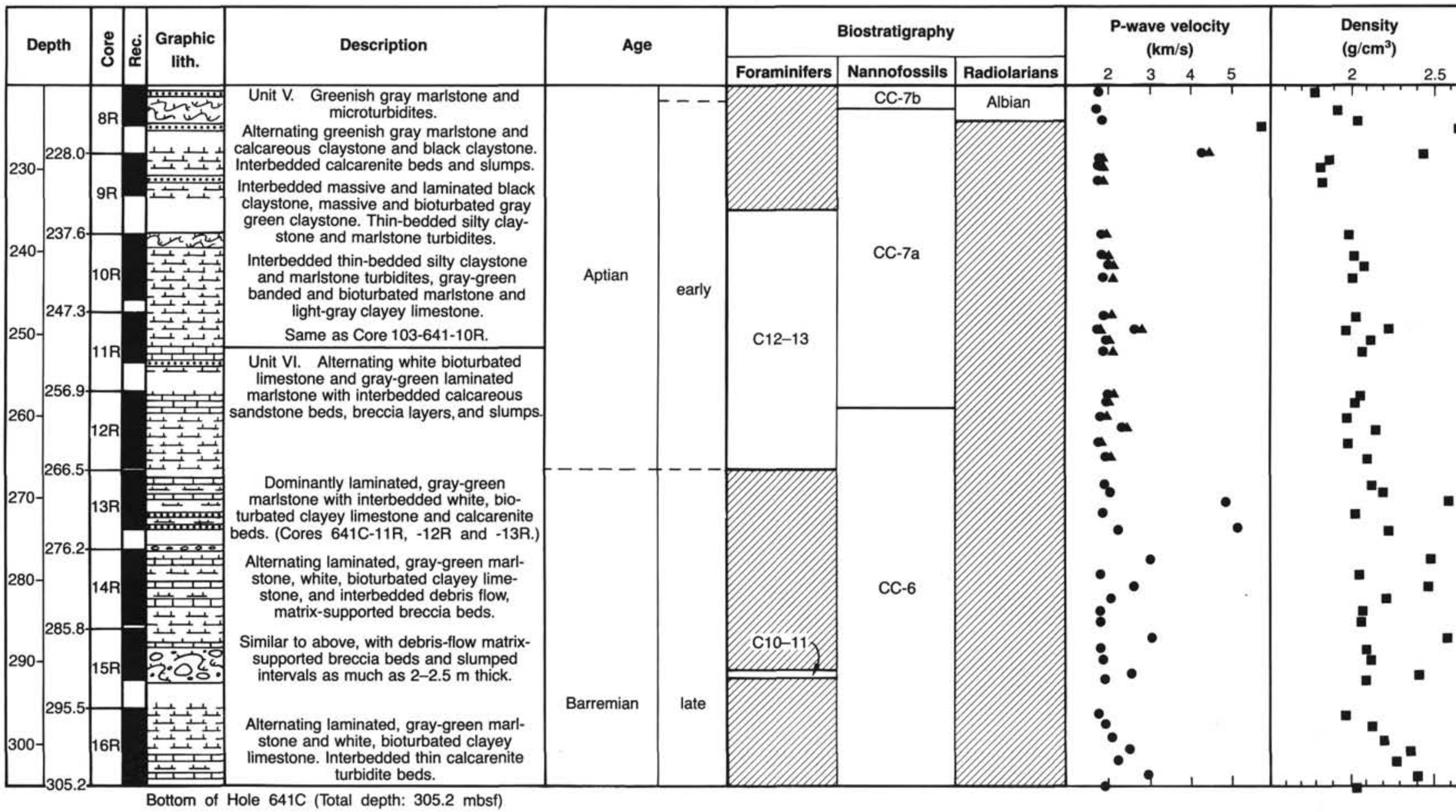

Figure 25 (continued).

SITE 641 HOLE A CORE 1X CORED INTERVAL 4635.5–4641.6 mbsl; 0–6.1 mbsf

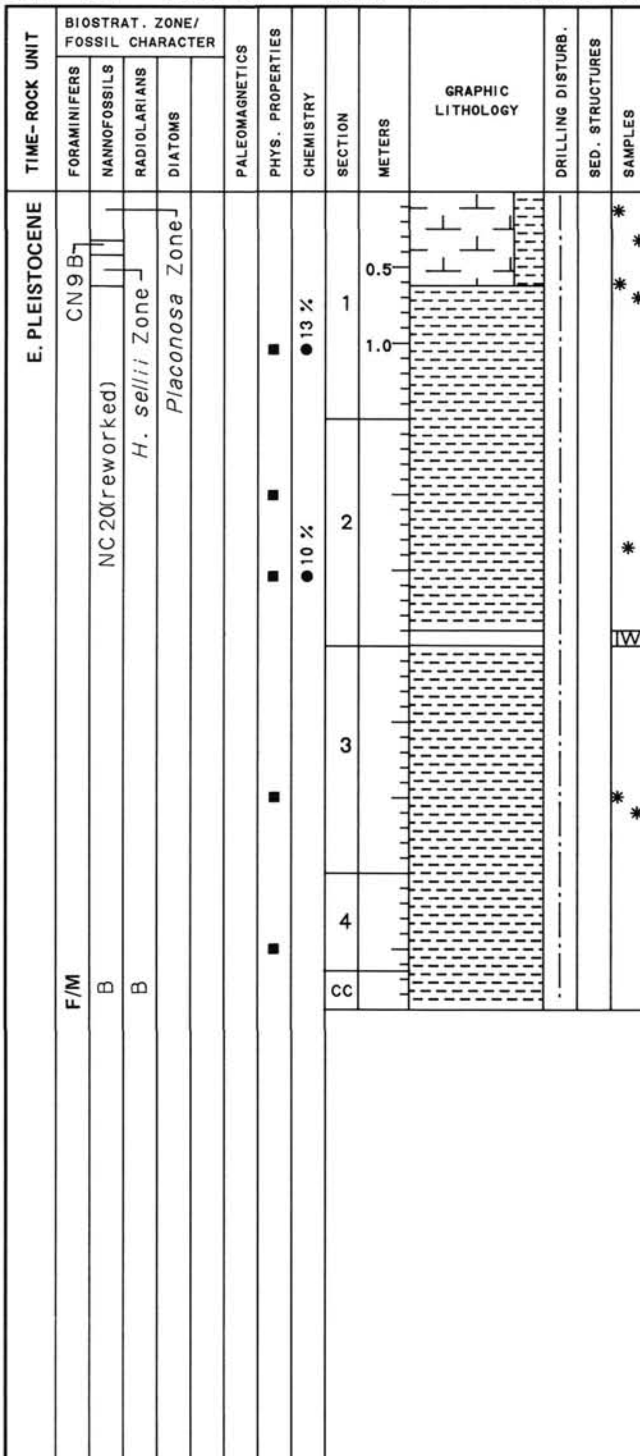

LITHOLOGIC DESCRIPTION

CLAYEY OOZE and BROWN CLAY.

The core consists of light yellowish brown (2.5Y6.5/4) and light gray (5Y7/1) clayey nannofossil ooze, overlying brown clay. The brown clay is slightly calcareous in the upper part. There are two clay lithologies: grayish brown (10YR5/2) and more reddish brown (7.5YR5/4) interbedded on a scale of 10-20 cm. The boundaries between them appear gradational. The brown clays are diffusely banded on a scale of 0.5-2.0 cm with very dark grayish brown (10YR3/2) clay (?richer in iron oxides and organic matter), and mottled with tiny black blebs of iron-manganese oxides. Both brown and reddish brown clays also show irregular light yellowish brown (10YR6/4) bands and blebs ranging 0.3-1.0 cm across. Minor dark brown and gray silt blebs (~0.1 cm) occur throughout. The entire core has been moderately deformed by drilling.

SMEAR SLIDE SUMMARY (%):

	1,12 D	1,32 D	1,60 M	1,65 D	2,86 M	3,105 D	3,109 D
TEXTURE:							
Silt	5	–	1	5	5	9	4
Clay	95	–	99	95	95	91	96
COMPOSITION:							
Quartz	–	–	–	Tr	–	–	4
Feldspar	–	–	–	–	–	–	Tr
Mica	–	–	–	–	2	–	5
Clay	10	10	2	10	95	91	89
Calcite/Dolomite	–	Tr	–	–	3	8	2
Accessory Minerals	–	–	–	–	–	Tr	Tr
Zeolites	Tr	–	–	–	2	–	–
Opaques	Tr	Tr	Tr	Tr	–	1	–
Fe Oxide	–	–	–	–	Tr	–	–
Foraminifers	5	1	1	5	–	–	–
Nannofossils	85	89	97	85	4	–	–
Fish Remains	Tr	Tr	–	–	–	–	–
Plant Debris	Tr	Tr	–	–	–	–	–
Ascidians	–	Tr	–	–	–	–	–

PHYSICAL PROPERTIES DATA:

	1,101	2,50	2,101	3,101	4,50
V_p (a)	1.58	–	1.51	1.55	–
ρ_b	1.79	–	1.74	1.75	–
T_c	–	2.66	–	–	2.52

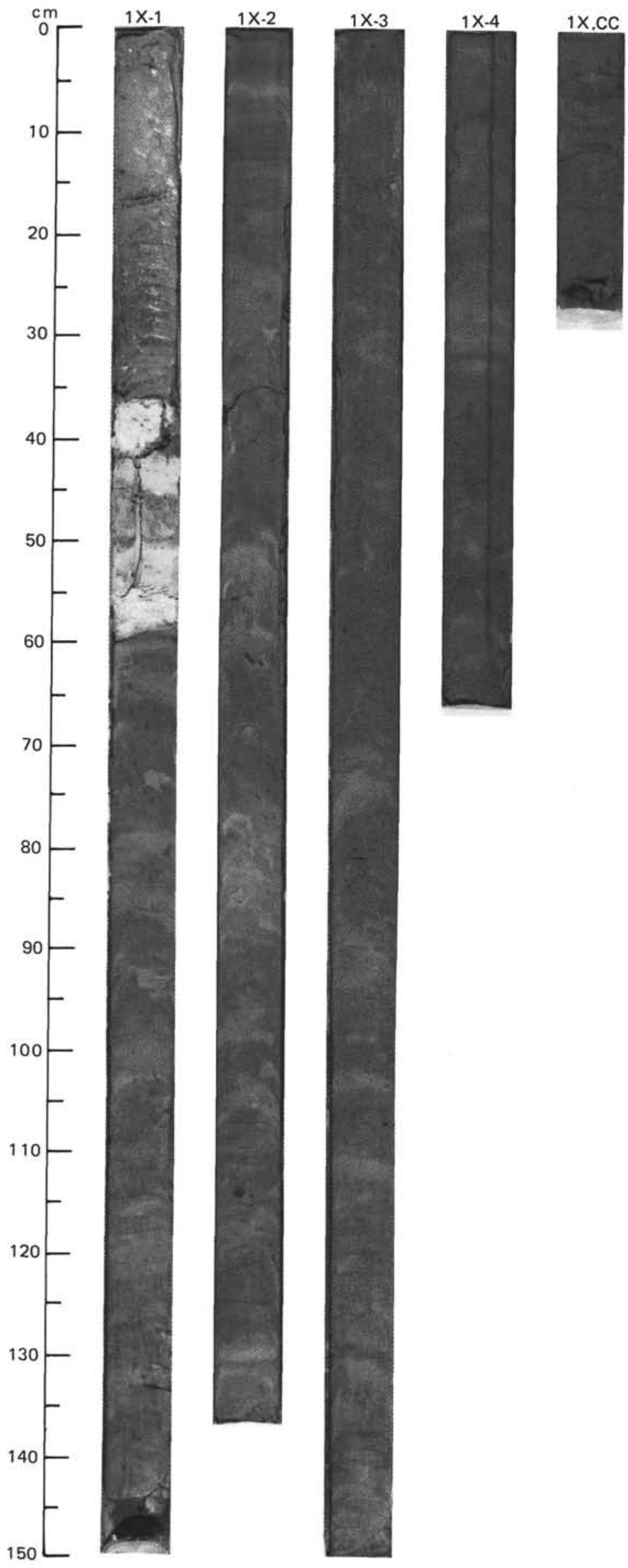
cm
0
10
20
30
40
50
60
70
80
90
100
110
120
130
140
150
1X-1
1X-2
1X-3
1X-4
1X,CC

SITE 641 HOLE A CORE 2 X CORED INTERVAL 4641.6-4651.2 mbsl; 6.1-15.7 mbsf

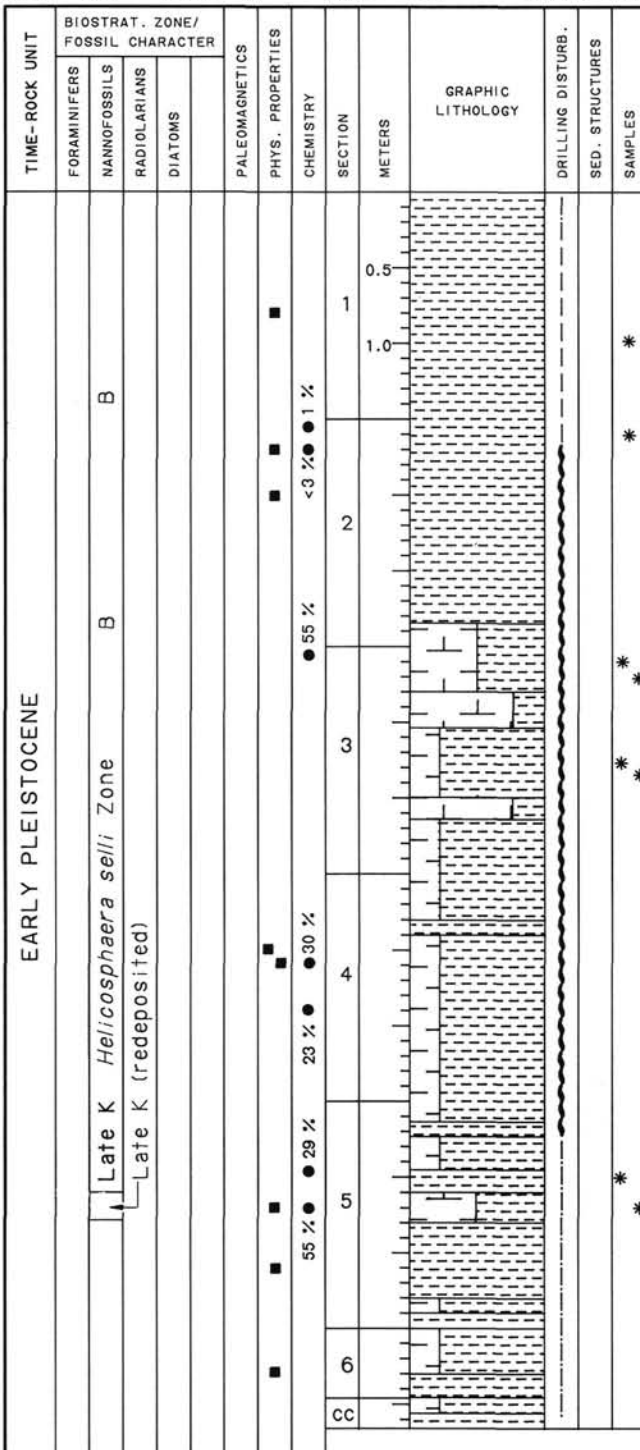

LITHOLOGIC DESCRIPTION

BROWN CLAY and CLAYEY OOZE and MARL

Down to Section 2, 26 cm the core consists of brown clay as in Core 1.

The remainder of Section 2 and Section 3 is a mixture of brown (10YR5/3) clay, bluish gray (5BG6/1) and black clay, light gray (5Y7/1) nannofossil marl, white (5Y8/1) clayey nannofossil ooze, and olive gray (5Y6/2) calcareous clay. Clasts range up to several centimeters across and appear to have been mixed by drilling and/ or as part of a natural slump. A pebble of sandstone or fine-grained acid igneous rock occurs at Section 3, 16 cm.

Below Section 3 the core consists of homogeneous olive gray (5Y 5.5/2) calcareous clay, light gray (2.5Y7/2) mottled nannofossil marl and brown clay.

SMEAR SLIDE SUMMARY (%):

	1,96 D	2,10 D	3,6 D	3,7 D	3,75 D	3,76 D	5,50 D	5,58 D
TEXTURE:								
Sand	—	—	4	—	Tr	—	—	—
Silt	5	5	11	7	7	5	17	2
Clay	95	95	85	93	93	95	83	98
COMPOSITION:								
Quartz	—	Tr	—	—	Tr	—	3	—
Feldspar	—	10	—	—	—	—	Tr	—
Mica	—	—	Tr	—	1	—	1	—
Clay	95	88	20	10	56	45	80	8
Calcite/Dolomite	3	—	—	—	Tr	Tr	10	1
Accessory Minerals	2	2	1	Tr	Tr	1	1	Tr
Foraminifers	—	—	12	7	3	3	2	—
Nannofossils	—	—	67	83	40	50	3	91

PHYSICAL PROPERTIES DATA:

	1,81	2,19	2,50	4,50
$V\rho$ (a)	1.46	1.50	—	—
ρ_b	1.80	1.76	—	—
T_c	—	—	2.04	2.16

	4,54	5,69	5,109	6,30
$V\rho$ (a)	1.46	1.61	1.49	—
ρ_b	1.50	1.88	1.72	—
T_c	—	—	—	2.43

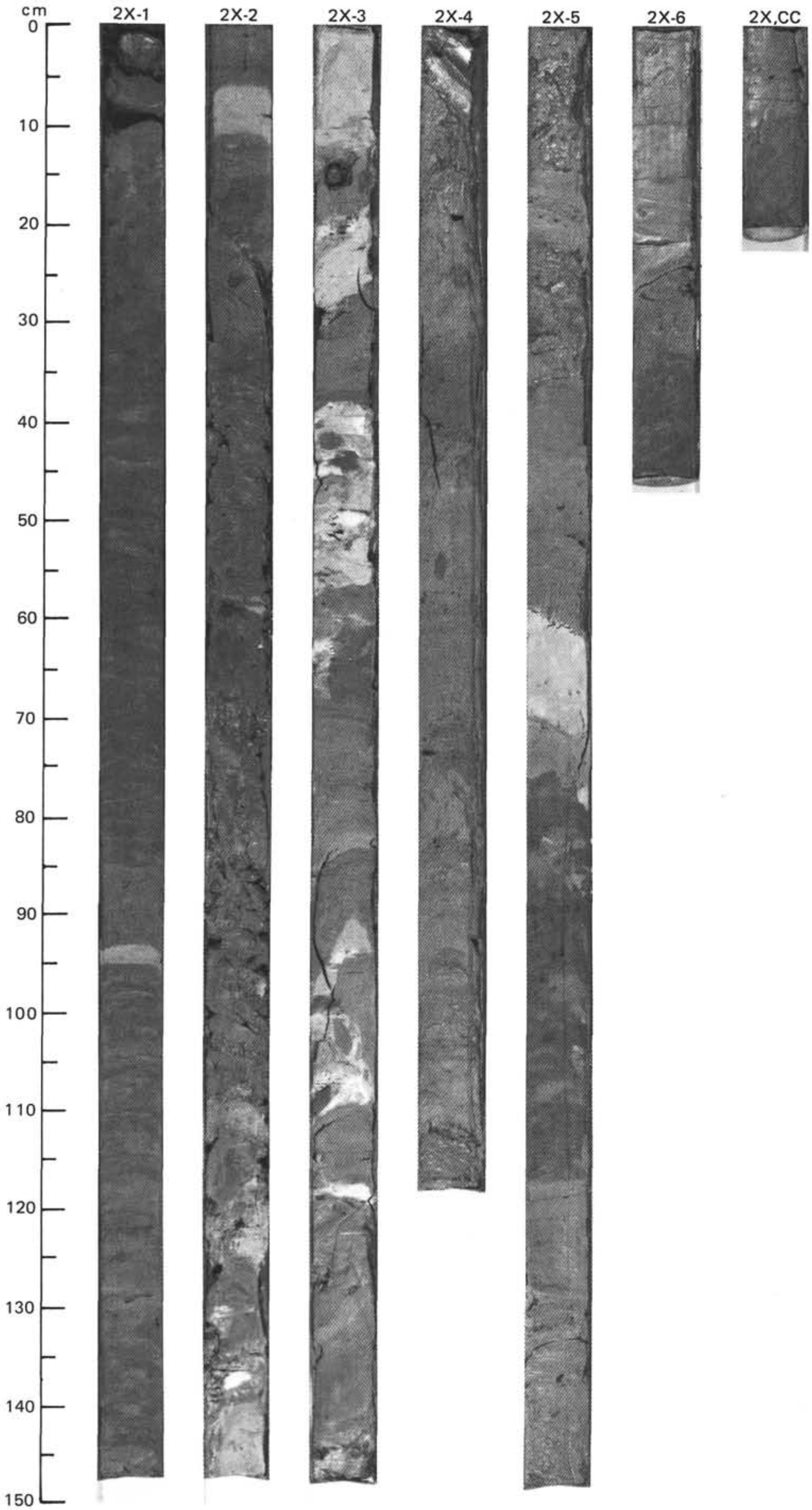
cm
0
10
20
30
40
50
60
70
80
90
100
110
120
130
140
150
2X-1
2X-2
2X-3
2X-4
2X-5
2X-6
2X,CC

SITE 641 HOLE A CORE 3X CORED INTERVAL 4651.2-4660.8 mbsl; 15.7-25.3 mbsf

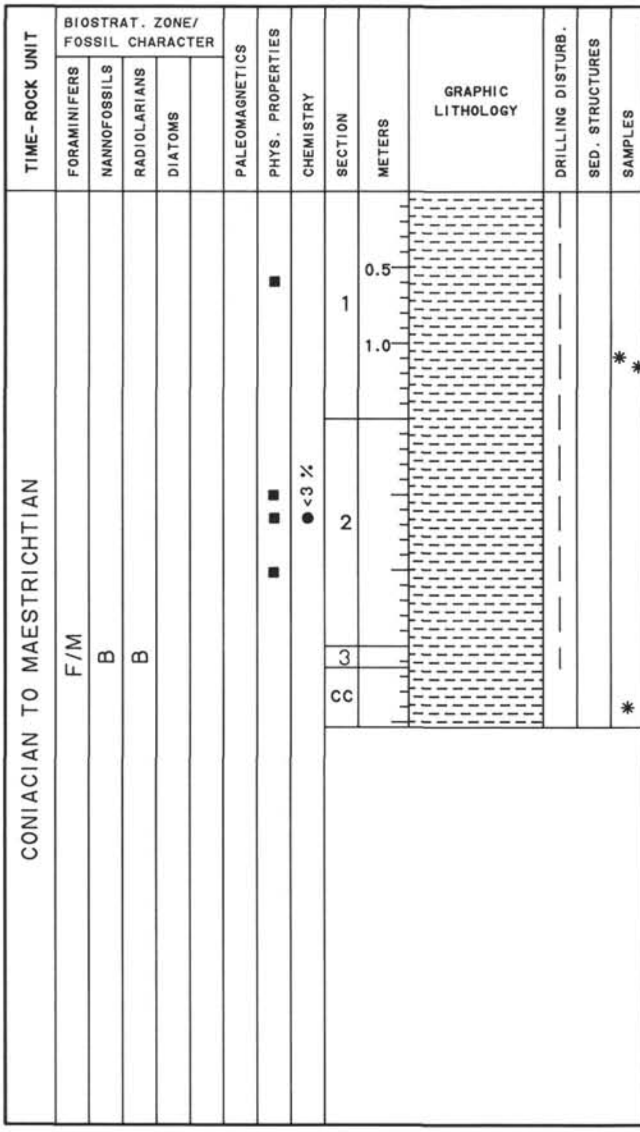

LITHOLOGIC DESCRIPTION

BROWN CLAY

The core consists of diffusely banded brown (7.5YR4.5/4) and dark grayish brown (10YR4.5/2) clay. Brown and dark brown clay alternate on a scale of 10-30 cm. Banding is on a scale of 0.5-5.0 cm. The clay is recrystallized. Dark gray-brown spots of iron-manganese oxide 0.1-0.2 cm across are present in the dark grayish brown clay. Red (10R4/6) and gray green (5GY7/1) patches, 1-2 cm across, occur at Section 1, 105-107 cm and 119-122 cm.

SMEAR SLIDE SUMMARY (%):

	1,105 M	1,112 D	CC,36 M
TEXTURE:			
Clay	100	100	100
COMPOSITION:			
Quartz	—	—	3
Mica	—	2	—
Clay	98	80	82
Calcite/Dolomite	—	—	1
Accessory Minerals	2	Tr	4
Zeolites	—	15	10
Fe-Oxide	—	3	—

PHYSICAL PROPERTIES DATA:

	1,61	2,50	2,61	2,100
V_p (a)	1.51	—	1.49	—
ρ_b	1.75	—	1.72	—
T_c	—	2.46	—	2.60

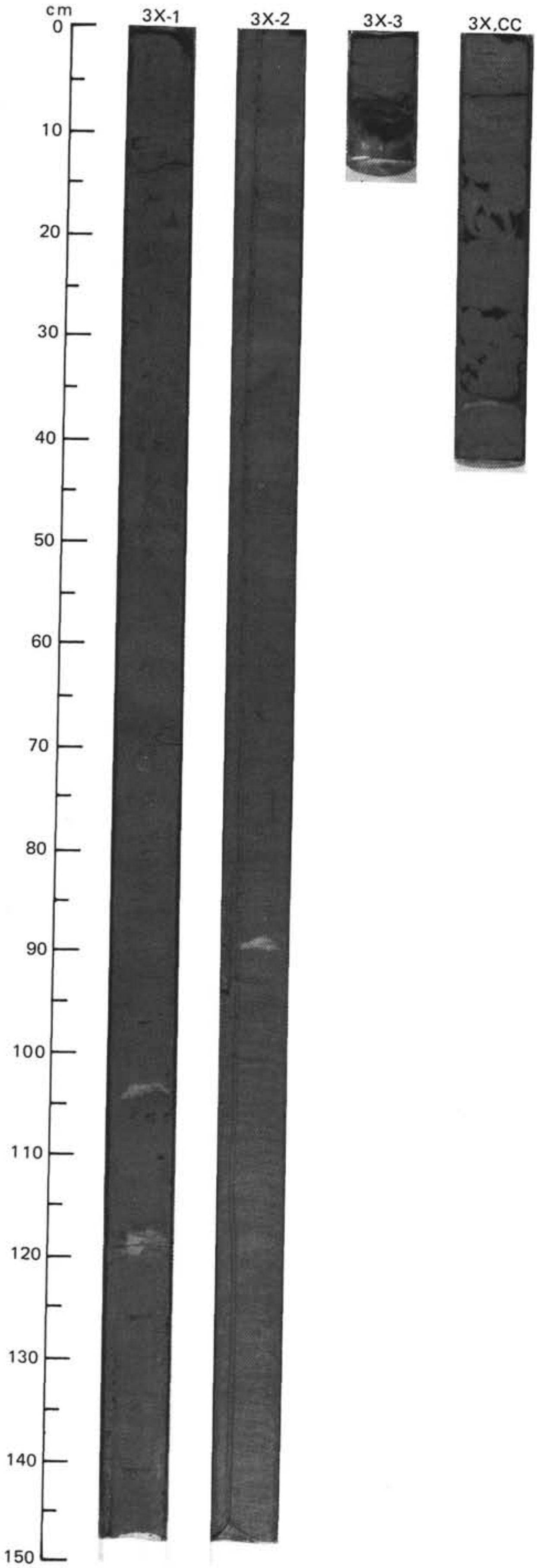
cm
0
10
20
30
40
50
60
70
80
90
100
110
120
130
140
150
3X-1
3X-2
3X-3
3X,CC

SITE 641 HOLE A CORE 4X CORED INTERVAL 4660.8-4670.4 mbsl; 25.3-34.9 mbsf

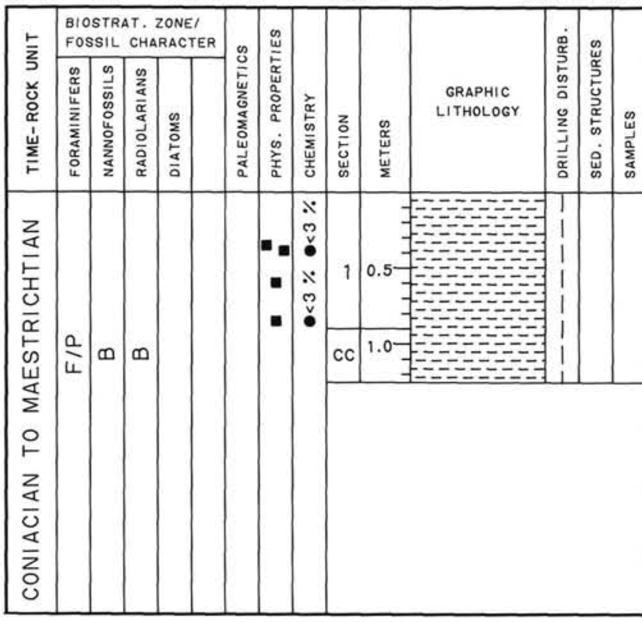

LITHOLOGIC DESCRIPTION

BROWN CLAY

The core consists of dark grayish brown (10YR4.5/2) and reddish brown (5YR5/3) clay, as in Core 3, alternating on a scale of 10-30 cm. Overall the color is redder and iron-manganese spots are rare. The core is very uniform and structureless, except for diffuse banding on a scale of 0.5-1.0 cm.

PHYSICAL PROPERTIES DATA:

	1,30	1,36	1,60	1,81
V_p (a)	–	1.57	–	1.56
ρ_b	–	1.75	–	1.76
T_c	2.41	–	2.21	–

SITE 641 HOLE A CORE 5X CORED INTERVAL 4670.4-4680.0 mbsl; 34.9-44.5 mbsf

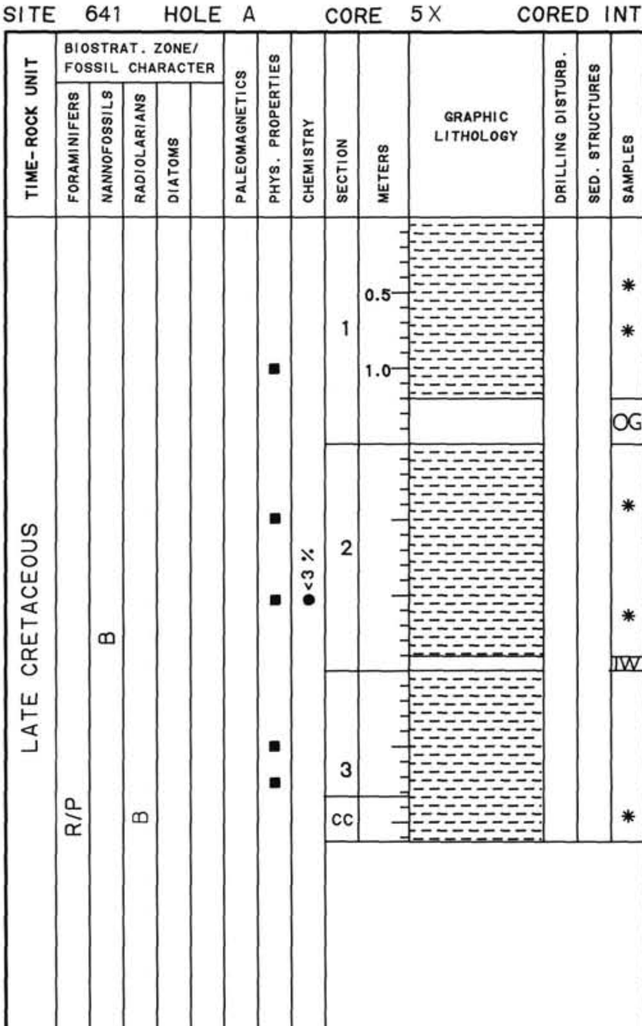

LITHOLOGIC DESCRIPTION

BROWN CLAY

The core consists of dark grayish brown (10YR4/2) and reddish brown (5YR5/4) clay, as in Core 3, alternating on a scale of 10-30 cm, moderately deformed by drilling so that the dark layers are mixed into lighter layers. No internal structures or lamination are visible, except for a slight suggestion of mottling.

SMEAR SLIDE SUMMARY (%):

	1,43 D	1,71 D	2,40 M	2,112 D	CC,17 D
TEXTURE:					
Silt	10	5	–	5	5
Clay	90	95	100	95	95
COMPOSITION:					
Quartz	15	10	Tr	5	5
Mica	Tr	Tr	Tr	Tr	Tr
Clay	80	87	100	95	95
Accessory Minerals	5	2	–	–	Tr
Zeolites	–	1	–	–	–

PHYSICAL PROPERTIES DATA:

	1,101	2,50	2,101	3,50	3,72
V_p (a)	1.54	–	1.54	–	1.54
ρ_b	1.76	–	1.74	–	1.75
T_c	–	2.66	–	2.49	–

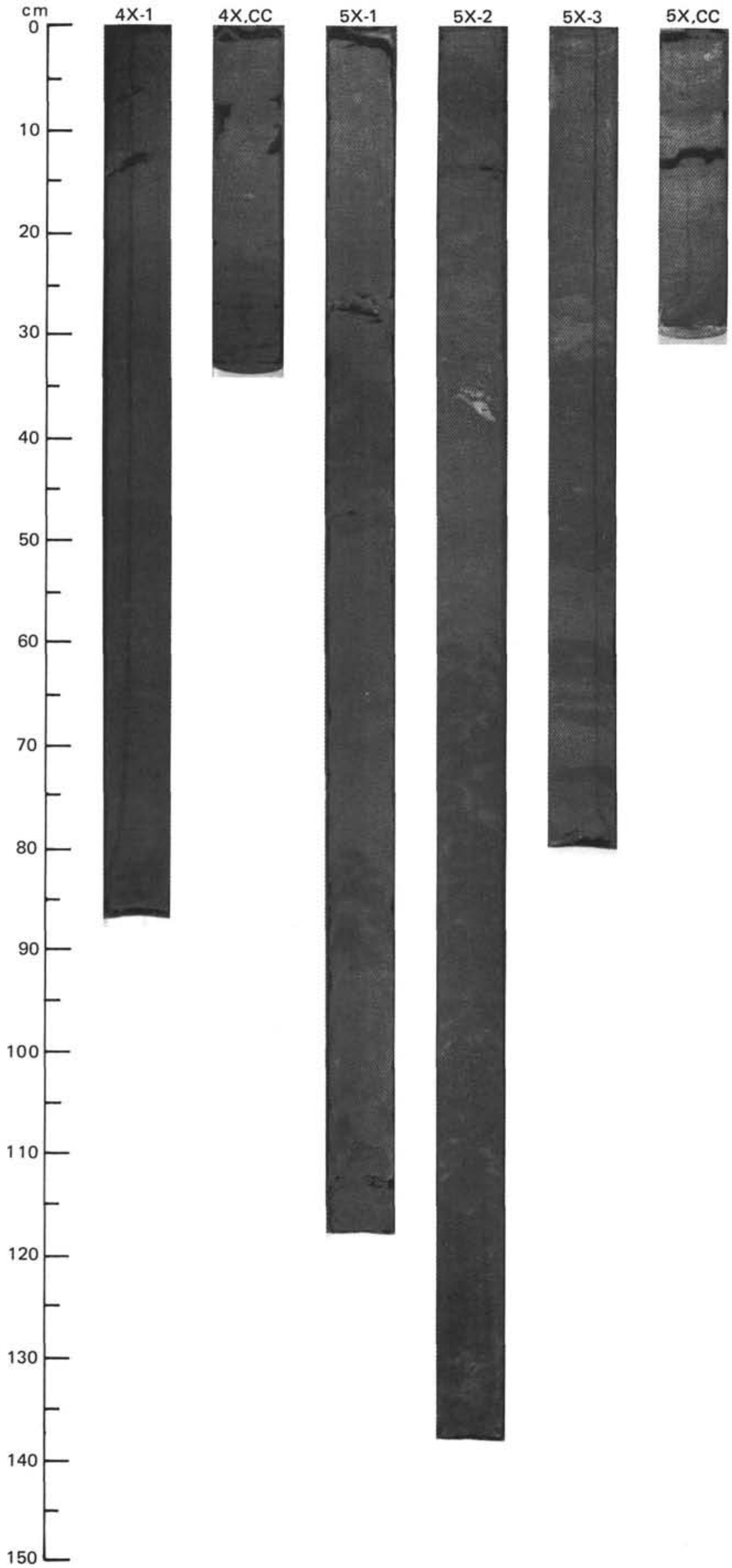
cm
0
10
20
30
40
50
60
70
80
90
100
110
120
130
140
150
4X-1
4X,CC
5X-1
5X-2
5X-3
5X,CC

SITE 641 HOLE A CORE 6X CORED INTERVAL 4680.0–4689.6 mbsl; 44.5–54.1 mbsf

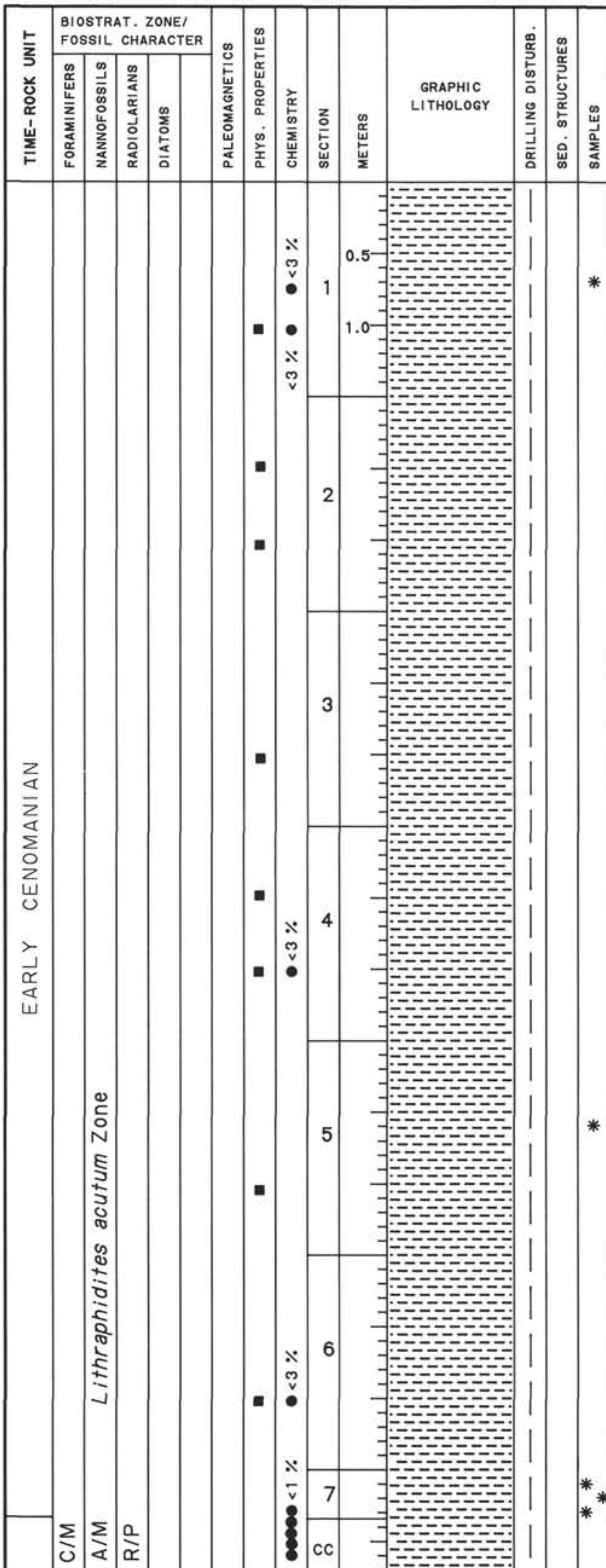

LITHOLOGIC DESCRIPTION

BROWN, GREEN-GRAY, and BLACK CLAY

Down to Section 7, 17 cm the core consists of structureless dark brown and reddish brown clay as in the preceding cores. Small (1-2 cm) patches of greenish gray clay occur at Section 2, 45 cm, and Section 3, 70-98 cm.

The sequence below Section 6 is:

(1) Section 7, 0-17 cm: uniform yellowish brown (10YR5/4) clay.

(2) Section 7, 17-27 cm: greenish gray (5G6/1) clay, becoming darker (5G5/1) downward.

(3) Section 7, 27-32 cm, and CC, 0-20 cm: homogeneous black (2.5Y2/0) clay.

(4) CC, 20-45 cm: greenish gray (5G5/1) to light greenish gray (5GY6/1) clay, faintly banded with darker gray blebs.

The color boundaries in Section 7 and CC are sharp, but disturbed by drilling.

SMEAR SLIDE SUMMARY (%):

	1,70 D	5,60 D	7,7 D	7,22 D	7,30 D
TEXTURE:					
Silt	5	2	5	–	5
Clay	95	98	95	100	95
COMPOSITION:					
Quartz	5	Tr	5	7	5
Mica	–	Tr	–	Tr	–
Clay	93	98	90	93	72
Accessory Minerals	2	–	5	Tr	3
Zeolite	Tr	–	–	Tr	10
Plant Debris/Organic	–	2	–	–	10

PHYSICAL PROPERTIES DATA:

	1,101	2,50	2,101	3,101
V_p (a)	1.54	–	1.44	1.49
ρ_b	1.73	–	1.66	1.73
T_c	–	2.30	–	–

	4,50	4,101	5,101	6,101
V_p (a)	–	1.55	1.56	1.58
ρ_b	–	1.67	1.75	1.77
T_c	2.18	–	–	–

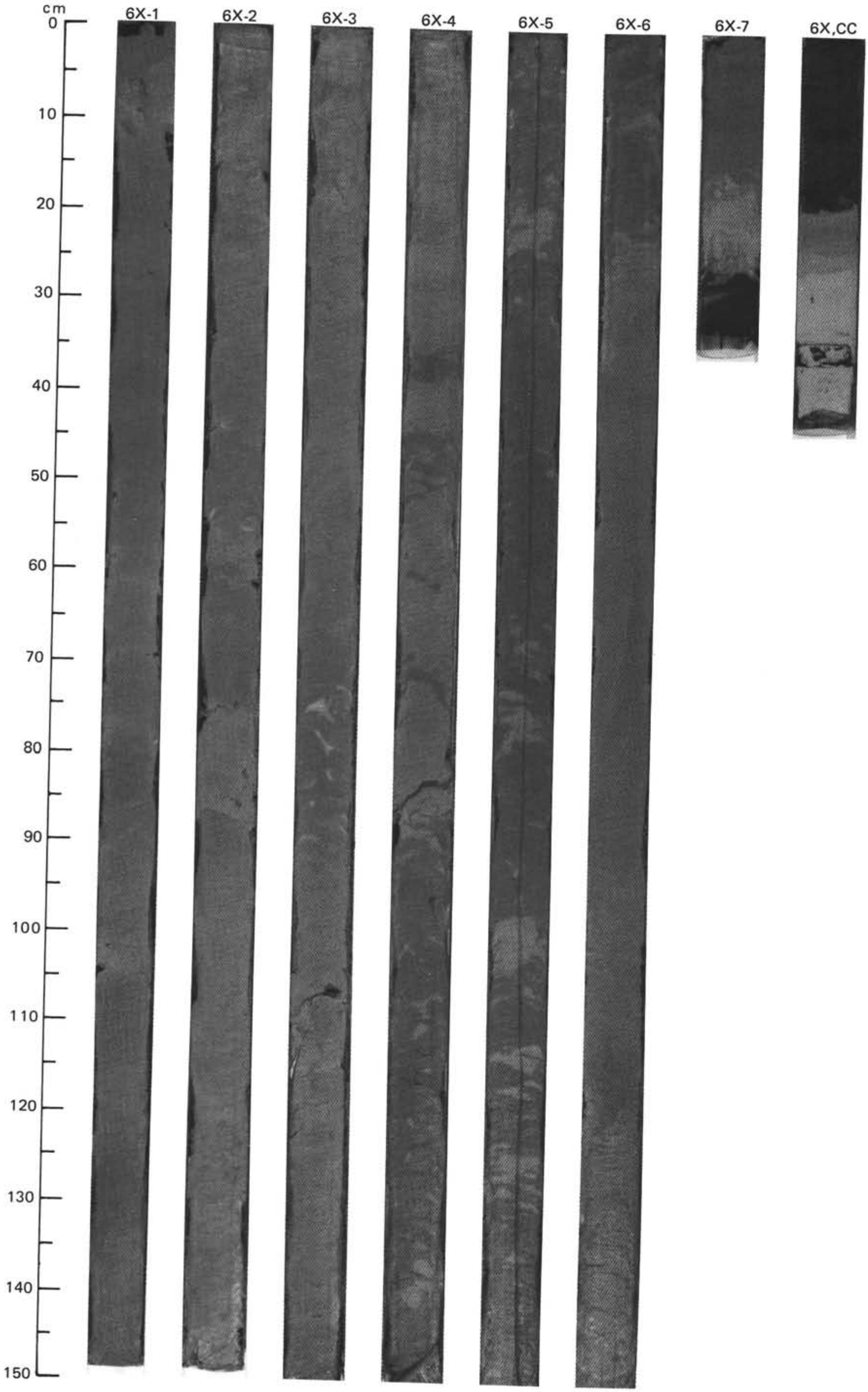
cm
0
10
20
30
40
50
60
70
80
90
100
110
120
130
140
150
6X-1
6X-2
6X-3
6X-4
6X-5
6X-6
6X-7
6X,CC

SITE 641 HOLE A CORE 7X CORED INTERVAL 4689.6-4699.1 mbsl; 54.1-63.6 mbsf

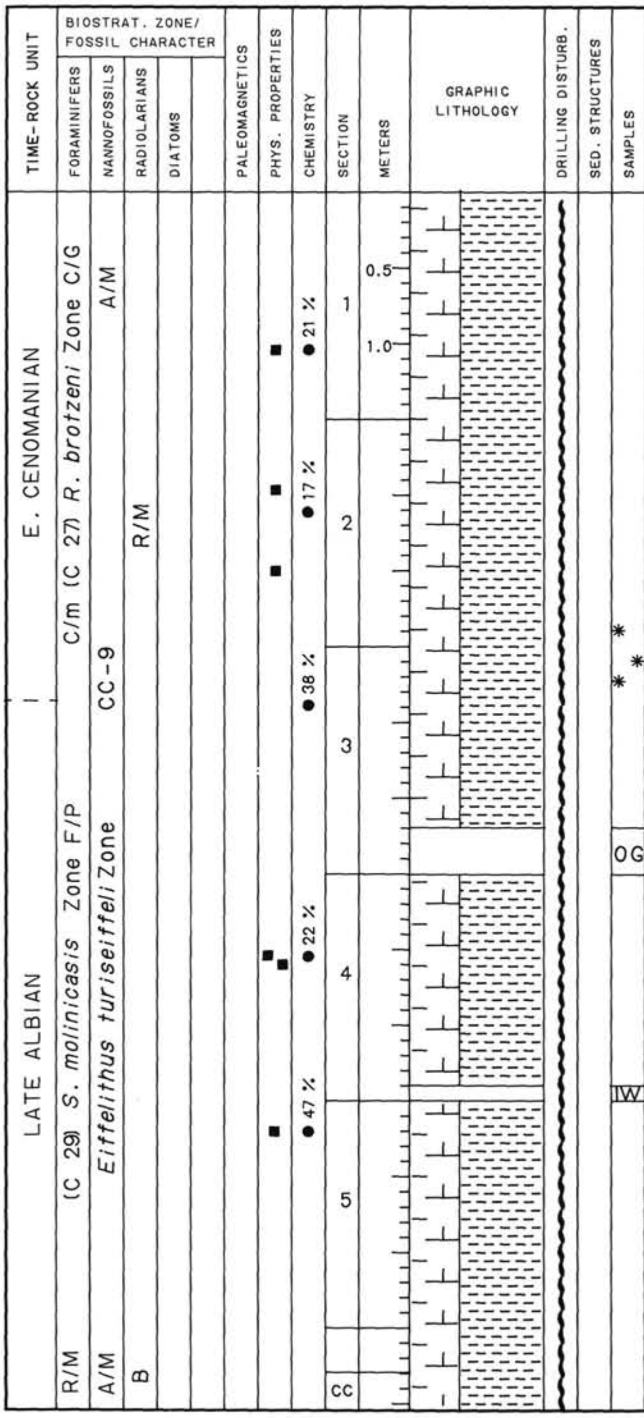

LITHOLOGIC DESCRIPTION

GREEN-GRAY CALCAREOUS CLAY and NANNOFOSSIL MARL

The core is a mixture of greenish gray (5G5/1), gray (5Y6/1, 5Y5/1) calcareous clay and nannofossil marl, badly disturbed by drilling. There is some suggestion of mottling and lamination, but drilling has obliterated the internal structure of the sediments. Section 3 is generally grayer than above and below.

SMEAR SLIDE SUMMARY (%):

	2,137 D	3,11 D	3,20 D
TEXTURE:			
Silt	3	5	2
Clay	97	95	98
COMPOSITION			
Quartz	3	–	Tr
Mica	–	Tr	Tr
Clay	74	50	50
Accessory Minerals	3	–	–
Zeolites	Tr	Tr	–
Foraminifers	–	5	2
Nannofossils	20	45	48

PHYSICAL PROPERTIES DATA:

	1,102	2,50	2,101	4,50	4,57	5,20
V_p (a)	1.51	–	1.50	–	1.55	1.44
ρ_b	1.71	–	1.64	–	1.65	1.71
Tc	–	2.61	–	2.53	–	–

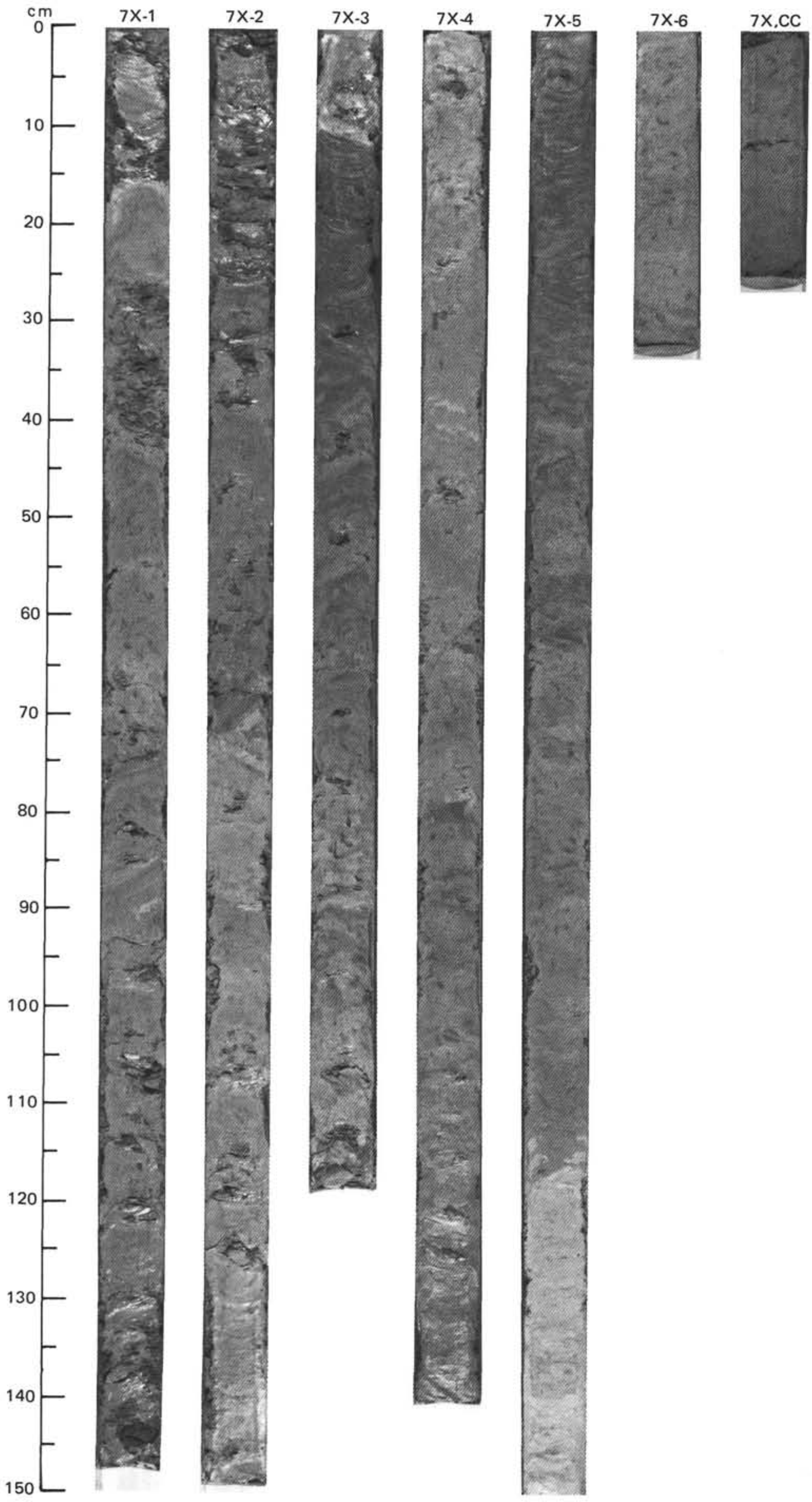
cm
0
10
20
30
40
50
60
70
80
90
100
110
120
130
140
150
7X-1
7X-2
7X-3
7X-4
7X-5
7X-6
7X,CC

SITE 641 HOLE C CORE 1 R CORED INTERVAL 4790.4-4800 mbsl; 150.9-160.5 mbsf

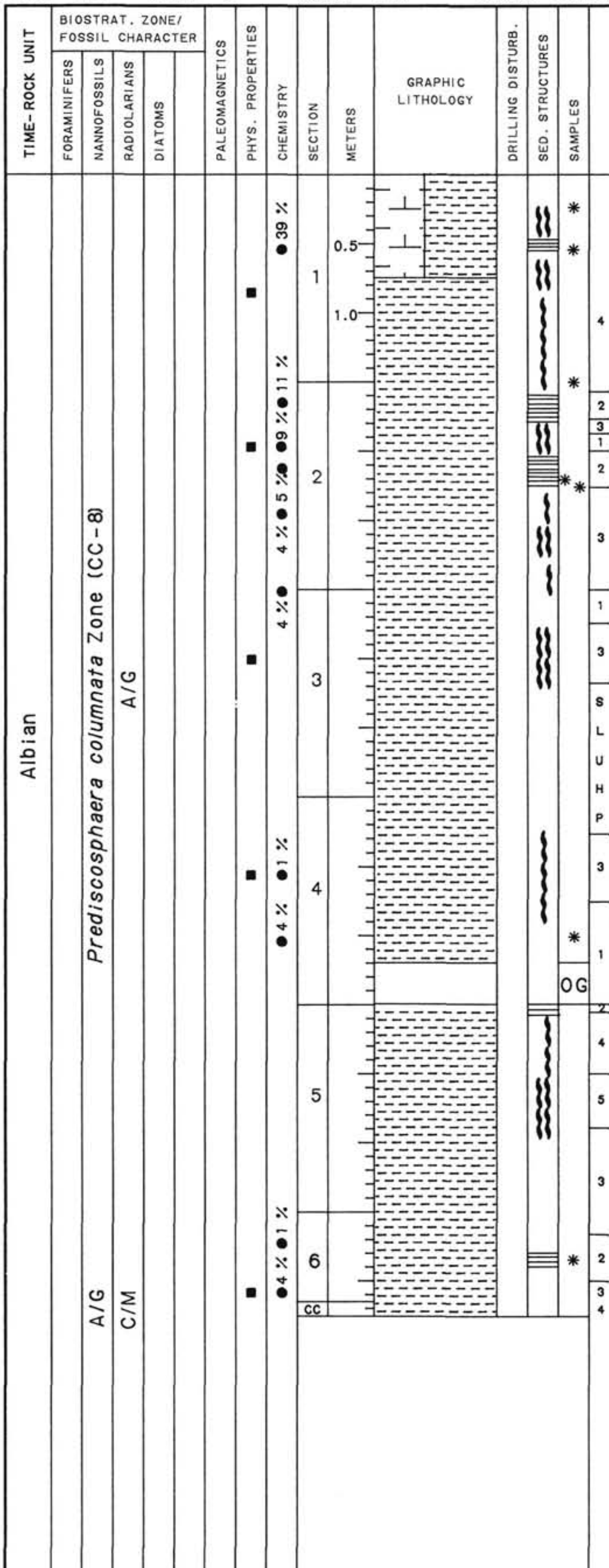

LITHOLOGIC DESCRIPTION

BLACK and GREENISH GRAY CLAYSTONE

The topmost 75 cm of the core are greenish gray, bioturbated marlstone. Below this, five distinct lithologies are present in this and succeeding cores:

(1) Massive black (5Y2.5/1) claystone;

(2) Laminated black (5Y2.5/1) claystone;

(3) Interbedded, on a scale of 0.1-1.5 cm, black (7.5YR3/0) and dark greenish gray (5BG4/1) claystone. The proportions of black and green are highly variable. Lamination is present but wispy, irregular and discontinuous. Laminae are generally black and <0.2 cm thick. Bioturbation is light to moderate.

(4) Greenish-gray (5GY6/1 & 5G5/1) claystone, lightly bioturbated with generally large (0.4-2 cm) black burrows. Lamination is faint or absent.

(5) Grayish green (5G5/2) and greenish gray (5G5/1) massive claystone.

These lithologies are interbedded on a scale of 10-80 cm. Lithologies 1-3 are most common. The rocks are largely undisturbed by drilling, and boundaries between lithologies are generally gradational. Burrows are commonly flattened parallel to the lamination(compaction).

Section 3, 70 cm to Section 4, 26 cm is a mixture of pebbles of all five lithologies. Clasts are <5 cm across and subhorizontal. This interval is considered to be a slump or debris flow.

Where lamination is present in Core 1, dips range up to 13°.

?Siderite nodules and laminae occur at Section 2, 75 cm, and Section 6, 35 cm.

SMEAR SLIDE SUMMARY (%):

	1,25 D	1,52 D	2,1 D	2,72 D	2,74 M	4,99 D	6,33 M
TEXTURE:							
Silt	–	3	2	7	100	3	100
Clay	100	97	98	93	–	97	–
COMPOSITION:							
Mica	2	2	–	Tr	–	1	–
Clay	90	62	36	8	–	92	–
Calcite/Dolomite	1	2	2	1	–	–	–
Accessory Minerals	–	Tr	–	–	–	–	–
Zeolites	2	2	2	3	–	2	–
Pyrite	–	–	–	5	1	1	1
Siderite	–	–	–	–	99	–	99
Foraminifers	–	1	–	–	–	–	–
Nannofossils	5	30	50	–	–	–	–
Organic matter	<1	1	–	7	Tr	2	Tr

PHYSICAL PROPERTIES DATA:

	1,86	2,48	3,52	4,54
V_p (a)	1.65	1.66	1.66	1.63
V_p (b)	1.73	1.71	1.75	1.68
V_p (c)	1.71	1.70	1.74	1.69
ρ_b	1.81	1.75	1.79	1.74

	5,47	5,50	5,100	6,57
V_p (a)	1.70	–	–	1.72
V_p (b)	1.77	–	–	1.82
V_p (c)	1.75	–	–	1.79
ρ_b	1.83	–	–	1.84
T_c	–	2.48	2.49	–

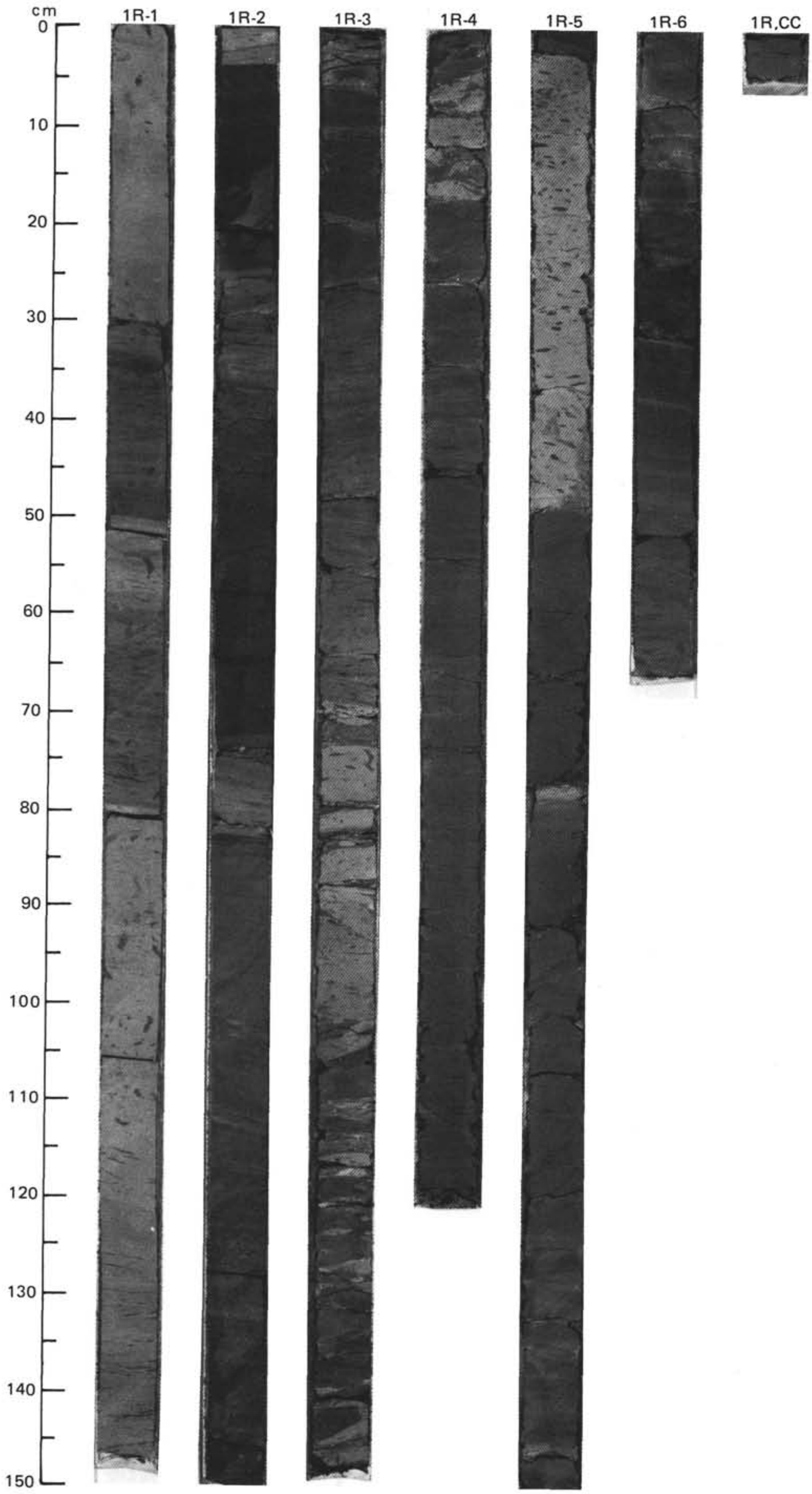
cm
0
10
20
30
40
50
60
70
80
90
100
110
120
130
140
150
1R-1
1R-2
1R-3
1R-4
1R-5
1R-6
1R,CC

SITE 641 HOLE C CORE 2 R CORED INTERVAL 4800–4809.6 mbsl; 160.5–170.1 mbsf

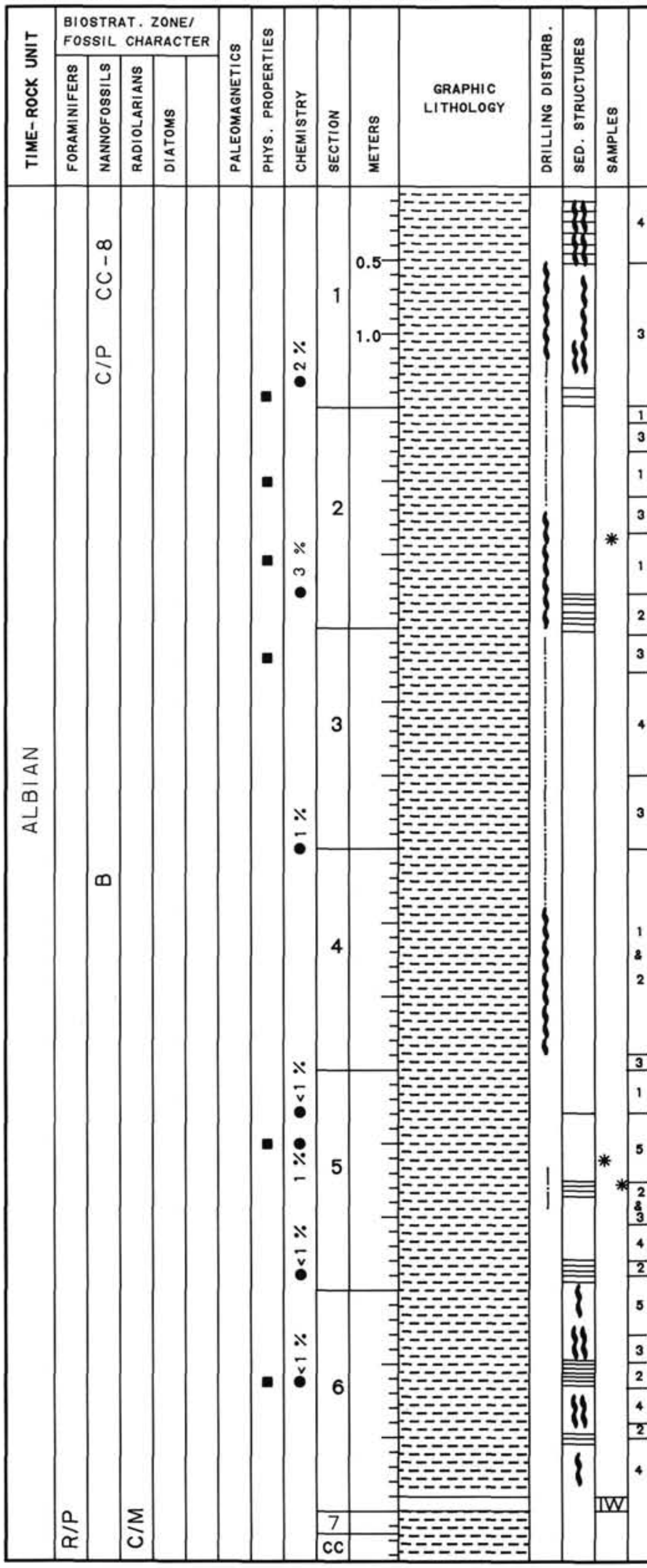

LITHOLOGIC DESCRIPTION

BLACK and GREENISH GRAY CLAYSTONE

The core consists of the same lithologies as Core 641C-1 (q.v.), but Lithologies 1-4 are dominant and subequal in amount. Lamination in Core 2 is near horizontal. ?Siderite nodules and laminae occur at Section 1, 130 & 139 cm, Section 2, 0-8, 39, 84-88, 92-93, 131, & 141 cm, Section 4, 27-30 cm, and Section 5, 73-74 cm.

SMEAR SLIDE SUMMARY (%):

	2,84	5,58	5,79
	M	D	M
TEXTURE:			
Silt	100	–	–
Clay	–	100	100
COMPOSITION:			
Mica	–	Tr	–
Clay	–	98	100
Accessory Minerals	–	Tr	–
Siderite	100	–	–

PHYSICAL PROPERTIES DATA:

	1,144	2,50	2,100	3,119	5,51	6,53
V_p (a)	1.79	–	–	1.76	1.72	1.74
V_p (b)	1.86	–	–	1.86	1.79	1.80
ρ_b	1.81	–	–	1.83	1.78	1.78
T_c	–	2.52	2.30	–	–	–

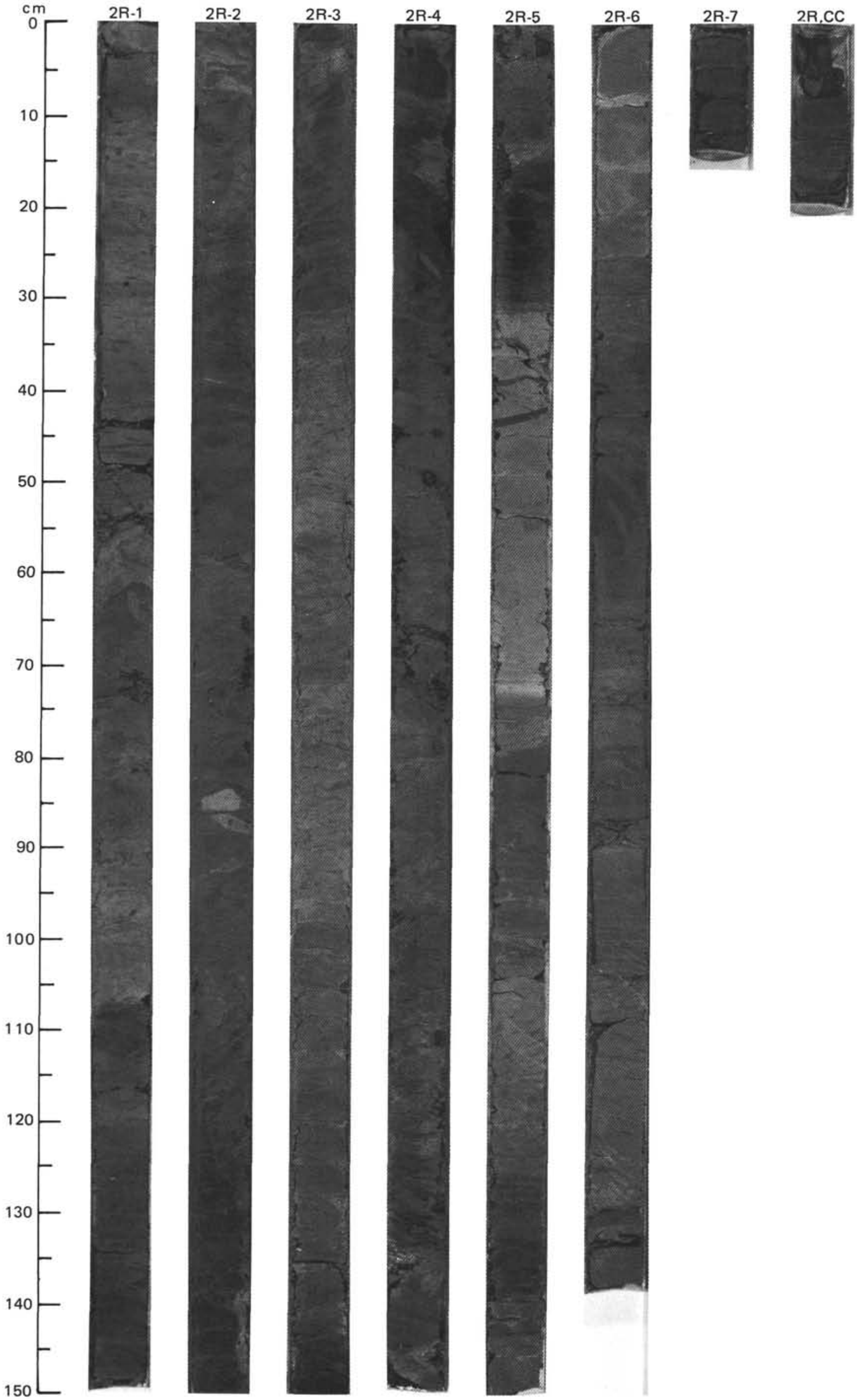
cm
0
10
20
30
40
50
60
70
80
90
100
110
120
130
140
150
2R-1
2R-2
2R-3
2R-4
2R-5
2R-6
2R-7
2R,CC

SITE 641 HOLE C CORE 3 R CORED INTERVAL 4809.6-4819.3 mbsl; 170.1-179.8 mbsf

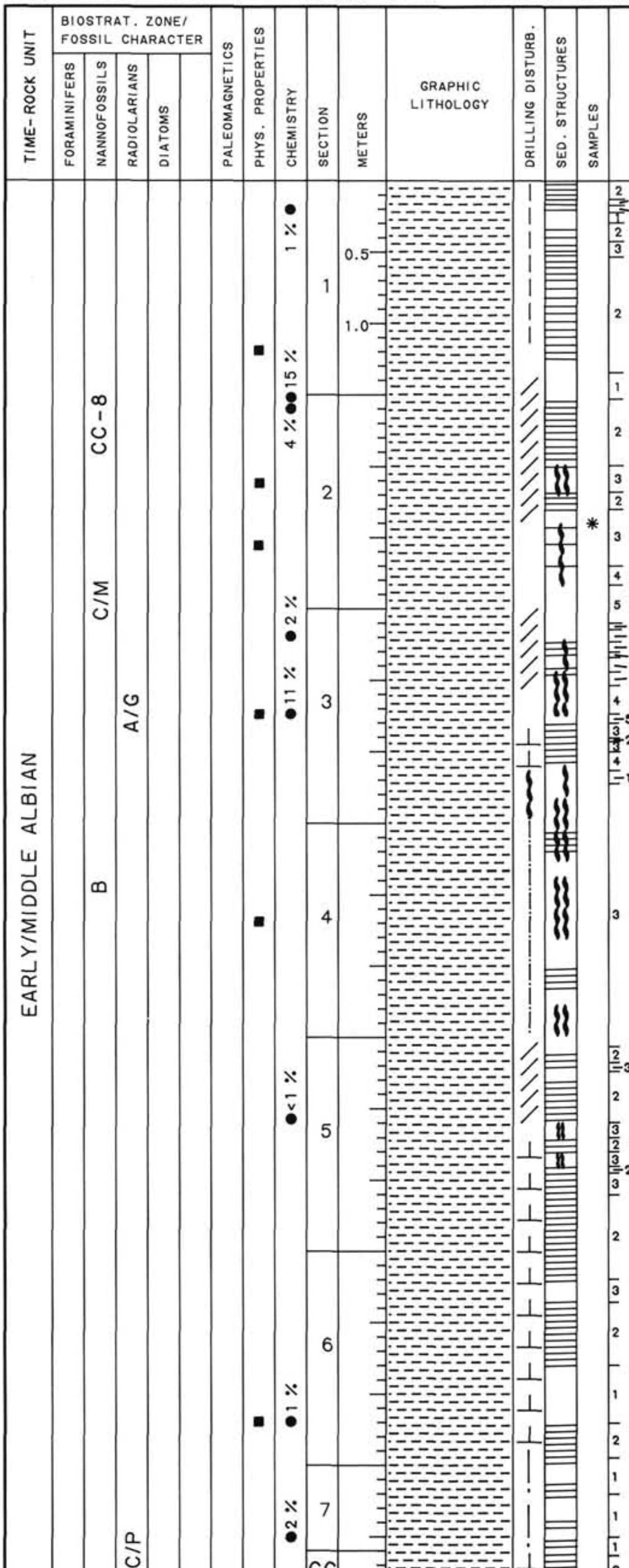

LITHOLOGIC DESCRIPTION

BLACK and GREENISH GRAY CLAYSTONE

The core consists of the same lithologies as Core 641C-1 (q.v.), but Lithologies 1, 2, and 3 are dominant. Thin brownish (2.5Y5/2) laminae occur at Section 2, 130 cm. Lamination in Core 3 dips up to 13°. Pyrite nodules occur at Section 1, 133-150, Section 2, 53-54 cm; pyritized wood at Section 5, 55-57 cm, and ?siderite nodules and laminae at Section 3, 42-43 cm, Section 6, 50-51 & 104-105 cm.

SMEAR SLIDE SUMMARY (%):

	2,84
	M
COMPOSITION:	
Mica	10
Clay	61
Accessory Minerals:	
Pyrite	20
Zeolite	2
Nannofossils	7

PHYSICAL PROPERTIES DATA:

	1,114	2,60	2,102	3,69	4,65	6,116
V_p (a)	1.73	–	–	1.81	1.74	1.75
V_p (b)	1.86	–	–	1.90	1.83	1.84
ρ_b	1.82	–	–	1.86	1.78	1.78
T_c	–	4.35	4.70	–	–	–

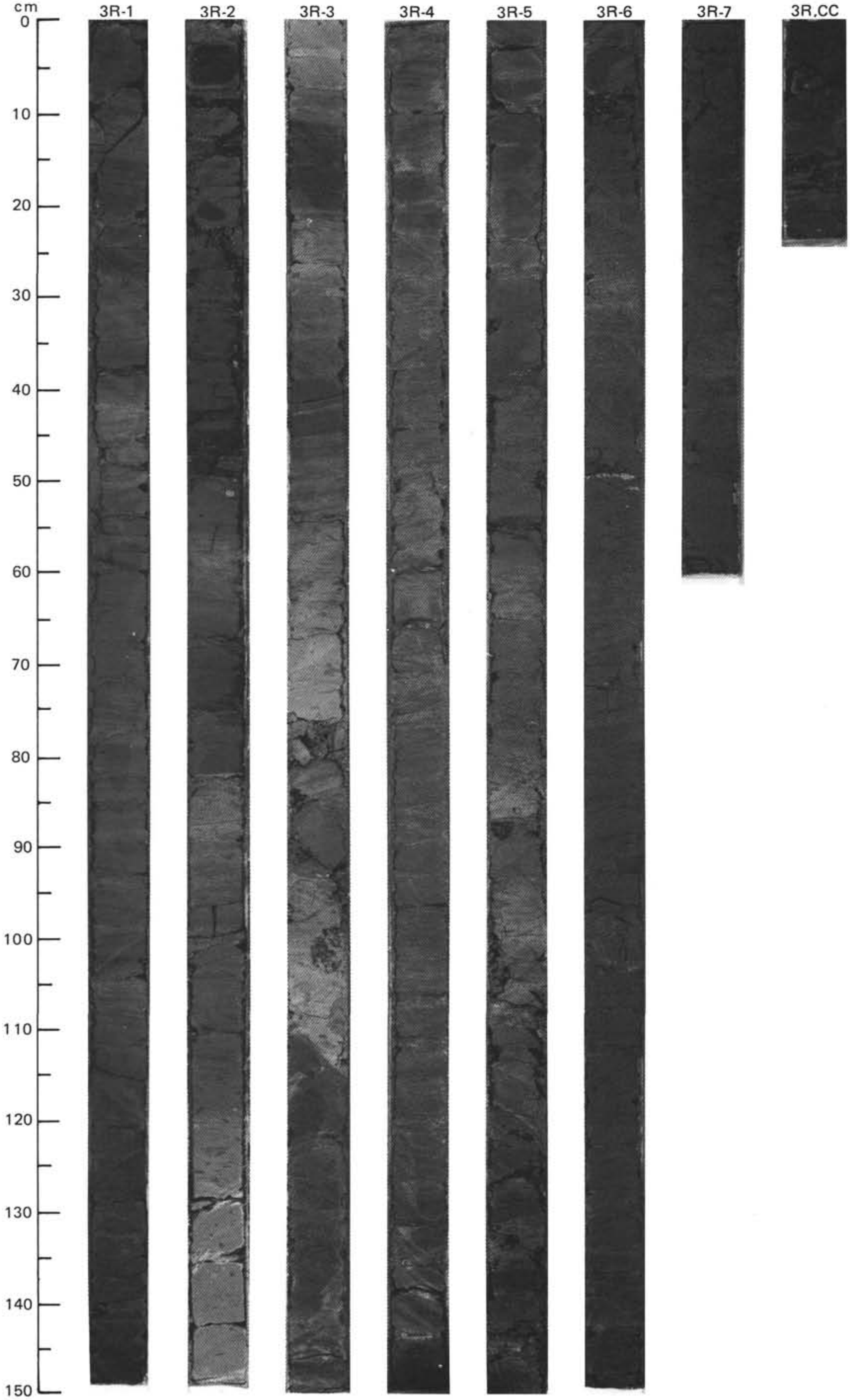
cm
0
10
20
30
40
50
60
70
80
90
100
110
120
130
140
150
3R-1
3R-2
3R-3
3R-4
3R-5
3R-6
3R-7
3R,CC

SITE 641 HOLE C CORE 4 R CORED INTERVAL 4819.3–4828.9 mbsl; 179.8–189.4 mbsf

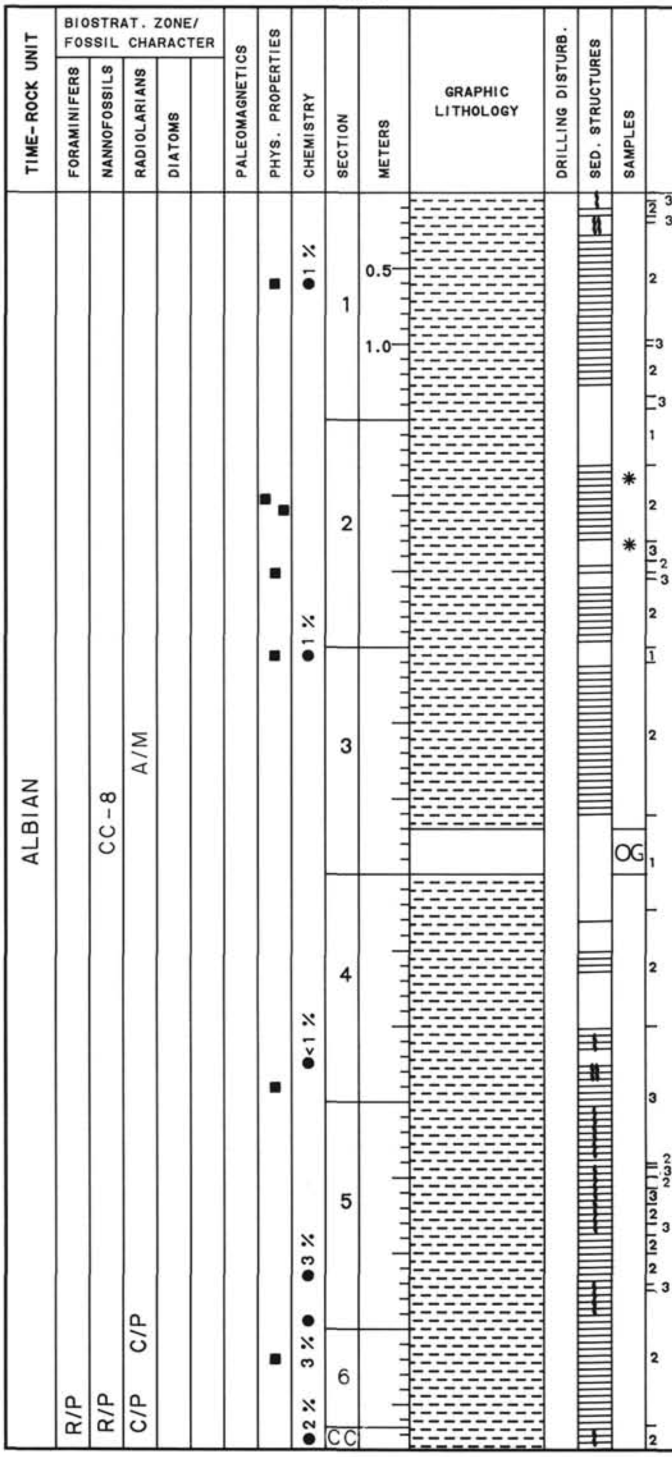

LITHOLOGIC DESCRIPTION

BLACK and GREENISH GRAY CLAYSTONE

The core consists of the same lithologies as Core 641C-1 (q.v.), but Lithologies 1, 2, and 3 are dominant. Interbedding of lithologies is on the scale of 5-100 cm.

Laminated quartz-rich siltstone and very fine sandstone layers up to 1 cm thick occur at Section 2, 102 cm, Section 5, 40, 134, & 144 cm and Section 6, 19 cm.

Lamination in Core 4 dips up to 11°.

SMEAR SLIDE SUMMARY (%):

	2,41 M	2,83 M
TEXTURE:		
Silt	10	–
Clay	90	–
COMPOSITION:		
Quartz	15	–
Clay	75	–
Calcite/Dolomite	–	93
Accessory Minerals	4	–
Zeolites	6	–
Opaques	–	5
Radiolarians	Tr	–

PHYSICAL PROPERTIES DATA:

	1,62	2,50	2,58	2,100
V_p (a)	1.74	–	1.72	–
V_p (b)	1.82	–	–	–
ρ_b	1.83	–	–	–
T_c	–	2.47	–	2.35

	3,4	4,141	6,15
V_p (a)	1.77	1.78	1.80
V_p (b)	1.85	1.86	1.90
ρ_b	1.82	1.81	1.80

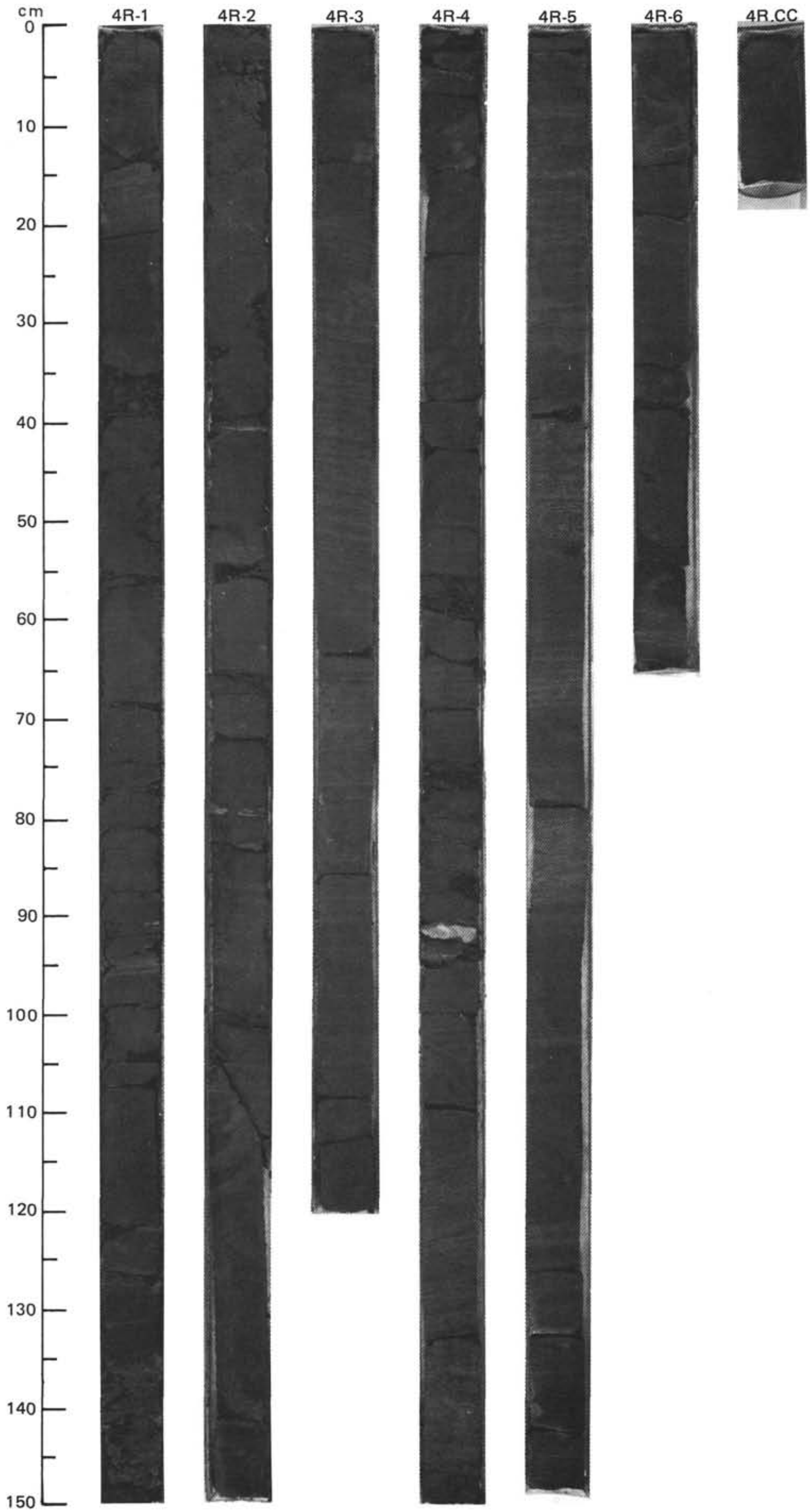
cm
0
10
20
30
40
50
60
70
80
90
100
110
120
130
140
150
4R-1
4R-2
4R-3
4R-4
4R-5
4R-6
4R,CC

SITE 641 HOLE C CORE 5 R CORED INTERVAL 4828.9-4838.5 mbsl; 189.4-199.0 mbsf

TIME-ROCK UNIT	BIOSTRAT. ZONE/ FOSSIL CHARACTER: FORAMINIFERS	NANNOFOSSILS	RADIOLARIANS	DIATOMS		PALEOMAGNETICS	PHYS. PROPERTIES	CHEMISTRY	SECTION	METERS	GRAPHIC LITHOLOGY	DRILLING DISTURB.	SED. STRUCTURES	SAMPLES	LITHOLOGIC DESCRIPTION
ALBIAN	R/P	B	A/P						1 CC			× ×			See below

BLACK and GREENISH GRAY CLAYSTONE

Core 641C-5R consists of several small (<5 cm) pieces of black laminated claystone (Lithology 2) and two pieces of interbedded black and greenish gray claystone (Lithology 3).

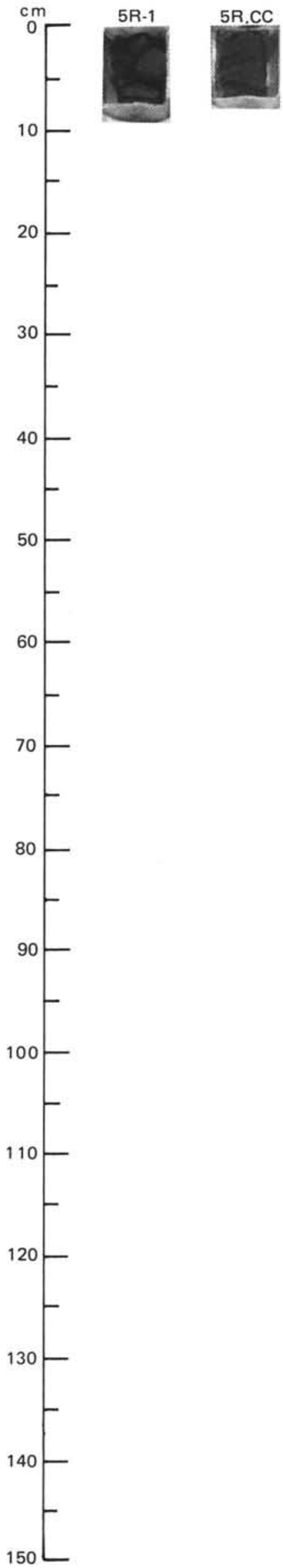
cm
5R-1
5R,CC
0
10
20
30
40
50
60
70
80
90
100
110
120
130
140
150

SITE 641 HOLE C CORE 6 R CORED INTERVAL 4838.5–4848.2 mbsl; 199.0–208.7 mbsf

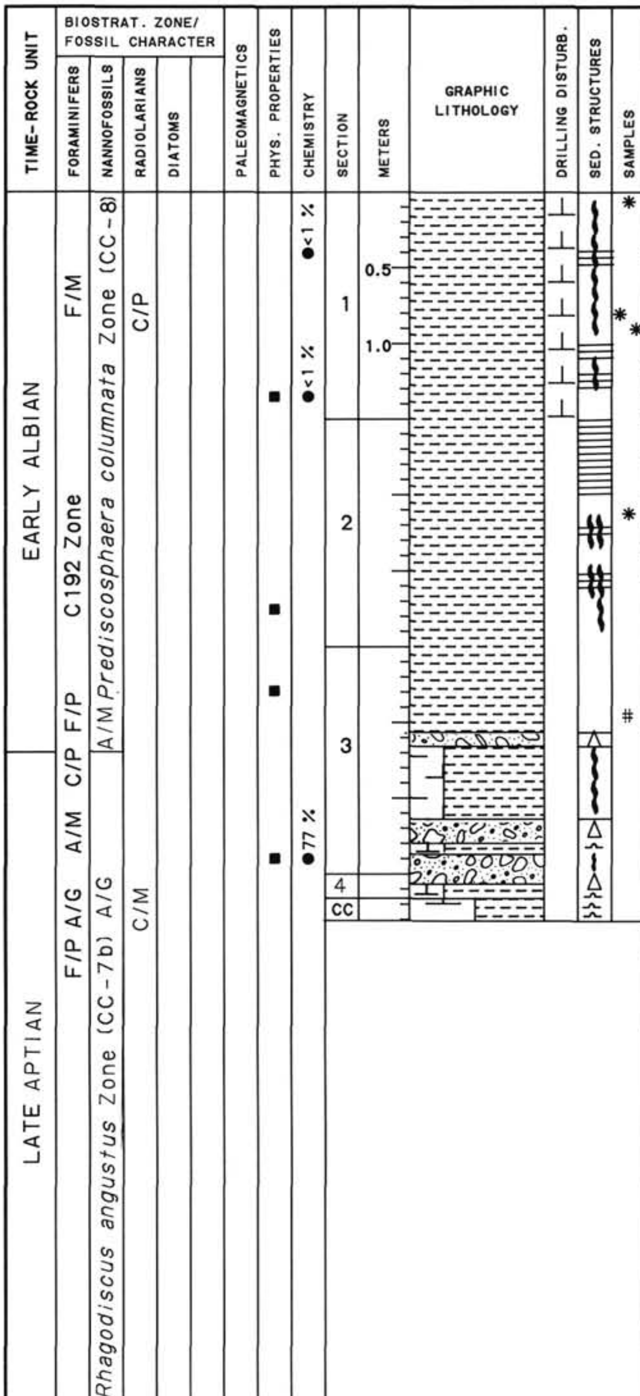

LITHOLOGIC DESCRIPTION

BLACK and GREENISH GRAY CLAYSTONE, and GRANULE CONGLOMERATE

Above Section 3, 58 cm the core consists of the same lithologies as Core 641C-1R but lithologies 1, 3, and 4 are dominant. Siderite concretions occur at Section 1, 0-5 cm.

Below Section 3, 58 cm the core consists of interbedded granule conglomerate (3 beds) and greenish gray (5Y6/1) calcareous clay. The conglomerate is composed of carbonate debris, including skeletal grains and large foraminifers, and rare rock fragments (limestones, shale and quartz sandstone). Conglomerate layers are as thick as 15 cm and do not appear to be graded. The calcareous claystone is massive and bioturbated.

SMEAR SLIDE AND THIN SECTION SUMMARY (%):

	1,4 M	1,81 D	1, 89 D	2, 65 D	3, 53-54 D
TEXTURE:					
Sand	–	10	–	–	–
Silt	40	–	25	10	6
Clay	60	90	75	90	94
COMPOSITION:					
Quartz	6	–	4	1	4
Feldspar	5	–	1	–	Tr
Rock Fragments	15	–	–	–	Tr
Mica	15	–	1	1	1
Clay	55	50	38	55	30
Calcite/Dolomite	–	10	25	10	64
Accessory Minerals	2	–	Tr	Tr	1
Opaques	2	–	–	1	–
Zeolites	–	–	–	2	–
?Cubes	–	–	–	5	–
Foraminifers	–	–	1	–	–
Nannofossils	–	40	30	25	–

PHYSICAL PROPERTIES DATA:

	1,134	2,124	3,23	3,137
V_p (a)	1.76	1.69	–	2.89
ρ_b	1.88	1.77	–	2.10
T_c	–	–	2.61	–

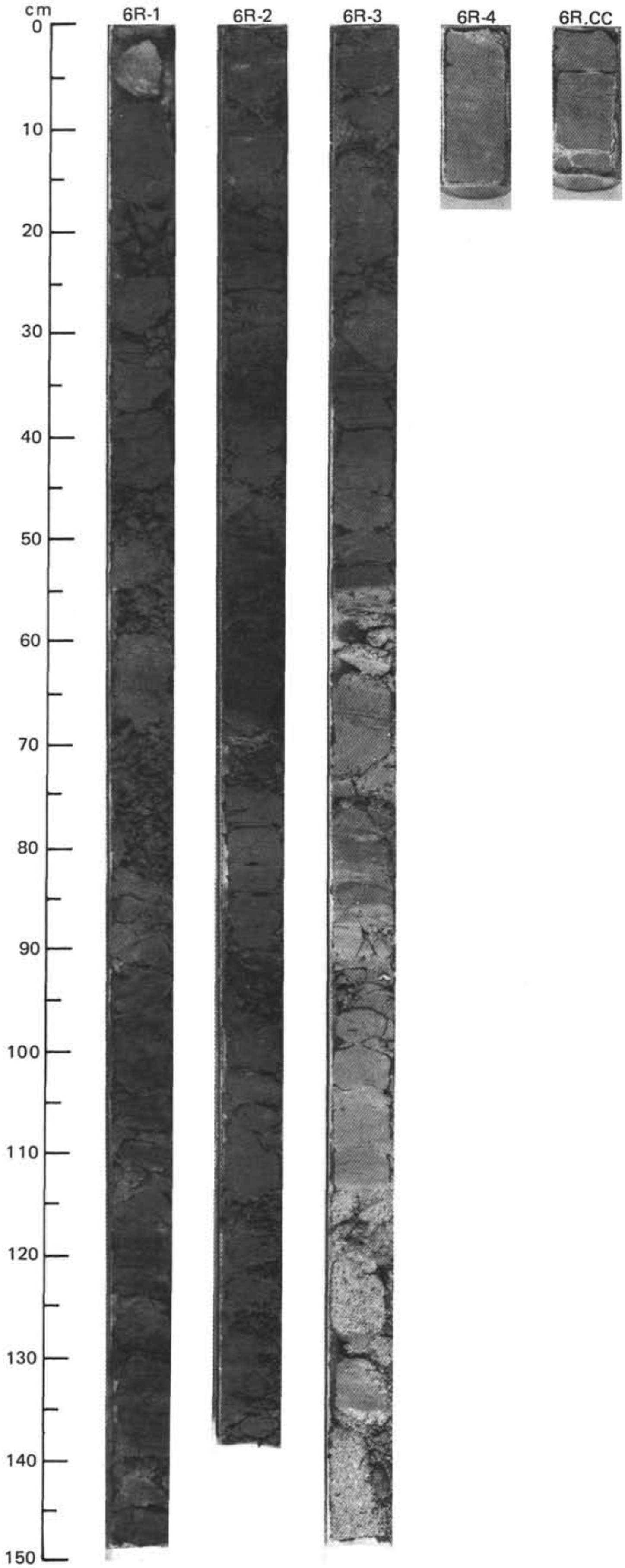
cm
0
10
20
30
40
50
60
70
80
90
100
110
120
130
140
150
6R-1
6R-2
6R-3
6R-4
6R,CC

SITE 641 HOLE C CORE 7 R CORED INTERVAL 4848.2-4857.9 mbsl; 208.7-218.4 mbsf

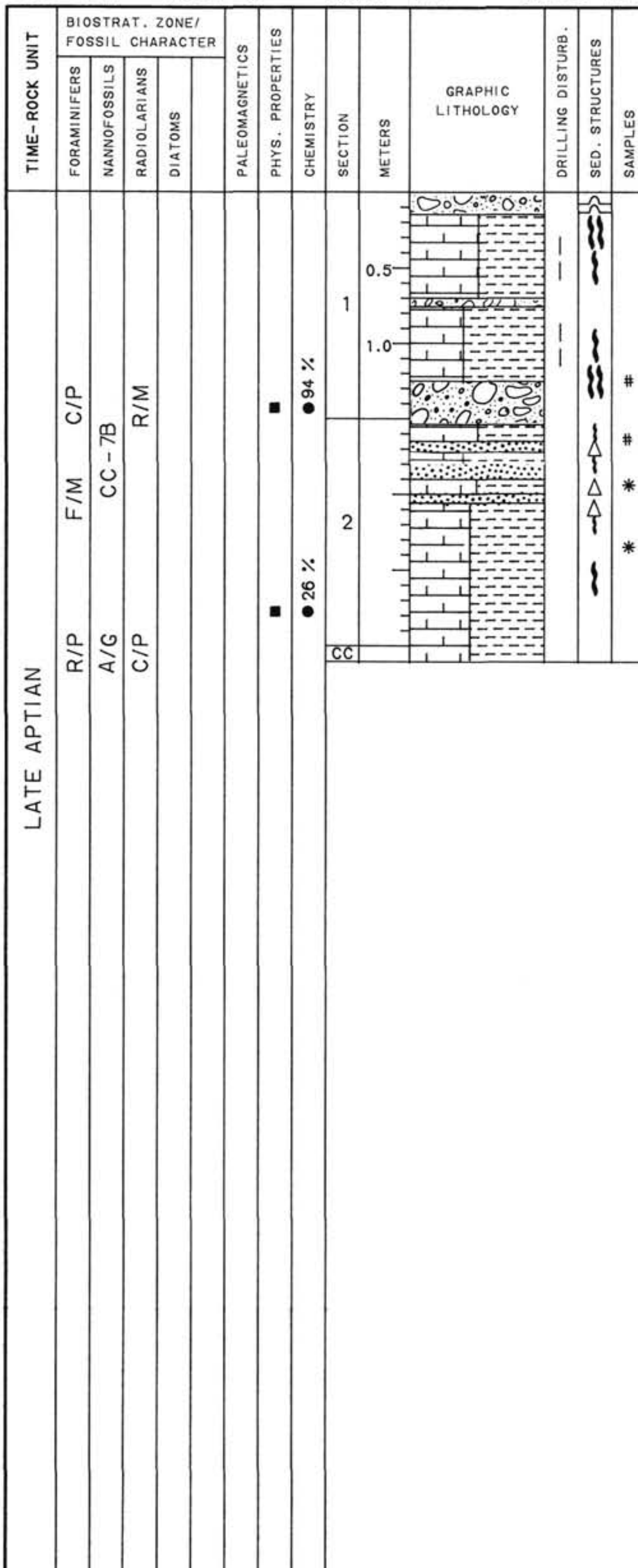

LITHOLOGIC DESCRIPTION

MARLSTONE, CALCAREOUS CLAYSTONE and CALCARENITE

This core is composed primarily of interbedded greenish gray (5GY5/1) nannofossil marlstone and dark greenish gray (5GY4/1) calcareous claystone. These lithologies are bioturbated, but faint lamination is preserved in Section 2, 39-47 cm and in the CC.

Coarse grained calcarenite and granule conglomerate (clasts <1 cm) occur at Section 1, 125 to Section 2, 5 cm, Section 2, 15-22, 36-39, & 47-57 cm. They are composed of carbonate debris similar to that in Core 641C-6R. The upper part of each bed is graded and laminated. The beds have sharp bases and gradational tops (?turbidites).

Slumped intervals occur at Section 1, 0-13 cm and 45-55 cm. These might be debris flow deposits.

SMEAR SLIDE AND THIN SECTION SUMMARY (%):

	1,128-130 D	1,132-134 D	2,16-18 D	2,44 D	2,85 D
TEXTURE:					
Sand	54	100	95	–	–
Silt	–	–	–	5	15
Clay	45	–	5	95	85
COMPOSITION:					
Quartz	–	1	Tr	Tr	3
Feldspar	–	Tr	–	–	1
Mica	–	Tr	Tr	1	4
Clay	10	–	–	60	65
Calcite/Dolomite	–	–	–	10	15
Accessory Minerals	2	Tr	Tr	Tr	–
Opaques	–	–	–	–	2
Nannofossils	–	–	–	30	10
Sponge Spicules	–	–	–	Tr	–
Radiolarians	1	–	–	–	–
Plant debris	1	–	–	–	–
Ooids	–	Tr	Tr	–	–
Bioclasts	54	50	50	–	–
Intraclast	1	14	10	–	–
Spar cement	5	–	5	–	–
Micrite	24	5	–	–	–
Pore space	2	30	35	–	–

PHYSICAL PROPERTIES DATA:

	1,144	2,128
V_p (a)	2.33	1.77
ρ_b	2.01	1.92

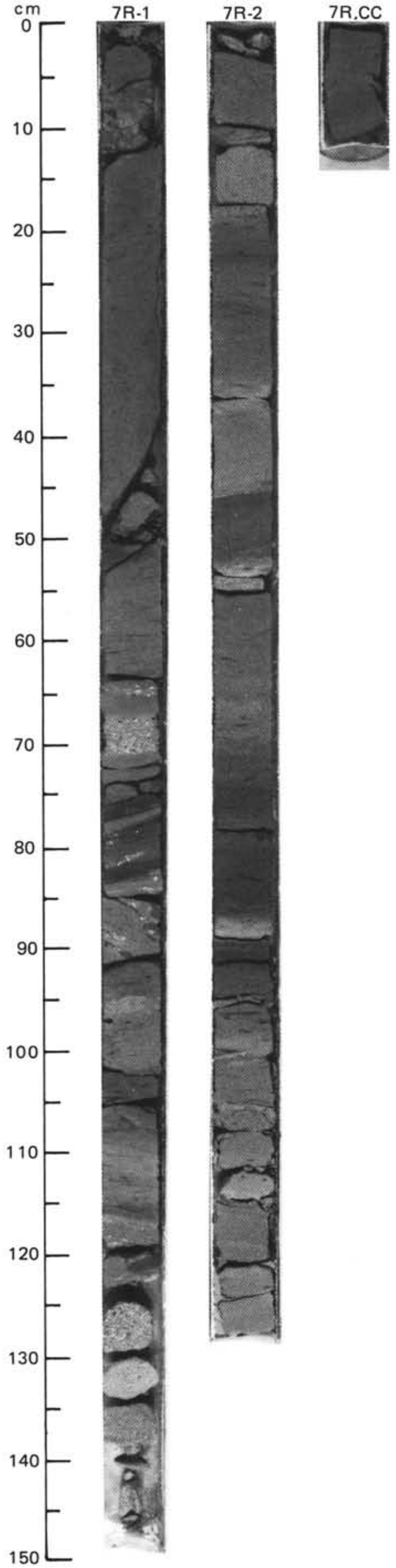
cm
0
10
20
30
40
50
60
70
80
90
100
110
120
130
140
150
7R-1
7R-2
7R,CC

SITE 641 HOLE C CORE 8 R CORED INTERVAL 4857.9-4867.5 mbsl; 218.4-228.0 mbsf

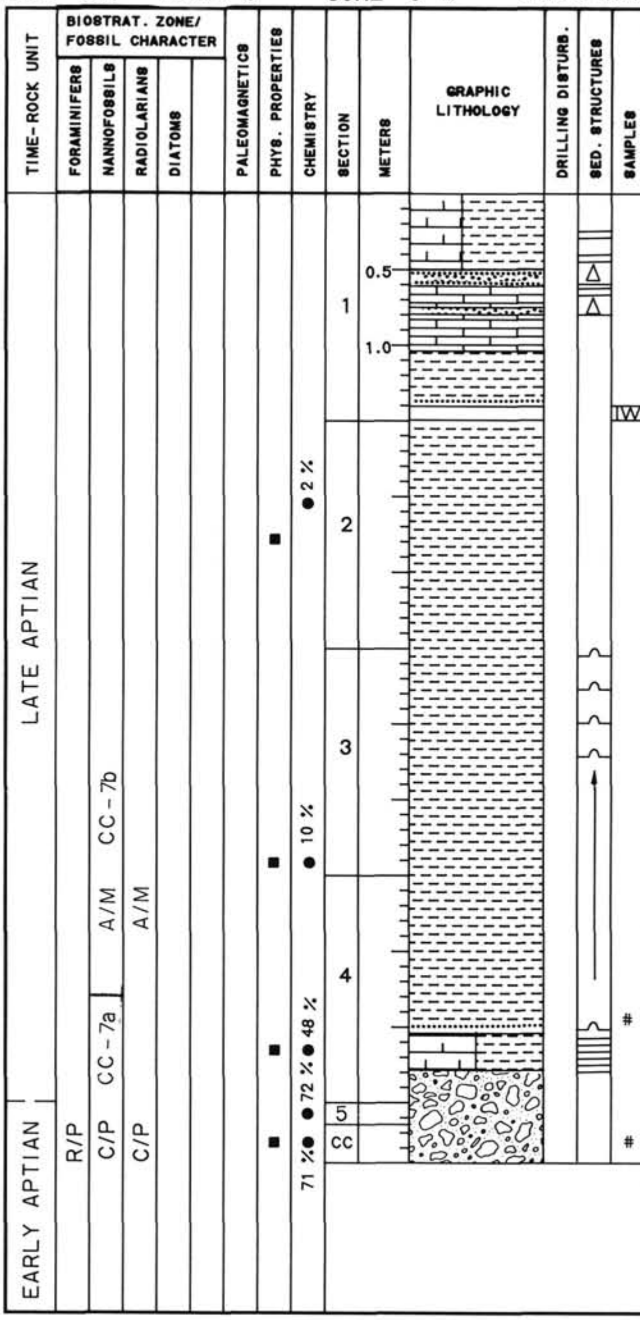

LITHOLOGIC DESCRIPTION

MARLSTONE, CALCAREOUS CLAYSTONE and CALCARENITE

Sections 1 and 2 are composed primarily of interbedded greenish gray (5GY5/1) nannofossil marlstone and dark greenish gray (5GY4/1) calcareous claystone and black (N5) claystone. These lithologies are highly bioturbated, but faint lamination is preserved locally. Graded and laminated beds of coarse-grained calcarenite, rich in claystone fragments, occur in Section 1. The graded beds pass up into calcisilitite and marlstone. The beds have sharp bases and gradational tops. Below Section 2 the core consists of a slumped mass of dark gray (5Y4/1)and black claystone with pebbles of white limestone and light bluish gray (5BG6/1) and grayish green (5G4/2) claystone. Convolute bedding is common. This interval has the appearance of pebbly mudstone. Silicified carbonate conglomerate occurs in the CC sample.

THIN SECTION SUMMARY (%):

	4, 107-108 D	CC, 16-19 D
TEXTURE:		
Sand	90	60
Silt	10	40
Clay	–	–
COMPOSITION:		
Quartz	Tr	5
Feldspar	–	Tr
Rock Fragments	Tr	–
Mica	Tr	–
Cement	2	5
Pore space	40	25
Foraminifers	Tr	–
Pellets	8	5
Bioclast	50	60

PHYSICAL PROPERTIES DATA:

	2,74	3,134	4,114	CC,16
V_p (a)	1.77	1.75	1.88	5.74
ρ_b	1.77	–	2.03	2.64

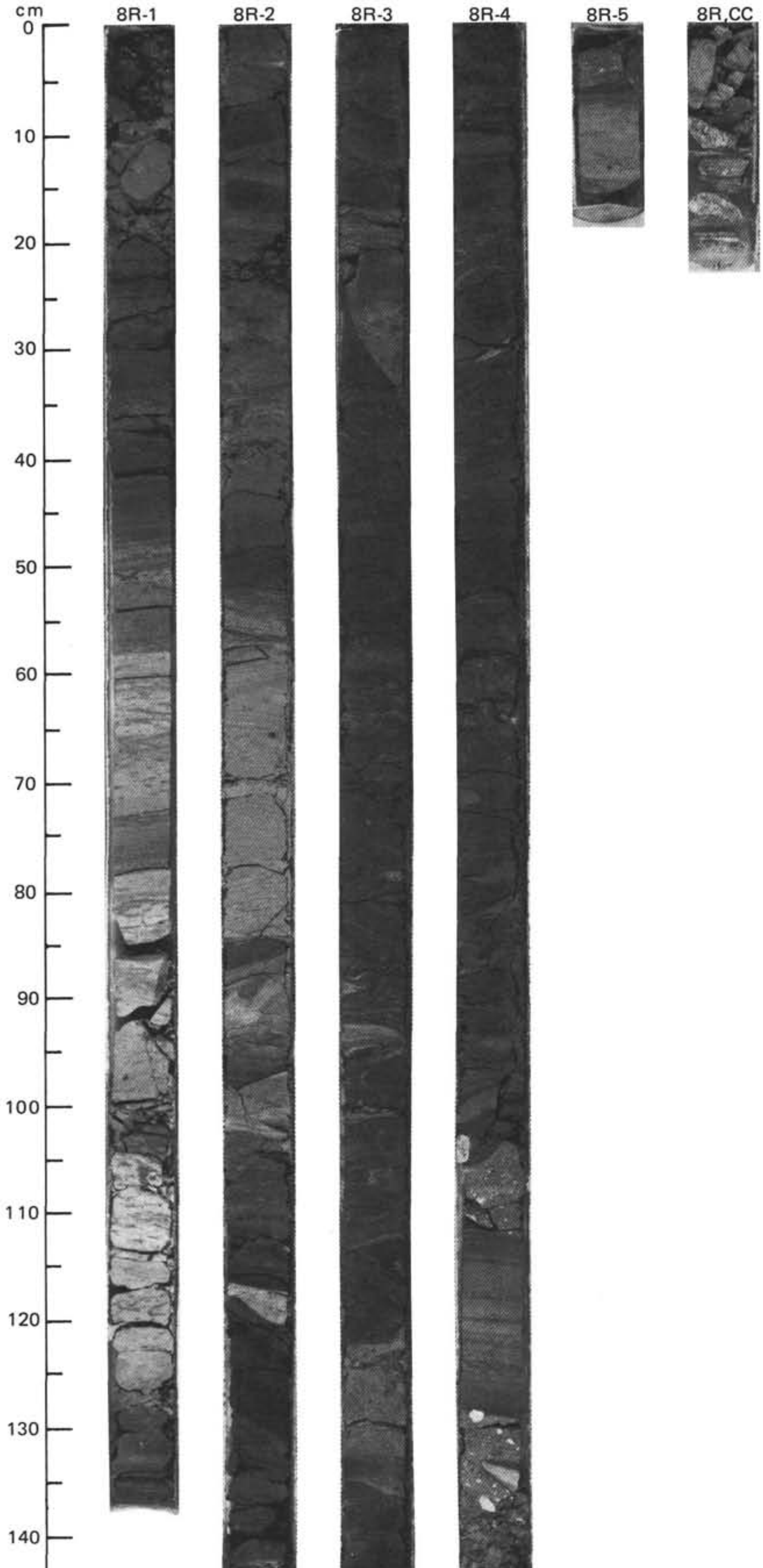
cm
0
10
20
30
40
50
60
70
80
90
100
110
120
130
140
150
8R-1
8R-2
8R-3
8R-4
8R-5
8R,CC

SITE 641 HOLE C CORE 9 R CORED INTERVAL 4867.5-4877.1 mbsl; 228.0-237.6 mbsf

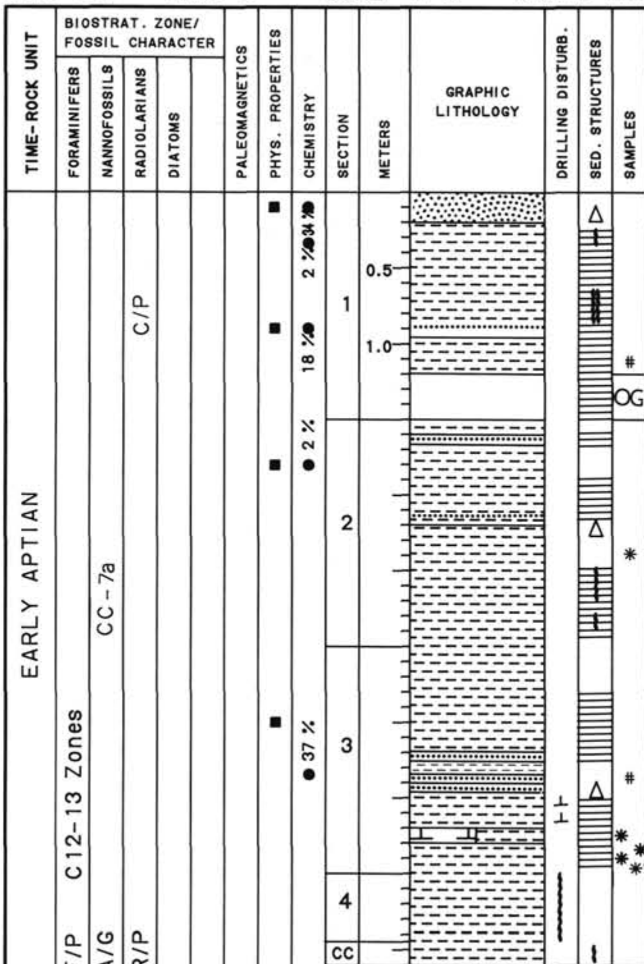

LITHOLOGIC DESCRIPTION

INTERBEDDED BLACK and GREENISH GRAY CLAYSTONE, CARBONATE-SAND TURBIDITES

There are six distinct lithologies present in Core 9 and succeeding cores:

(1) Massive black (5Y3/2) claystone;

(2) Laminated black (5Y3/2) claystone;

(3) Interbedded, on a scale of 1-1.5cm, black (5Y3/1)and greenish gray (5G4/1) claystone. Lamination is irregular and discontinuous. Bioturbation is light to moderate with the burrows severely flattened. Burrows are typically 0.1 x 1.0 cm;

(4) Greenish gray (5G4/1) to grayish green (5G5/2) claystone. Lamination is rare to absent. Bioturbation is weak;

(5) Dark olive gray (5Y3/2), slightly calcareous, microturbidites. The base is siltstone and very fine sandstone grading upward into calcareous claystone and silty calcareous claystone. Beds are laminated (Td-e). Each microturbidite unit is commonly capped by 0.2 cm light gray (5Y7/1) marlstone. Both upper and lower boundaries are very sharp. Microturbidites are rarely as thick as 9 cm and average 1 cm;

(6) Greenish gray (5GY6/1) to gray (5Y6/1), lightly to moderately bioturbated marlstone. Burrows are severely flattened. Diffuse banding, 0.3-2.0 cm thick, due to variations in amount of clay, is present. Interbedding with other lithologies is usually on a scale of 5-50 cm and contacts are usually gradational over at least 1 cm.

Coarse sand and granule conglomerate composed of carbonate debris are present at the top of the core. Thin beds of carbonate sand are also present at Section 2, 10-13 cm, and Section 3, 70-74, 83-90, & 93-95 cm.

A large wood fragment occurs at Section 1, 83-84 cm.

Lamination in Core 9 dips up to 11°.

SMEAR SLIDE AND THIN SECTION SUMMARY (%):

	1,117-121 D	2,87 D	3,85-89	3,127 M	3,137 D	3,138 D	3,144 M
TEXTURE:							
Sand	–	–	7	–	–	–	10
Silt	15	3	–	3	1	4	18
Clay	85	97	93	97	99	96	72
COMPOSITION:							
Quartz	1	–	–	–	Tr	–	1
Clay	78	–	78	–	–	–	–
Mica	Tr	97	5	65	63	70	52
Calcite/Dolomite	–	–	–	–	Tr	–	1
Accessory Minerals	1	Tr	–	–	–	–	–
Pyrite	–	2	–	3	1	3	5
Zeolite	–	–	–	2	1	1	–
Foraminifers	–	–	7	–	–	–	3
Nannofossils	–	–	–	30	25	25	20
Organic matter	–	1	–	–	–	–	–
Bioclasts	–	–	7	–	–	–	4
Radiolarians	15	–	–	–	–	–	–
Plant debris	5	–	–	–	–	–	–
Micrite	–	–	3	–	–	–	–

PHYSICAL PROPERTIES DATA:

	1,8	1,89	2,30	3,49
V_p (a)	4.29	1.80	1.77	1.79
V_p (b)	4.48	1.93	1.91	1.92
ρ_b	2.43	1.86	1.81	1.82

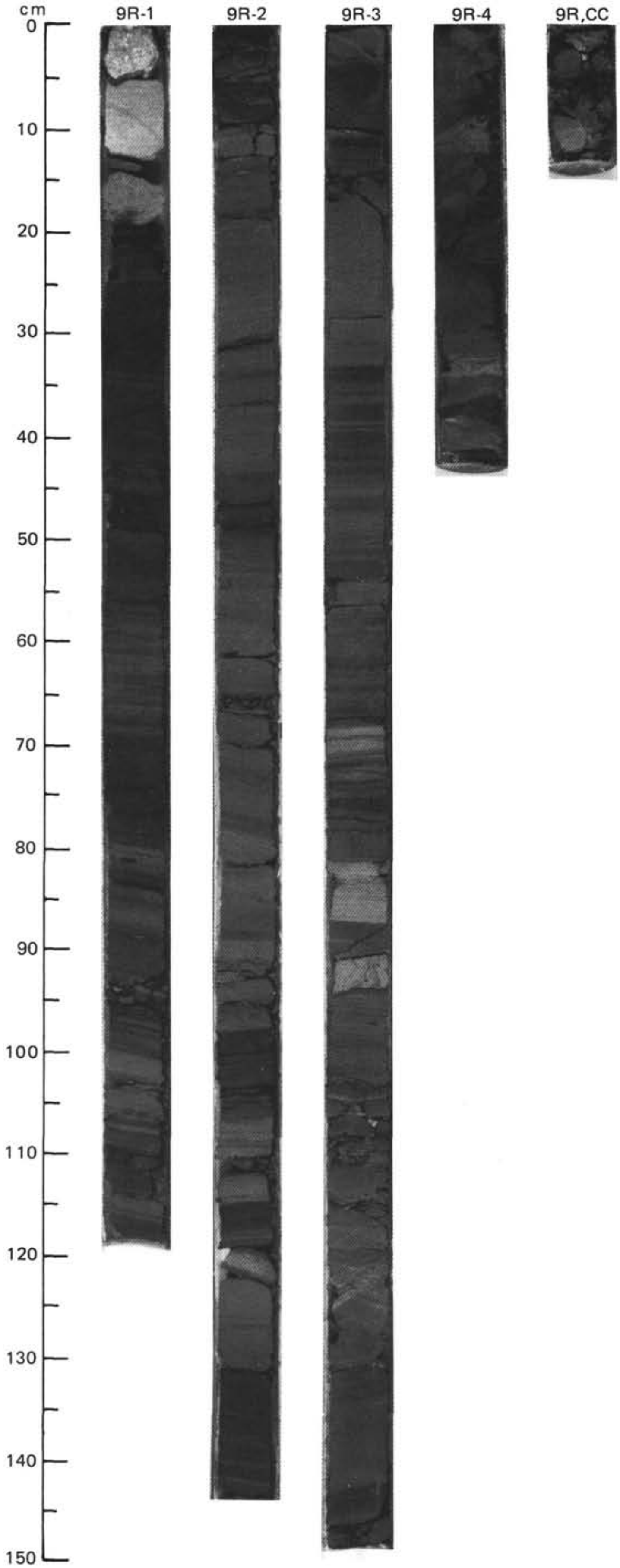
cm
0
10
20
30
40
50
60
70
80
90
100
110
120
130
140
150
9R-1
9R-2
9R-3
9R-4
9R,CC

SITE 641 HOLE C CORE 10 R CORED INTERVAL 4877.1-4886.8 mbsl; 237.6-247.3 mbsf

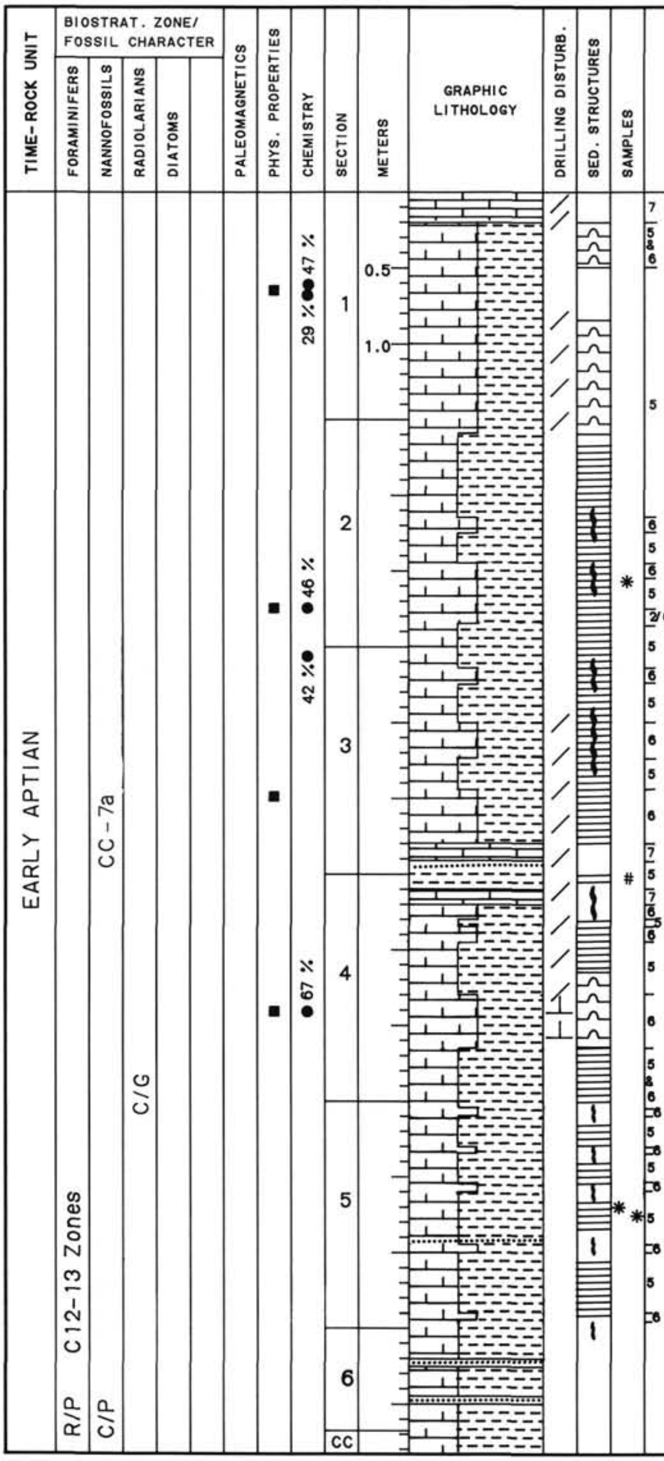

LITHOLOGIC DESCRIPTION

CALCAREOUS MICROTURBIDITES MARLSTONE and CLAYEY LIMESTONE

Core 10 is composed of the same lithologies as described for Core 9 (q.v.), with the addition of:

(7) Light greenish gray (5GY7/1) and light gray (5Y7/1) clayey limestone, lightly to moderately bioturbated. Burrows range up to 0.5 x 3.0 cm and are subhorizontal due to flattening.

Slumps occur at Section 1, 20-52 cm, Section 1, 85 cm to Section 2, 10 cm, and Section 4, 65-115 cm.

Lamination in Core 10 dips up to 17°.

Finely laminated carbonate sandstone occurs at Section 3, 141-144 cm, and Section 6, 21-26 & 45-50 cm. In Section 6 the sandstone is interbedded with marlstone.

SMEAR SLIDE AND THIN SECTION SUMMARY (%):

	2, 105 D	4, 13-16 D	5,71 M	5,73 M
TEXTURE:				
Silt	–	3	7	7
Clay	100	97	93	93
COMPOSITION:				
Quartz	–	2	–	–
Feldspar	–	Tr	–	–
Mica	–	Tr	–	–
Clay	51	77	57	63
Calcite/Dolomite	1	15	5	2
Accessory Minerals	–	Tr	Tr	–
Zeolites	2	–	1	1
Pyrite	1	–	1	1
Foraminifers	–	Tr	Tr	Tr
Nannofossils	45	–	35	50
Organic matter	–	–	–	1
Bioclasts	–	–	–	3
Radiolarians	–	1	–	–
Plant debris	–	5	–	–

PHYSICAL PROPERTIES DATA:

	1,67	2,124	3,96	4,94
V_p (a)	1.85	1.90	2.05	1.93
V_p (b)	2.00	2.07	2.20	2.17
ρ_b	1.98	2.02	2.08	2.01

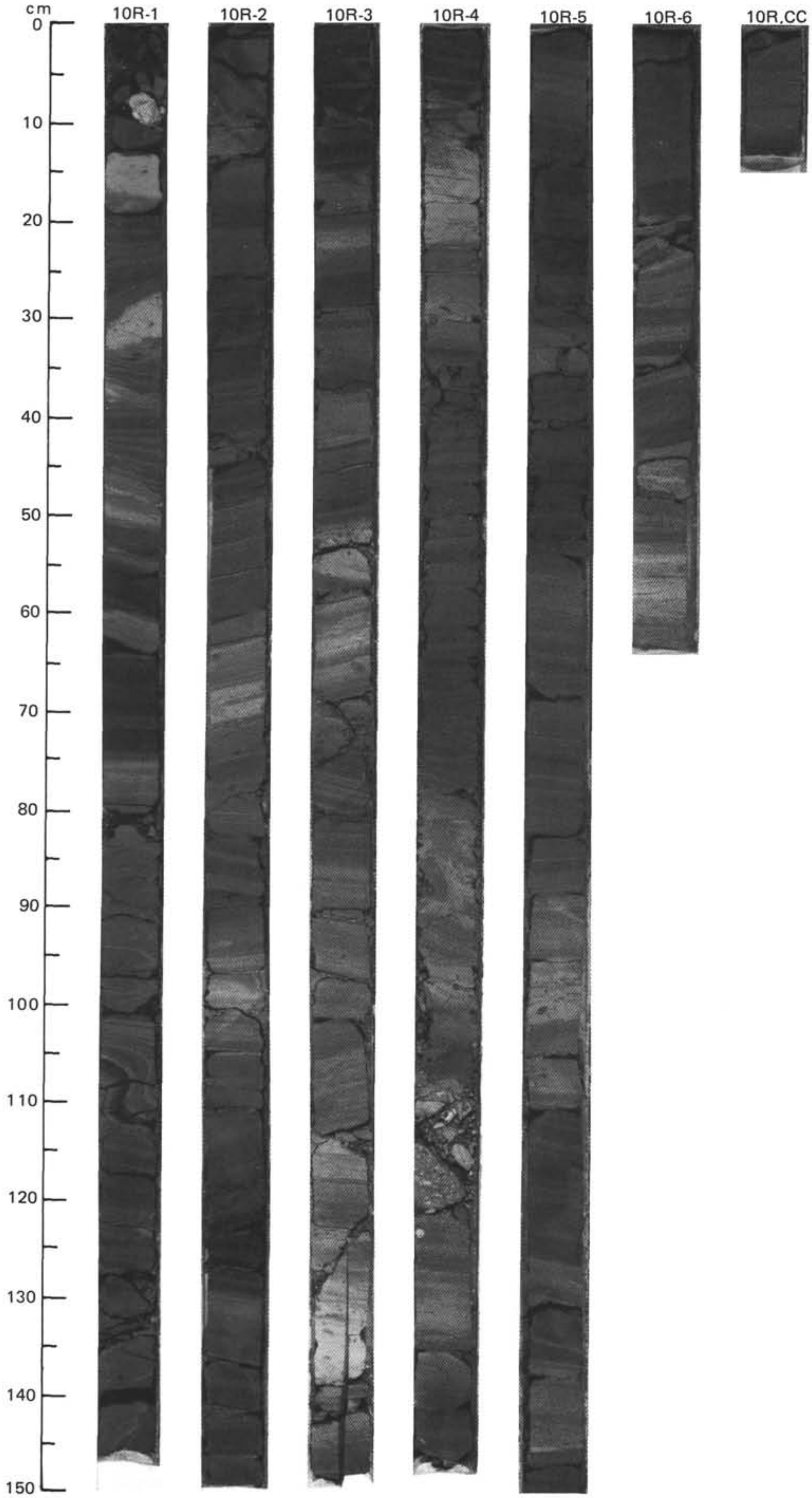
cm
0
10
20
30
40
50
60
70
80
90
100
110
120
130
140
150
10R-1
10R-2
10R-3
10R-4
10R-5
10R-6
10R,CC

SITE 641 HOLE C CORE 11 R CORED INTERVAL 4886.8-4896.4 mbsl; 247.3-256.9 mbsf

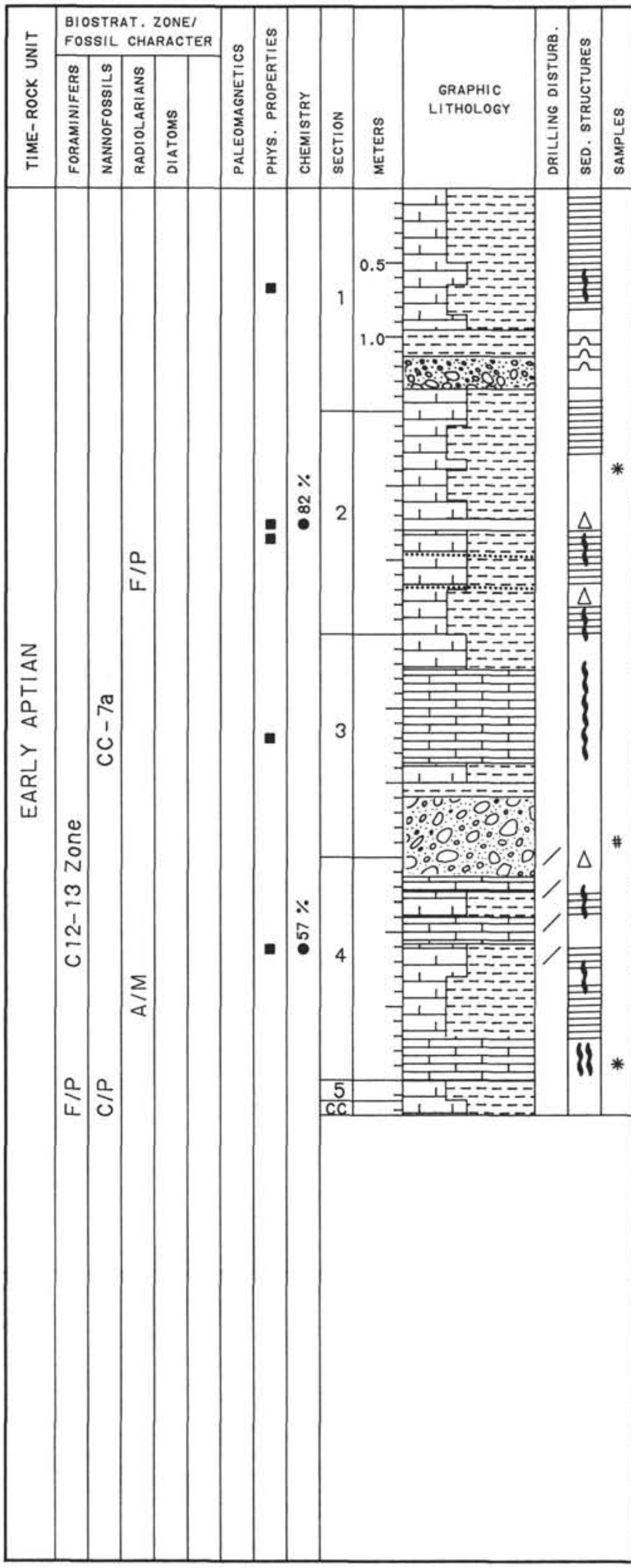

LITHOLOGIC DESCRIPTION

CALCAREOUS MICROTURBIDITES, MARLSTONE and CLAYEY LIMESTONE

Core 11 is composed of the same lithologies as described for Cores 9 and 10 (q.v.).

A slump occurs in Section 1, 93-112 cm, overlying debris flow composed of limestone clasts in a dark claystone matrix.

Calcarenite turbidites occur at Section 2, 73-80 and 115-120 cm. A coarsely graded, from pebble conglomerate to very coarse sand, carbonate bed occurs at Section 3, 120 cm to Section 4, 17 cm.

SMEAR SLIDE AND THIN SECTION SUMMARY (%):

	2, 38 D	3, 146-150 D	4, 140 M
TEXTURE:			
Sand	–	55	–
Silt	6	–	5
Clay	94	45	95
COMPOSITION:			
Quartz	1	5	–
Feldspar	–	3	–
Mica	44	Tr	75
Clay	–	5	–
Calcite/Dolomite	Tr	5	1
Accessory Minerals	Tr	Tr	–
Pyrite	2	–	4
Zeolite	1	–	–
Nannofossils	50	–	20
Sponge Spicules	1	–	–
Microspar	2	–	–
Rock fragment	–	5	–
Bioclast (corals, echinoderms, rudists, algae)	–	37	–
Intraclast	–	5	–

PHYSICAL PROPERTIES DATA:

	1,63	2,76	2,84	3,73	4,61
V_p (a)	1.93	2.70	1.83	2.07	1.98
V_p (b)	2.13	2.88	1.86	2.11	2.17
ρ_b	2.03	2.23	1.97	2.12	2.07

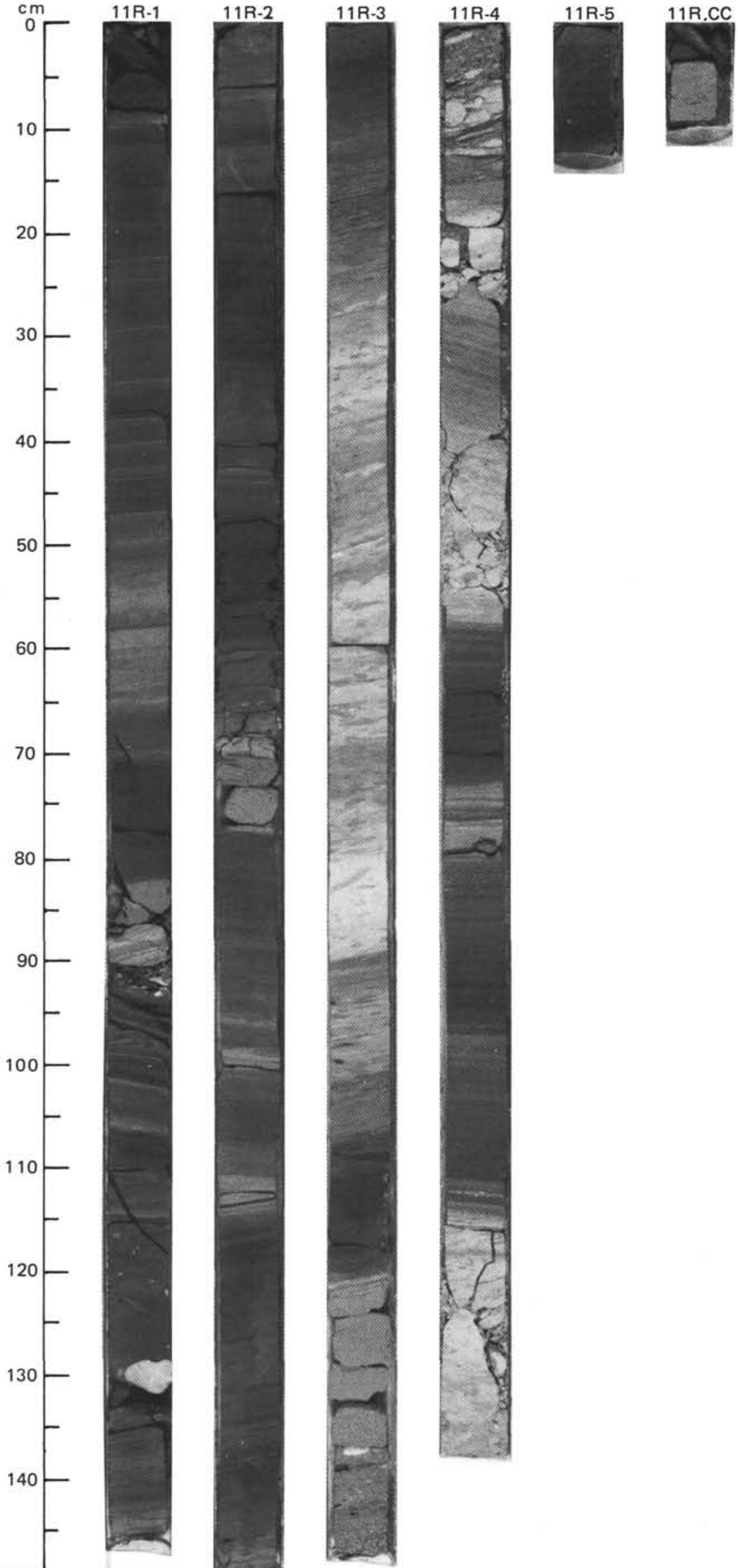
cm
0
10
20
30
40
50
60
70
80
90
100
110
120
130
140
150
11R-1
11R-2
11R-3
11R-4
11R-5
11R,CC

SITE 641 HOLE C CORE 12 R CORED INTERVAL 4896.4-4906 mbsl; 256.9-266.5 mbsf

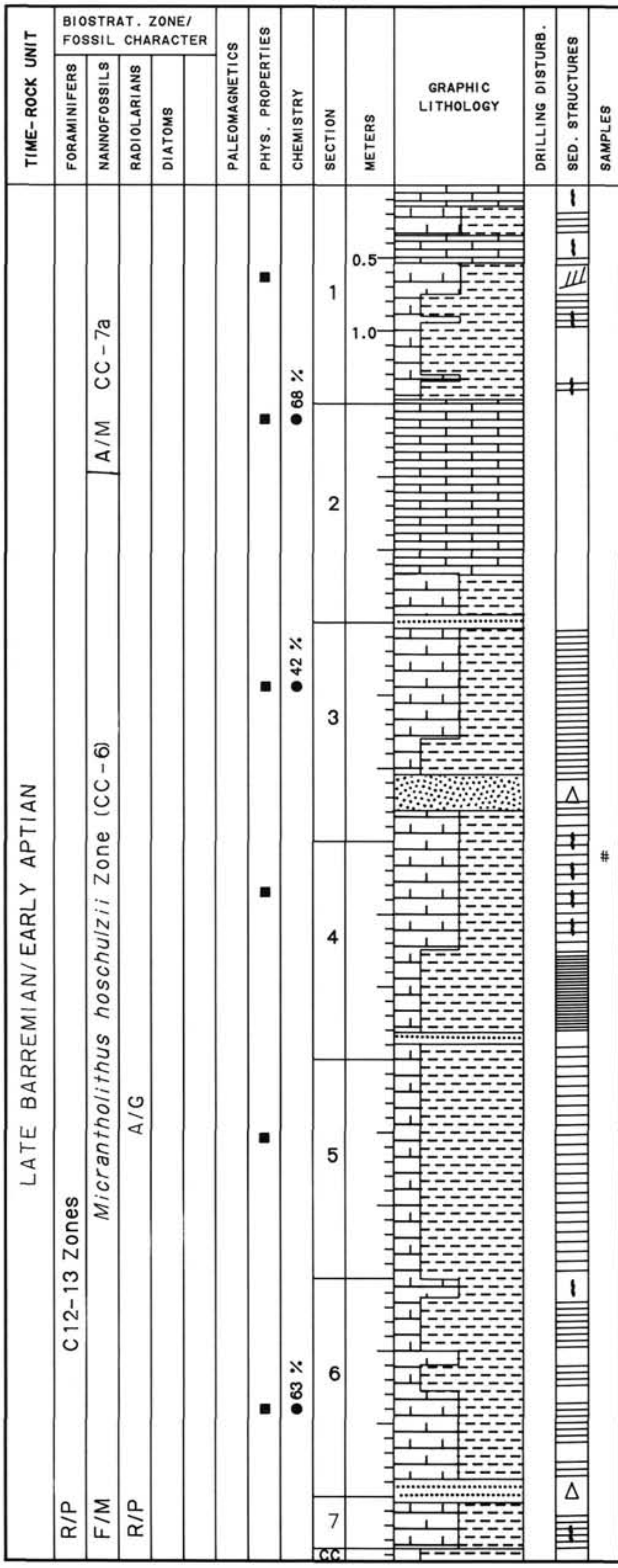

LITHOLOGIC DESCRIPTION

CALCAREOUS MICROTURBIDITES, MARLSTONE and CLAYEY LIMESTONE

Core 12 is composed of the same lithologies as described for Cores 9 and 10 (q.v.).

Clayey limestone (lithology 7) is a much more significant proportion of the core than in cores above.

Lamination in Core 12 dips up to 11°.

THIN SECTION SUMMARY (%):

	4, 17 D
TEXTURE:	
Silt	15
Clay	85
COMPOSITION:	
Mica	Tr
Clay	30
Accessory minerals:	
Pyrite, Opaques	Tr
Radiolarians	15
Plant debris	2
Bioclasts	Tr
Micrite	53

PHYSICAL PROPERTIES DATA:

	1,60	2,5	3,41	4,36	5,51	6,89
V_p (a)	2.04	2.04	2.85	2.38	1.85	2.00
V_p (b)	2.17	2.07	2.00	2.48	1.91	2.09
ρ_b	2.05	2.02	1.97	2.15	1.98	2.10

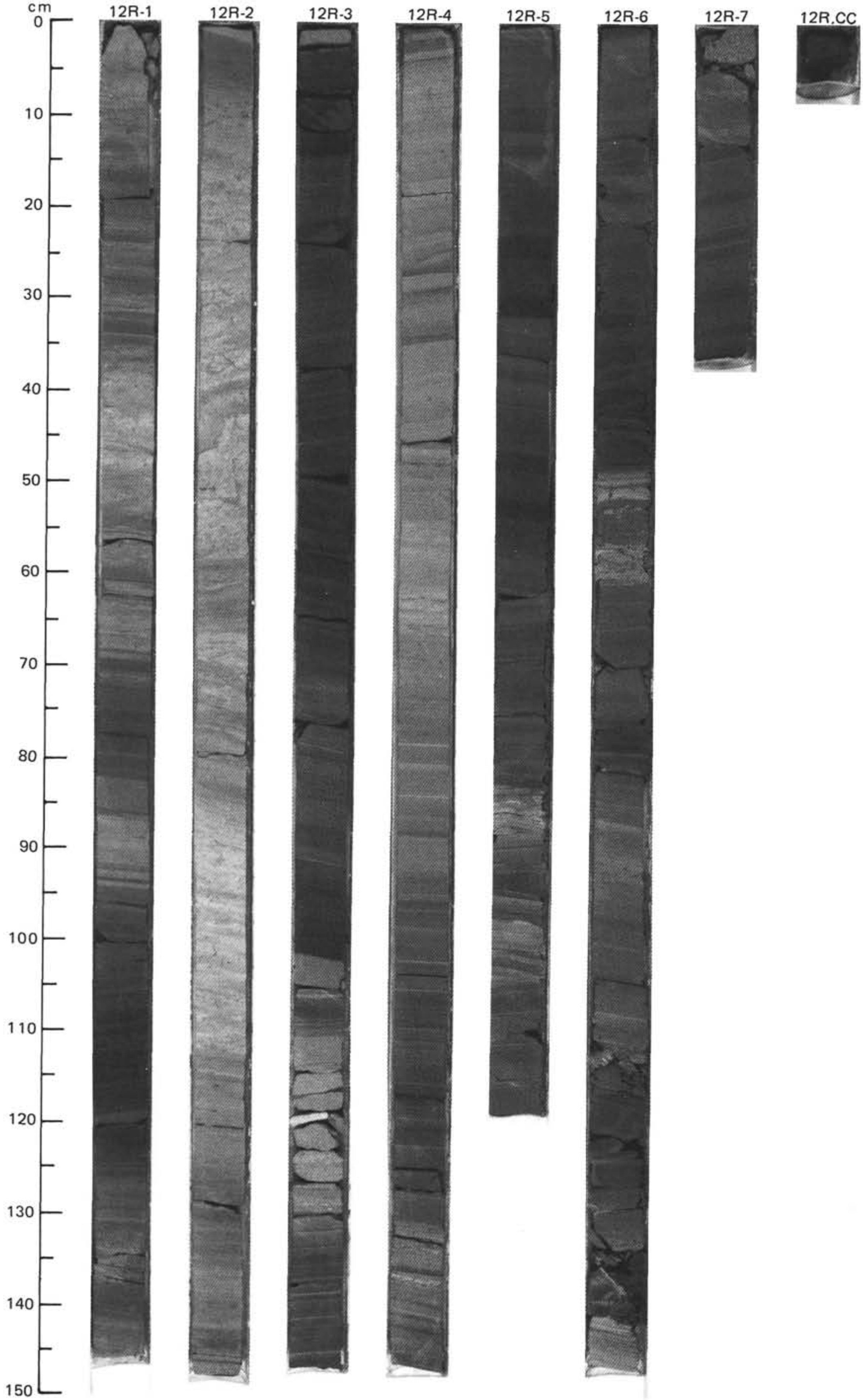
cm
0
10
20
30
40
50
60
70
80
90
100
110
120
130
140
150
12R-1
12R-2
12R-3
12R-4
12R-5
12R-6
12R-7
12R,CC

SITE 641 HOLE C CORE 13 R CORED INTERVAL 4906.0-4915.7 mbsl; 266.5-276.2 mbsf

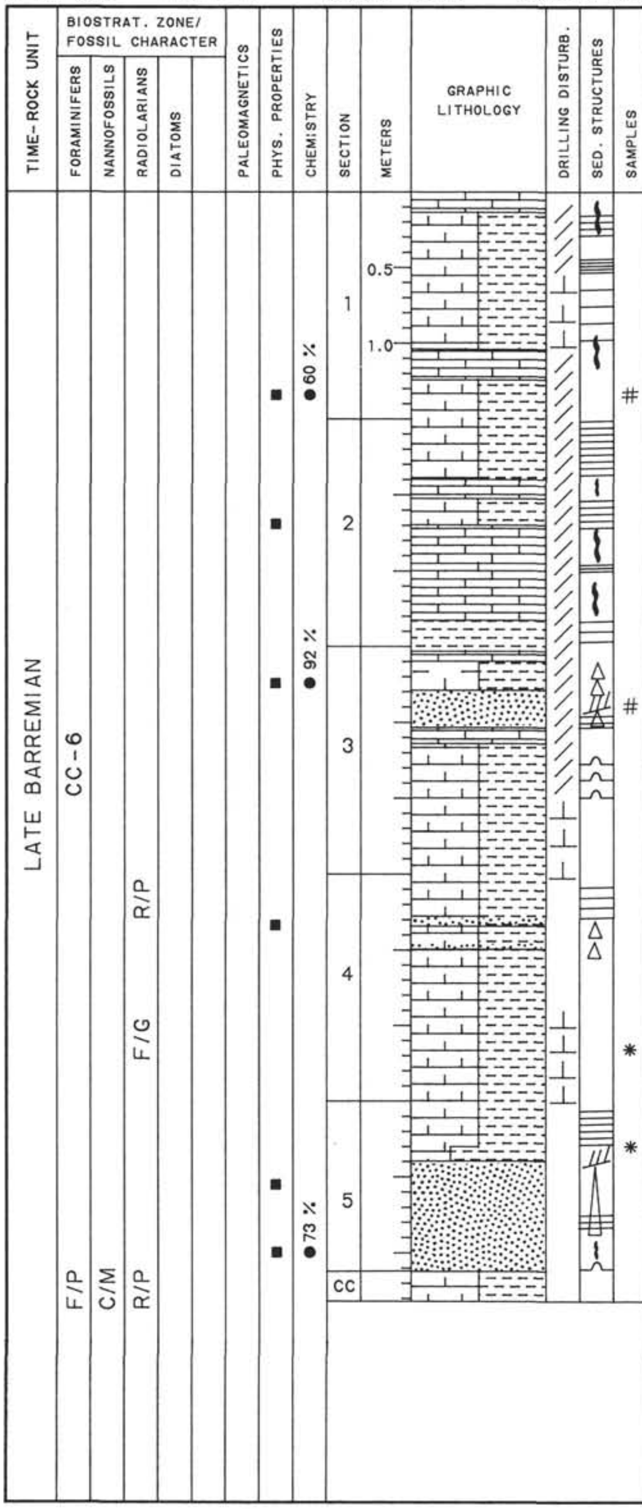

LITHOLOGIC DESCRIPTION

CLAYEY LIMESTONE, CALCAREOUS MICROTURBIDITES and TURBIDITES

The upper part of the core consists of gray (5Y6/1) bioturbated clayey limestone interbedded on a scale of 15-100 cm with gray (5Y5/1) and greenish gray (5GY5/1) marlstone. The marlstone occurs as both massive, bioturbated beds and as laminated beds. Laminated intervals are as thick as 3 cm and locally are graded. 0.1 cm thick white nannofossil marlstone laminae are common at the top of each interval. The laminated marlstone was deposited as microturbidites. Intervals of massive marlstone may represent the upper portions of turbidites. Below Section 2 coarse-grained, graded carbonate sandstone (turbidite) is present. In some cases the sandstone beds show cross bedding and climbing ripples.

SMEAR SLIDE AND THIN SECTION SUMMARY (%):

	1, 130 D	1, 138 D	3, 49 D	4, 115 D	5, 34 D
TEXTURE:					
Sand	–	–	60	–	–
Silt	Tr	3	–	–	10
Clay	100	97	40	100	90
COMPOSITION:					
Quartz	Tr	3	2	Tr	Tr
Feldspar	Tr	–	Tr	–	–
Mica	1	–	Tr	–	–
Clay	55	40	Tr	95	62
Calcite/Dolomite	10	46	50	–	5
Silica (chalcedony)	–	3	Tr	–	–
Accessory minerals	2	Tr	Tr	–	3
Foraminifers	–	Tr	–	–	Tr
Nannofossils	29	–	–	5	20
Radiolarians	Tr	3	–	–	3
Plant Debris	3	5	Tr	–	3
Bioclast (orbitolina, echinoids, algae, bivalves)	–	–	25	–	–
Intraclasts	–	–	22	–	–

PHYSICAL PROPERTIES DATA:

	1,134	2,71	3,25	4,31	5,54	5,94
V_p (a)	1.91	2.04	4.86	1.88	5.17	2.27
ρ_b	2.11	2.18	2.57	2.01	2.69	2.21

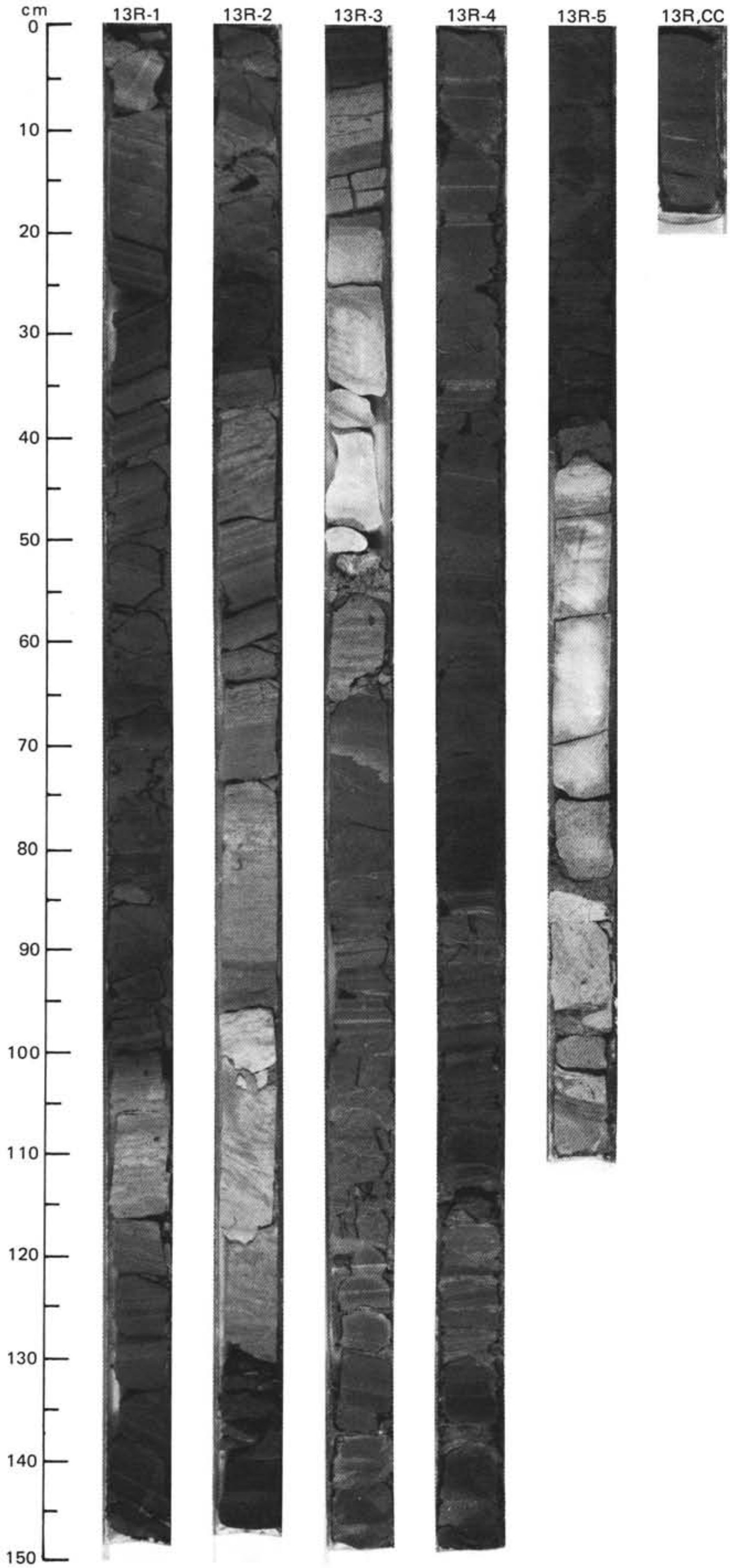
cm
0
10
20
30
40
50
60
70
80
90
100
110
120
130
140
150
13R-1
13R-2
13R-3
13R-4
13R-5
13R,CC

SITE 641 HOLE C CORE 14 R CORED INTERVAL 4915.7-4925.3 mbsl; 276.2-285.8 mbsf

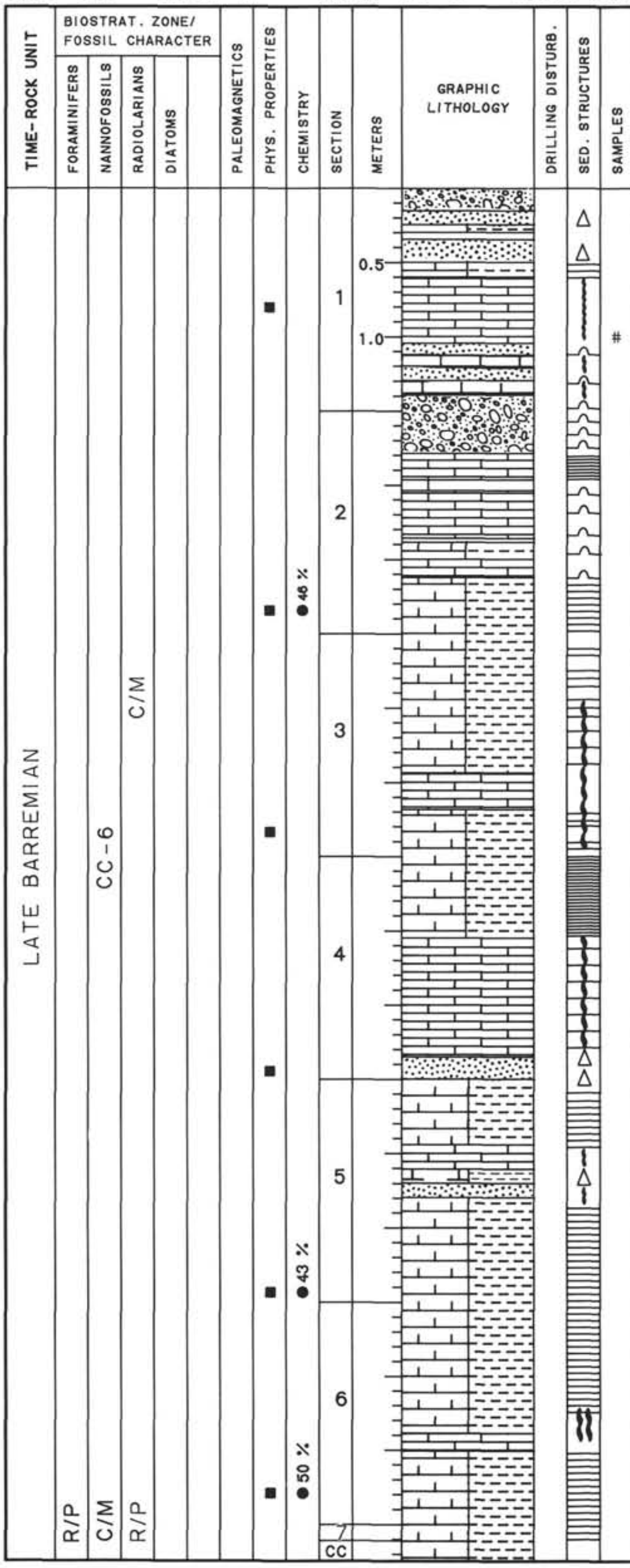

LITHOLOGIC DESCRIPTION

CLAYEY LIMESTONE, CALCAREOUS MICROTURBIDITES and MARLSTONE DEBRIS FLOW DEPOSITS

The core consists of bioturbated, gray (5Y7/1) clayey limestone, laminated and bioturbated dark gray (5Y4/1) marlstone, and fine grained skeletal carbonate sandstone. The laminated marlstone is microturbidite.

Debris flows composed of laminated and bioturbated marlstone clasts (<2 cm across) in a marlstone matrix occur at Section 1, 0-15, 30-35, 107-112, 120-128, 137 through Section 2, 27 cm. Slumps occur in Section 2 and in the middle of Section 5.

Graded sandstone composed of skeletal carbonate fragments and wood fragments occurs in Section 5. The sandstone grades up into massive clayey limestone/marlstone.

THIN SECTION SUMMARY (%):

	1, 96
	D
TEXTURE:	
Sand	–
Silt	30
Clay	–
COMPOSITION:	
Quartz	Tr
Mica	Tr
Clay	15
Calcite	55
Radiolarians	25
Plant debris	5
Short filaments	Tr

PHYSICAL PROPERTIES DATA:

	1,79	2,132	3,131	4,140	5,146	6,129
V_p (a)	3.03	1.83	2.68	2.09	1.83	1.85
ρ_b	2.47	2.04	2.45	2.20	2.06	2.05

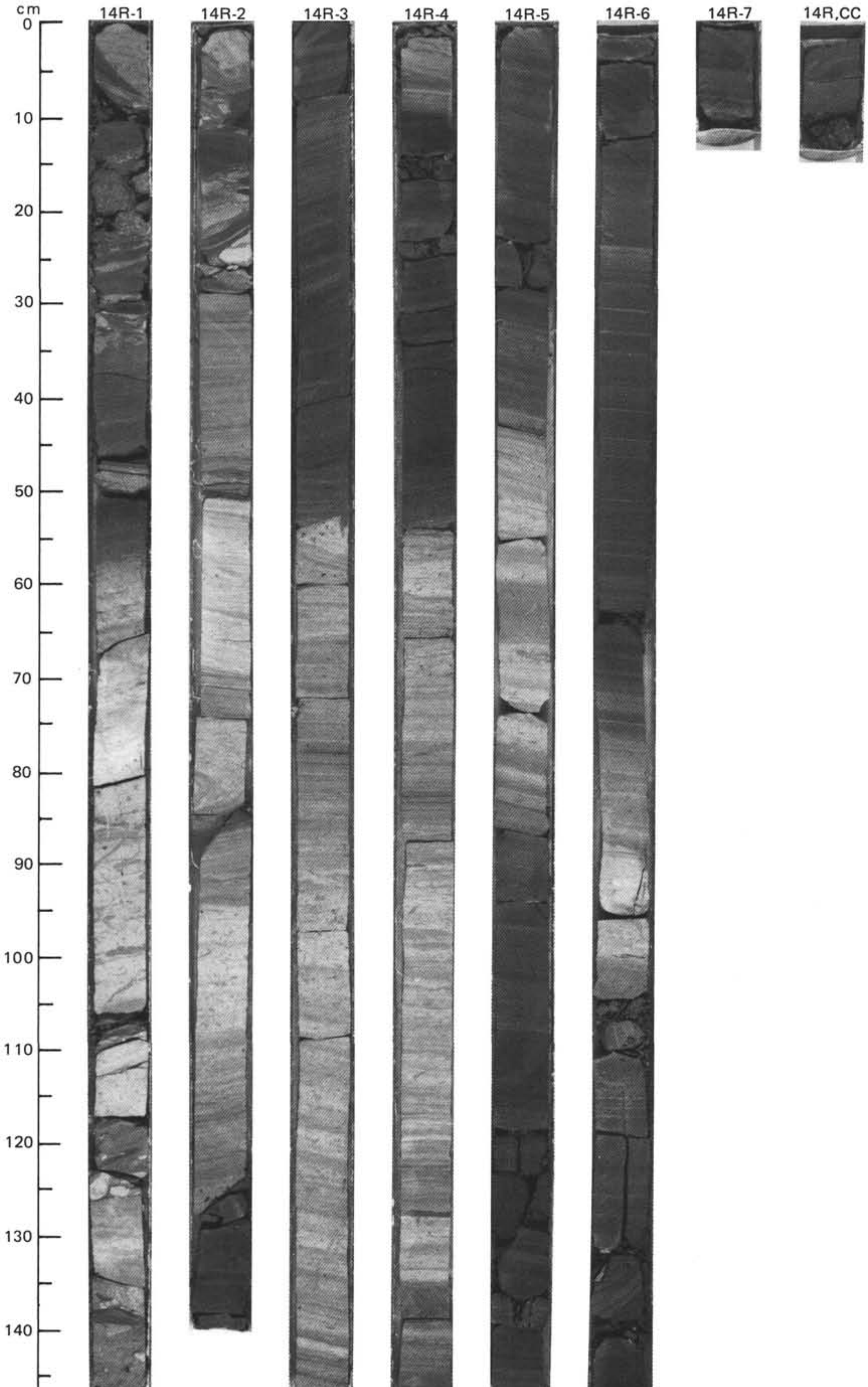
cm
0
10
20
30
40
50
60
70
80
90
100
110
120
130
140
150
14R-1
14R-2
14R-3
14R-4
14R-5
14R-6
14R-7
14R,CC

SITE 641 HOLE C CORE 15 R CORED INTERVAL 4925.3-4935.0 mbsl; 285.8-295.5 mbsf

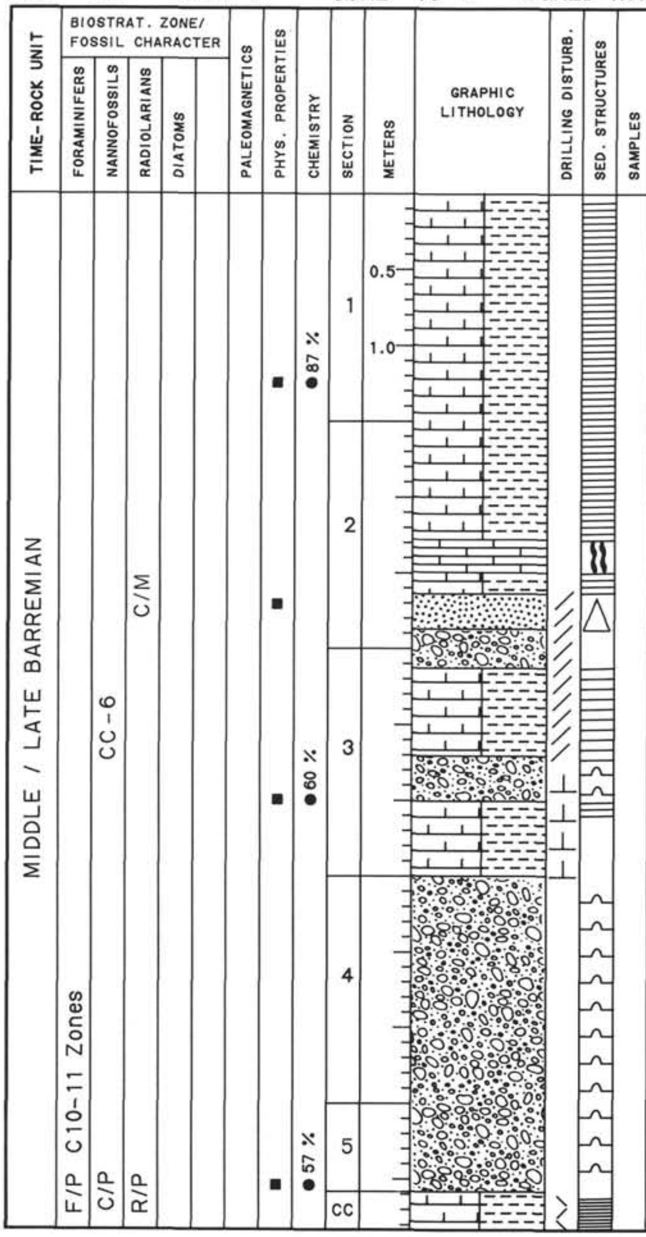

LITHOLOGIC DESCRIPTION

CALCAREOUS MICROTURBIDITES, MARLSTONE, DEBRIS FLOW and SLUMP DEPOSITS

Sections 1, 2, and 3 of the core consist of a succession of <3 cm thick gray marlstone/claystone microturbidites similar to those described in Core 9 (q.v.), though more calcareous. A thin clayey limestone bed is intercalated at Section 2, 77-97 cm. Debris flow deposits occur at the bottom of Section 2 and in the middle of Section 3.

Sections 4 and 5 consist of a single slump composed of fragments(<5 cm) of all the lithologies seen above in Sections 1-3: clayey limestone, bioturbated and laminated marlstones, and wood fragments.

PHYSICAL PROPERTIES DATA:

	1,129	2,119	3,102	4,139	5,51
V_p (a)	3.09	1.84	1.90	2.59	1.94
ρ_b	2.57	2.08	2.11	2.40	2.08

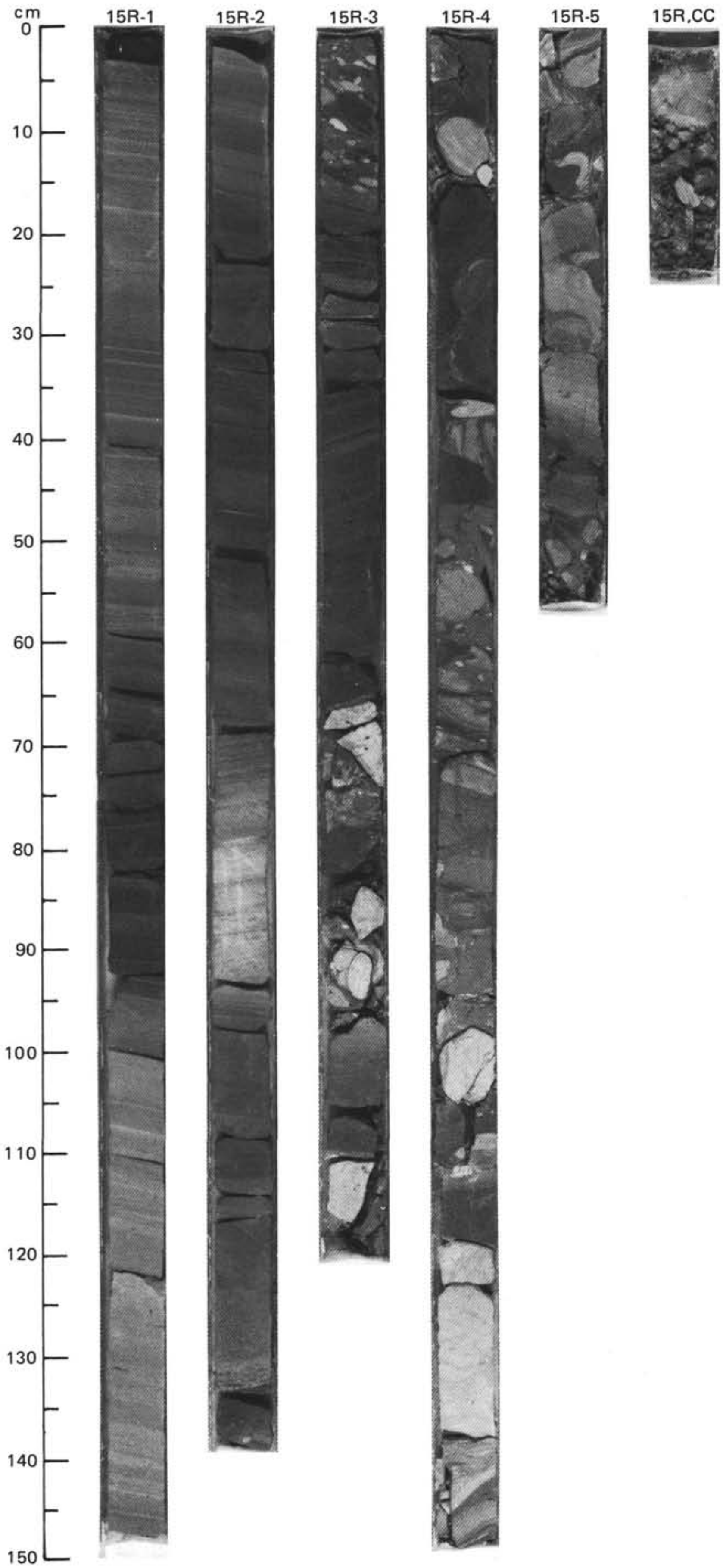
cm
0
10
20
30
40
50
60
70
80
90
100
110
120
130
140
150
15R-1
15R-2
15R-3
15R-4
15R-5
15R,CC

SITE 641 HOLE C CORE 16 R CORED INTERVAL 4935.0-4944.7 mbsl; 295.9-305.2 mbsf

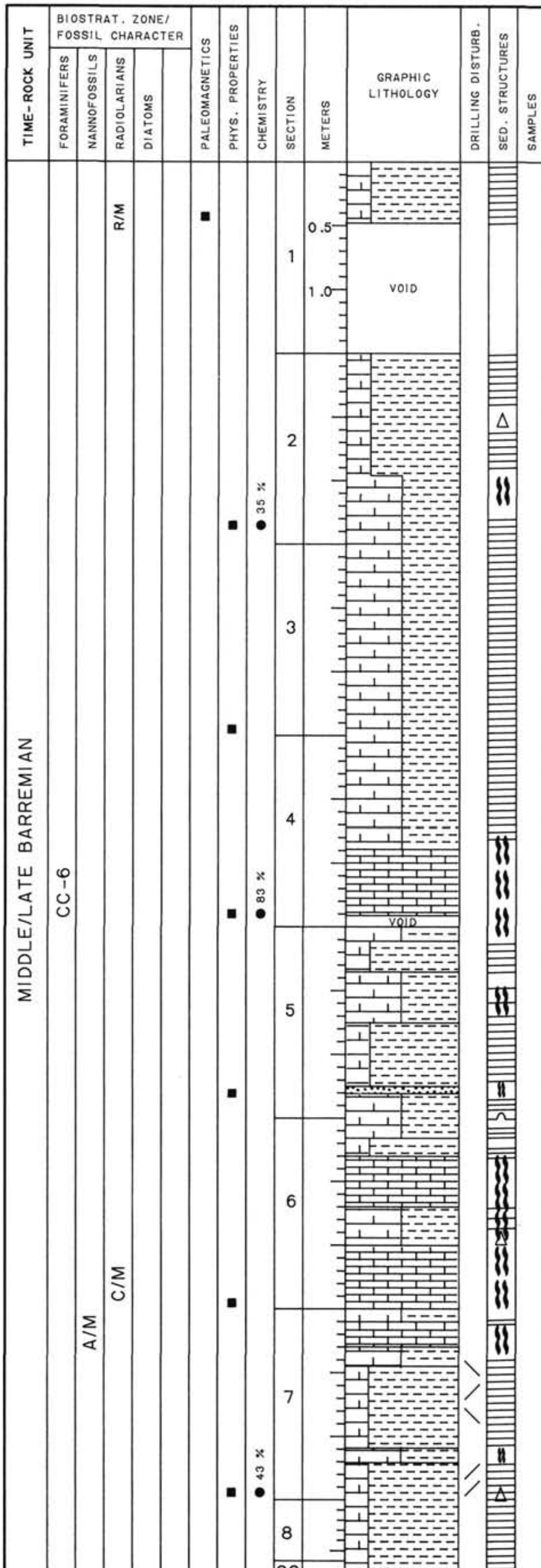

LITHOLOGIC DESCRIPTION

CALCAREOUS MICROTURBIDITES, MARLSTONE and CLAYEY LIMESTONE

The core consists of a thick sequence of dark gray (5Y3/1.5) marlstone and calcareous claystone microturbidites similar to those seen in cores above. Individual turbidites range from 0.4 to 4.0 cm in thickness, averaging 1.0cm. Interbedded with the turbidite sequence, on a scale of 15 to 120 cm, are gray (5Y6/1) bioturbated clayey limestone beds, as thick as 50 cm, and less common massive, bioturbated, gray (5Y6/1) marlstone layers.

Rip-up clasts of calcareous claystone occur in Section 3, 57-58 cm and coalified wood in Section 4, 38-41 cm.

Laminations dip up to 13°.

PHYSICAL PROPERTIES DATA:

	1, 42	2, 134	3, 147	4, 134	5, 124	6, 147	7, 144
V_p(a)	1.79	1.97	2.12	2.55	2.23	3.01	1.91
ρ_b	1.95	2.12	2.19	2.35	2.26	2.39	2.02

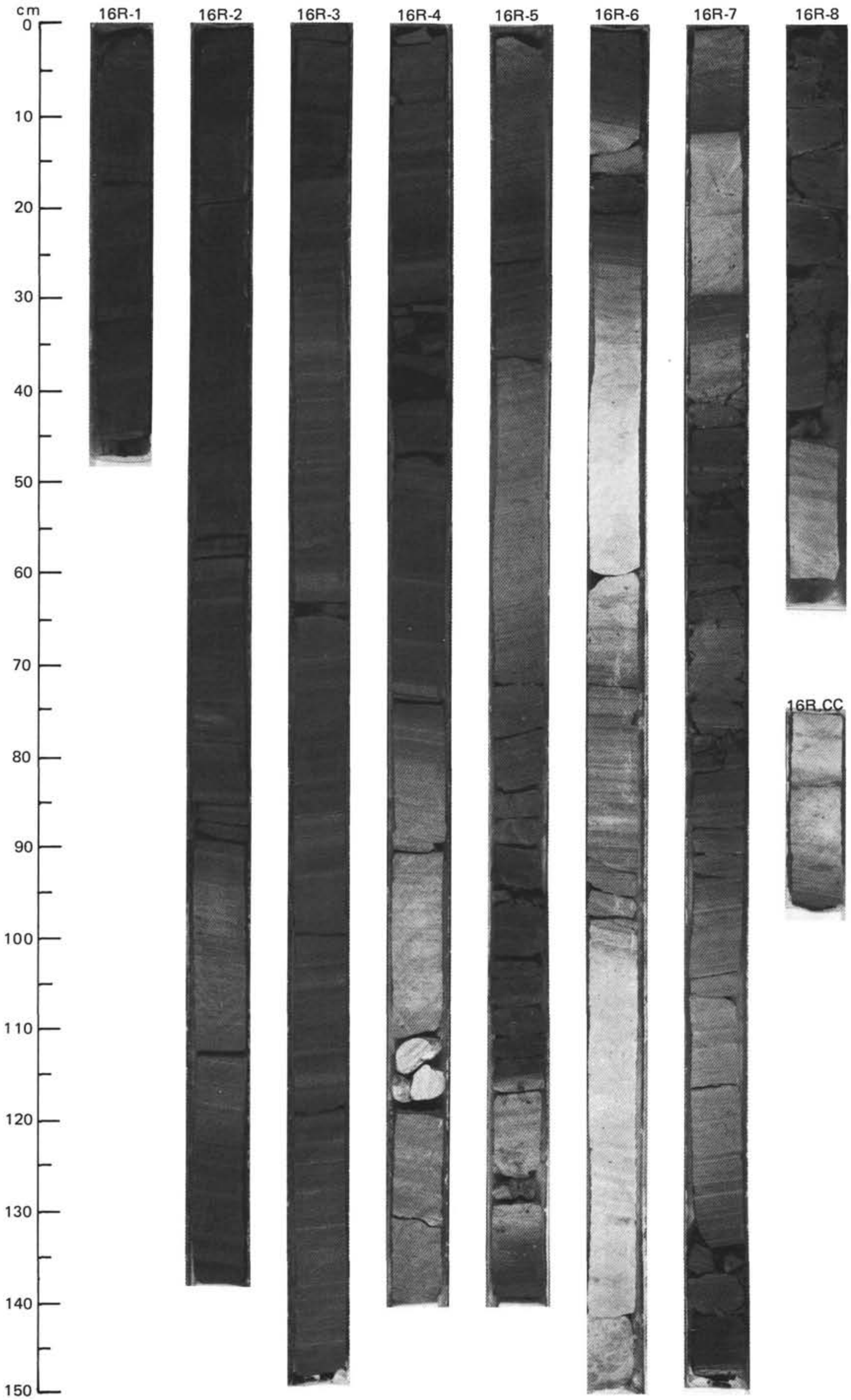
cm
0
10
20
30
40
50
60
70
80
90
100
110
120
130
140
150
16R-1
16R-2
16R-3
16R-4
16R-5
16R-6
16R-7
16R-8
16R,CC